

**CROSS-LAYER DYNAMIC SPECTRUM MANAGEMENT  
FRAMEWORK FOR THE COEXISTENCE OF WHITE  
SPACE APPLICATIONS**

A Thesis  
Presented to  
The Academic Faculty

by

Seungil Yoon

In Partial Fulfillment  
of the Requirements for the Degree  
Doctor of Philosophy



School of Electrical and Computer Engineering  
Georgia Institute of Technology  
August 2011

# CROSS-LAYER DYNAMIC SPECTRUM MANAGEMENT FRAMEWORK FOR THE COEXISTENCE OF WHITE SPACE APPLICATIONS

Approved by:

Professor Jongman Kim,  
Committee Chair  
School of Electrical and Computer  
Engineering  
*Georgia Institute of Technology*

Dr. Chang-Ho Lee  
School of Electrical and Computer  
Engineering  
*Georgia Institute of Technology*

Professor Sung Ha Kang  
School of Mathematics  
*Georgia Institute of Technology*

Professor Shyh-Chiang Shen  
School of Electrical and Computer  
Engineering  
*Georgia Institute of Technology*

Professor Kevin T Kornegay  
School of Electrical and Computer  
Engineering  
*Georgia Institute of Technology*

Date Approved: May 2, 2011

*To myself,*

*Seungil Yoon,*

*to my lovely wife,*

*Oksun Kim,*

*to my beautiful daughters,*

*Eunseo, Hyunseo, and Hannah,*

*and to my parents and parents-in-law*

## ACKNOWLEDGEMENTS

First of all, I would like to appreciate my advisor, Prof. Jongman Kim, for the monumental support and the invaluable opportunity on my Ph.D research. Without his inspiration, I certainly would not have achieved this goal. I would also like to thank Dr. Chang-Ho Lee, Prof. Shyh-Chiang Shen, Prof. Kevin T. Kornegay, and Prof. Sung Ha Kang, for their time in reviewing my dissertation and serving as my defense committee members.

I am very grateful to Dr. Joy Laskar for his great support and guidance throughout this study. Furthermore, I am also indebted to Dr. Kyutae Lim for his efforts to provide me the best research environment. Dr. Jongmin Park and Dr. Sangmin Lee deserve a special acknowledgement for their comments, help in the design, and their tremendous contributions in this research. I would like to acknowledge Samsung Design Center engineers for their assistance.

The support from members of Microwave Application Group has been invaluable: Taejoong Song, Kwanwoo Kim, Sanghyun Woo, Joonhoi Hur, Jaehyouk Choi, Michael Lee, Sungho Beck, Taejin Kim, Hyungsoo Kim, and Kilhoon Lee. I would also like to acknowledge all the members of power amplifier group: Hyungwook Kim, Jeongwon Cha, Eungjung Kim, Jihwan Kim, Youngchang Yoon, Hamhee Jeon, Hyunwoong Kim, Kun Seok Lee, and Kwanyeob Chae. I also thank to all students, who have been doing Ph.D study together, Jeewhan Lee, Junghyuk Park, Jehoon Lee, Yongnam Cho, Sehun Kim, and their family. I am very grateful to Robert Lee for his great support in Atlanta over five years and also Paul and Shawn Allen for giving us a good opportunity to meet great people. I wish to thank Angelika Braig and GEDC staffs for their continuous support.

And most of all, I cannot express my love and gratitude enough to my wife, Oksun Kim, for her love and support throughout all my life. My daughters, Eunseo, Hyunseo, and Hannah have also been a great source of joy. I am especially grateful to my parents, Samjoong Yoon and Mirim Ko, and my parents-in-law, Hong-am Kim and Yeonja Kim for their unconditional love. Without their encouragement and support, this dissertation would not have been possible. I would also like to recognize my sister, Seunghui Yoon, and my brother, Seungsoo Yoon, who also deserve a special thank for their support.

# TABLE OF CONTENTS

<b>DEDICATION</b> . . . . .	<b>iii</b>
<b>ACKNOWLEDGEMENTS</b> . . . . .	<b>iv</b>
<b>LIST OF TABLES</b> . . . . .	<b>ix</b>
<b>LIST OF FIGURES</b> . . . . .	<b>x</b>
<b>SUMMARY</b> . . . . .	<b>xiii</b>
<b>I INTRODUCTION</b> . . . . .	<b>1</b>
1.1 Technical Trends . . . . .	3
1.2 Motivation of Dissertation . . . . .	6
1.3 Organization of Dissertation . . . . .	10
<b>II CROSS-LAYER SPECTRUM MANAGEMENT</b> . . . . .	<b>12</b>
2.1 Motivation of Cross-layer Architecture . . . . .	12
2.2 Dynamic Spectrum Map Architecture . . . . .	14
2.2.1 Network Reference Model . . . . .	14
2.2.2 Structure of Spectrum Map . . . . .	15
2.2.3 Spectrum Map Lifecycle . . . . .	16
2.2.4 General Flow of Spectrum Selection with Extended Spectrum Map . . . . .	17
2.2.5 Technical Challenges and Solutions . . . . .	21
2.3 Dynamic Spectrum Map Management . . . . .	22
2.3.1 Spectrum Map Information Management . . . . .	23
2.3.2 Spectrum Map Creation Procedure . . . . .	26
2.3.3 Spectrum Sensing Result Retrieval . . . . .	27
2.3.4 Spectrum Selection Procedure . . . . .	28
2.3.5 Spectrum Map Update Procedure . . . . .	31
2.4 Theoretical Analysis . . . . .	32
2.4.1 Accuracy of Extended Spectrum Map . . . . .	35

2.4.2	Probability of Success in Channel Search . . . . .	38
2.4.3	Average Spectrum Sensing Time . . . . .	42
2.4.4	Burden of Updating the Spectrum Map . . . . .	45
2.5	Conclusions . . . . .	45
<b>III</b>	<b>FAST RETRIEVAL OF THE SPECTRUM MAP . . . . .</b>	<b>47</b>
3.1	Motivation of Fast Retrieval of the Spectrum Map . . . . .	47
3.2	Extension of the DHCP . . . . .	49
3.2.1	Aggressive Approach . . . . .	49
3.2.2	Cautious Approach . . . . .	51
3.3	Analytical Model . . . . .	52
3.3.1	Network Model and Evaluations Procedures . . . . .	52
3.3.2	Setup Time of Network Selection . . . . .	55
3.4	Numerical Results . . . . .	56
3.4.1	Decrease in Setup Time . . . . .	57
3.4.2	Probability of the Success of Call Setup . . . . .	57
3.4.3	Delay in the Internet access . . . . .	60
3.5	Conclusions . . . . .	62
<b>IV</b>	<b>FREQUENCY-DOMAIN COEXISTENCE BEACON . . . . .</b>	<b>63</b>
4.1	Motivation of Frequency-domain Coexistence Beacon . . . . .	63
4.2	Frequency-domain Coexistence Beacon for White Space Applications	64
4.3	Performance Analysis of FCBv1 . . . . .	68
4.3.1	Analysis of Detection Probability . . . . .	68
4.3.2	Analysis of Network Capacity Increase . . . . .	69
4.4	Performance Analysis of FCBv2 . . . . .	74
4.4.1	Queuing Network for Evaluation of FCBv2 . . . . .	74
4.5	Conclusions . . . . .	78
4.6	Appendix A. . . . .	78

<b>V</b>	<b>INTER-CELL TRANSMIT POWER ADAPTATION . . . . .</b>	<b>79</b>
5.1	Motivation of Inter-cell Transmit Power Adaptation . . . . .	79
5.2	Inter-cell Transmit Power Adaptation Algorithm . . . . .	80
5.2.1	Basic Functions . . . . .	80
5.2.2	ITPA Algorithm Description . . . . .	82
5.2.3	ITPA Negotiation . . . . .	85
5.3	Theoretical Analysis . . . . .	88
5.3.1	Network and Channel Models . . . . .	88
5.3.2	Performance Evaluation Metrics . . . . .	90
5.3.3	Parameters for Numerical Evaluation . . . . .	96
5.3.4	Calculation of Expected Number of Detected Neighboring WS- APs . . . . .	97
5.3.5	Numerical Results . . . . .	99
5.3.6	Summary of Theoretical Analysis . . . . .	105
5.4	Analysis of Simulation . . . . .	105
5.4.1	The Simulation Model . . . . .	106
5.4.2	Parameters for Simulation . . . . .	107
5.4.3	The Probability of Success in Channel Assignment . . . . .	108
5.4.4	The Probability of Success in Service Continuity . . . . .	112
5.4.5	Comparison of $S_{ITPA}^{pc}$ and $S_{ITPA}^c$ . . . . .	116
5.4.6	Summary of Simulation . . . . .	118
5.5	Conclusions . . . . .	118
<b>VI</b>	<b>CONCLUSIONS . . . . .</b>	<b>120</b>
<b>APPENDIX A</b>	<b>— COEXISTENCE SCHEMES IN PHY/MAC . .</b>	<b>123</b>
<b>REFERENCES</b>	<b>. . . . .</b>	<b>124</b>
<b>VITA</b>	<b>. . . . .</b>	<b>129</b>

## LIST OF TABLES

1	Comparison of Feature Detection and Energy Detection. . . . .	5
2	Parameters for evaluation of the cross-layer framework. . . . .	33
3	The expected success probability of the second spectrum sensing, $P_{ss}(t)$ , with $R_s = 0.9$ , $R = 120 m$ , and $N = 30$ . . . . .	43
4	The expected success probability of the second spectrum sensing, $P_{ss}(t)$ , with $R_s = 0.9$ , $R = 180 m$ , and $N = 30$ . . . . .	43
5	Parameters for the performance valuation of the enhanced DHCP. . .	56
6	The threshold, $\lambda$ , with fixed $u$ and $P_f$ . . . . .	68
7	Parameters for performance evaluation of the $FCB_{v1}$ in the probability of detection. . . . .	69
8	Parameters for performance evaluation of the $FCB_{v1}$ in network capacity.	71
9	the difference of the expected number of detected WSDs between energy detection using the $FCB_{v1}$ and a typical energy detection. . . .	71
10	The increase of a total MAC throughput of white space channels. . .	73
11	Parameters for the numerical evaluation of the ITPA-based spectrum sharing . . . . .	96
12	$COR(\alpha)$ without the ITPA for $P_{snr} = 10, 20$ and $30$ dB . . . . .	98
13	$COR(\alpha)$ with the ITPA for $P_{snr} = 10, 20$ and $30$ dB . . . . .	98
14	Average of $COR(\alpha)$ with the ITPA vs. without ITPA for $P_{snr} = 10, 20$ and $30$ dB . . . . .	98
15	Parameters for the ITPA-based spectrum sharing simulation . . . . .	108
16	Calculated number of detected neighboring WSAPs during the simulation	108

## LIST OF FIGURES

1	The example of the spectrum map management . . . . .	2
2	The coexistence of heterogeneity . . . . .	7
3	A network reference model for the spectrum map management. . . . .	15
4	A general flow of a channel selection procedure with the extended spectrum map. . . . .	18
5	An example of a channel selection procedure with the proposed framework . . . . .	20
6	Calculation of the accuracy index of the $i^{th}$ channel . . . . .	25
7	The expected number of activated WSAPs with $R = 120 m$ and error-less spectrum sensing methods when the density of WSAPs ( $\rho$ ), the average rate of the service time ( $\mu$ ), and the expected number of activated WSAPs, $E(N_\beta)$ , are known (Subfigure (a)). vs. the expected number of activated WSAPs with erroneous spectrum sensing methods (Subfigure (b)). Subfigure (c) depicts the extent to which the Spectrum Sensing Reliability Index (SSRI) is affected with the known $P_m$ , $P_f$ , $\rho$ , $\mu$ and $E(N_\beta)$ . . . . .	36
8	With the spectrum sensing reliability index, $R_s = 0.9$ , the analysis results of the expected probability of success in the first spectrum sensing, $P_{fs}(t)$ , with $R = 120 m$ and $N = 30$ in (a) and (c) are presented. In subfigure (b), for $N = 50$ , $\rho$ varies from 0.010 to 0.018. Subfigure (a) and (b) illustrate that a higher $\rho$ contributes to the drastic drop of the probability of success, which we observe in labels (c) of subfigure (a) and (b). In subfigure (c), with a lower $\nu = 0.4$ , $P_{fs}$ still approaches 80 % for $\rho = 0.004$ and $\rho = 0.006$ . A subfigure (d) depicts the extent to which $P_{fs}$ will decrease if we have consecutive expiration of $R_{to}$ timers	41
9	With the spectrum sensing reliability index, $R_s = 0.9$ , the analysis results of the expected spectrum sensing time, $E(T_{ss})(t)$ , with $N = 30$ are presented. Subfigure (b) is the analysis results of $E(T_{ss})(t)$ for $R = 180 m$ . Three subfigures depict that $E(T_{ss})(t)$ rather steeply increases when $\rho$ becomes greater than a saturation point. In subfigure (c), with a lower $\nu = 0.4$ , $E(T_{ss})(t)$ still could be reduced significantly when $\rho$ is less than or equal to 0.008. . . . .	44
10	The general call flow of the handover from WiFi <sup>TM</sup> to White Space Network . . . . .	48
11	The new call flow of the DHCP in the aggressive approach. . . . .	50

12	The new call flow of the DHCP in the cautious approach. . . . .	51
13	Queuing model for the performance evaluation of the extended DHCP	53
14	The calculated $P_{to}$ with $\lambda_1 = \lambda_2 = \lambda_3$ . . . . .	58
15	The $\rho'$ with $T_{sa} + T_{hd}$ versus The $\rho'$ with $T_{sa} + T_{hr}$ (Subfigure(a)). Probability of the success in handover calls with $\lambda_1 = \lambda_2 = \lambda_3$ (Sub- figure (b)) . . . . .	59
16	Calculated delay in the retrieval of the spectrum map . . . . .	61
17	A new proposal of white space channel for the proposed pilot detection scheme. The proposed scheme assumes that the total power of 10 kHz of the frequency-domain coexistence beacon is equal to the total power of energy detection of 100 kHz of 6 MHz. . . . .	65
18	The average probability, $\bar{P}_{d,nak}$ , of detection in a typical energy de- tection and the proposed pilot detection scheme. The SNR of the proposed scheme is 10 dB greater than the SNR of energy detection. . . . .	70
19	The expected number, $E'(N_b)$ , of occupied channels with $R = 120 m$ . Symbols for $P_d \approx 0.95$ represent $E'(N_b)$ of $FCB_{v1}$ -based energy detec- tion while symbols for $P_d \approx 0.86$ represent $E'(N_b)$ of a typical energy detection with $SNR(\bar{\gamma}) = 10 dB$ and $u = 2$ . . . . .	72
20	Queuing networks for performance evaluation . . . . .	74
21	Differences between blocking probabilities, $P_{B1}$ , $P_{B2}$ , and $P_{B3}$ . . . . .	75
22	The average number of active WSDs ( $E''(N_b)$ versus $E(N_b)$ ) with $\alpha_1$ , $\alpha_2$ , and $\alpha_3$ . . . . .	76
23	The total spectrum sensing time, $T_{ss}$ , of a WSD conducting $FCB_{v2}$ - based energy detection . . . . .	77
24	Reference model of the ITPA algorithm . . . . .	82
25	Diagram of the extent to which the ITPA algorithm works . . . . .	84
26	A message flow for the ITPA negotiation. . . . .	87
27	A reference model for the analysis of the probability of continuity in the ITPA-based spectrum sharing with a time-stationary location of clients. . . . .	95
28	$S_{ITPA}^{pr}$ versus $S_{ITPA}^{sr}$ with $\alpha \approx 2.9$ and MF = 2. . . . .	100
29	$S_{ITPA}^{pr}$ versus $S_{ITPA}^{sr}$ with $\alpha \approx 2.9$ and MF = 10. . . . .	102
30	$S_{ITPA}^{pr}$ versus $S_{ITPA}^{sr}$ with $\alpha \approx 3.3$ and MF = 2 and 10. . . . .	103
31	$S_{ITPA}^{pc}$ versus $S_{ITPA}^{sr}$ with $\alpha \approx 2.9$ and 3.3 for MF = 2. . . . .	104

32	$S_{ITPA}^{pc}$ versus $S_{ITPA}^{sr}$ with $\alpha \approx 3.3$ for MF = 10. . . . .	105
33	The simulation model for the ITPA performance evaluation . . . . .	106
34	The procedures for activating WSAPs in the simulation . . . . .	107
35	$S_{wITPA}^{ca}$ versus $S_{woITPA}^{ca}$ with M = 0. . . . .	110
36	$S_{wITPA}^{ca}$ versus $S_{woITPA}^{ca}$ with M = 1. . . . .	111
37	The difference between $S_{wITPA}^{ca}$ for M = 0 and $S_{wITPA}^{ca}$ for M = 1 at MF = 2 (represented by the solid symbols).The difference between $S_{wITPA}^{ca}$ for M = 0 and $S_{wITPA}^{ca}$ for M = 1 at MF = 10 (represented by the open symbols) . . . . .	112
38	$S_{ITPA}$ and $S_{ITPA}^c$ for M = 0 . . . . .	114
39	The average distance of neighboring WSAPs with AR = 0.448 . . . . .	115
40	The probability of real success in channel assignment with M = 0 and MF = 2 . . . . .	116
41	The difference between $S_{ITPA}$ for M = 0 and $S_{ITPA}$ for M = 1 . . . . .	117
42	Comparison of $S_{ITPA}^{pc}$ and $S_{ITPA}^c$ . . . . .	117
43	The cross-layer architecture layers with all proposed schemes . . . . .	122
44	The example of the cross-layer spectrum map management . . . . .	122
45	Coexistence Schemes in PHY/MAC layers of licensed and/or unlicensed access network standards . . . . .	123

## SUMMARY

The objective of this dissertation is to propose the cross-layer spectrum management architecture for white space applications that improves the main functions of the spectrum management: spectrum sensing, spectrum decision, spectrum sharing and spectrum mobility. In addition, the objective is to propose specific methods that aim to assist white space devices (WSDs) to achieve a higher accuracy of spectrum sensing, smart spectrum decision, interoperable spectrum sharing, and effective spectrum mobility.

This dissertation proposes the cross-layer spectrum management framework for white space applications that enables white space network devices such as WSDs and a spectrum map server to cooperate to build a dynamic spectrum map that provides not only a location-based list of available white space channels but also the channel occupancy-status, either *occupied* or *unoccupied*. The newly-joining WSDs with the extended spectrum map can avoid unnecessary spectrum sensing against the channels that are marked as unoccupied, which results in decreasing not only the possibility of causing interference to neighboring WSDs but also the total spectrum sensing time that WSDs spend to sense all channels listed in the retrieved spectrum map. In addition, for a faster retrieval of the extended spectrum map, this dissertation proposes extending the role of the Dynamic Host Configuration Protocol (DHCP) server that provides the extended spectrum map retrieved from the spectrum map server in advance during establishing the Internet connection through the licensed or unlicensed wireless networks. The early retrieval of the spectrum map contributes to a faster attachment to white space networks than the case of retrieving the spectrum map after the setup of the licensed or unlicensed wireless networks. Decrease in the

establishment time to white space networks after all contributes to increase in the capacity of white space channels since WSDs can release their operating channel early as much as the decreased time in the network establishment.

Along with the optimization of the target list for spectrum sensing, to increase the detection capability of spectrum sensing methods, this dissertation suggests the frequency-domain coexistence beacon (FCB) that is allotted to the same location of the DTV pilot as the pilot of WSDs. As we have a higher signal-to-noise ratio (SNR) of the DTV pilot than that of the total bandwidth of one channel, using the FCB as a new transceiver framework, we can achieve a better detection of the signals of neighboring WSDs at a rather low SNR compared to other spectrum sensing methods while we can implement the FCB at a low cost by adopting the DTV pilot detector. In addition, the FCB can broadcast channel information of channel bonding or aggregation so that the FCB has a further contribution in shortening the total spectrum sensing time and increasing the total capacity of white space channels.

However, the cross-layer spectrum management and the FCB are dedicated on assisting WSDs to search unoccupied channels effectively and quickly with the assumption that they have unoccupied channels. Thus, in the dissertation, we propose the inter-cell transmit power adaptation (ITPA) as a collaboration-based spectrum sharing framework when newly-joining WSDs or any WSDs in need of their new operating channel fail to find unoccupied channels. Using the ITPA-base spectrum sharing, WSDs, which failed to search their operating channel, can afford to find shareable channels among the channels belonging to neighboring WSDs and negotiate the adjustment of their transmit power in a cooperative way. In the ITPA-based spectrum sharing, the spectrum map server acts as the intermediary to support the ITPA negotiation between homogeneous and/or heterogeneous WSDs. The ITPA-based spectrum sensing contributes to accommodating more WSDs that after all increase the utilization of white space channels.

The proposed cross-layer spectrum management framework consists of the extended spectrum map, the faster retrieval of the spectrum map, the FCB, and the ITPA, which all contribute to improvement in spectrum sensing, spectrum decision, spectrum sharing and spectrum mobility.

In November 2008, the Federal Communications Commission (FCC) [17] released the rules of white space, locally unused TV spectrum, stating that unlicensed devices that will not interfere with incumbent users can use white space for wireless broadband Internet access. In addition, in September 2010 [18], the FCC approved use of white spaces for unlicensed data, the so-called “Super WiFi” proposal. The FCC rules and approvals mainly focus on providing the guidelines that protect incumbent users such as TV broadcasting and wireless microphone service from the access of unlicensed devices, so-called “white space devices (WSDs).” For the protection of incumbent users, with spectrum sensing techniques, WSDs attempts to detect the presence of incumbent users and then avoid selecting their operating channel among any channels where they detect the signals of incumbent users. After they succeed in finding and occupying unused or unoccupied channel through spectrum sensing, they start transmitting their signals on the channel.

However, all activated WSDs during their activation time continue to conduct spectrum sensing periodically and/or manually to detect not only the signals of incumbent users but also the signals of their neighboring WSDs. Thus, they conduct periodically spectrum sensing against not only their operating channel but also other white space channels. Sensing their operating channel aims to detect a sudden appearance of incumbent users on their operating channel, and if the detection is positive,

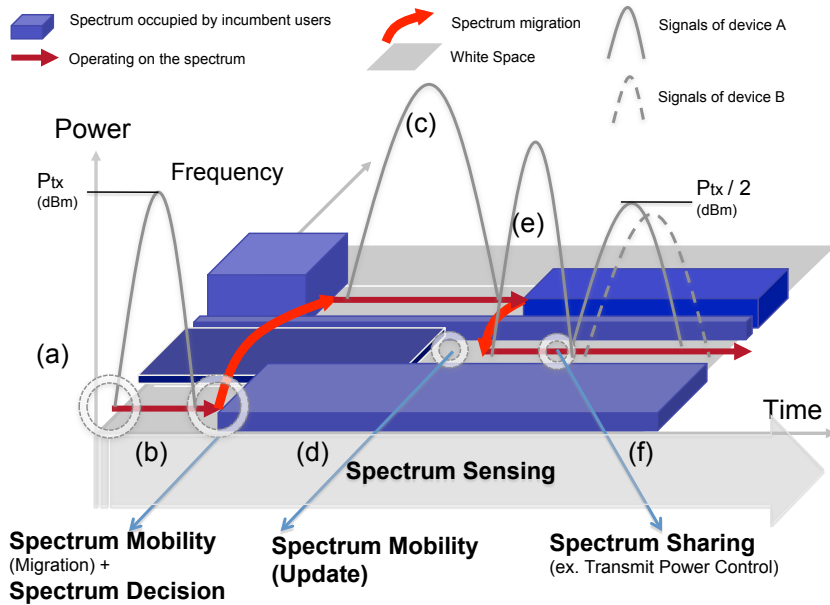


**Figure 1:** The example of the spectrum map management

they should immediately switch over to another unused channel. Meanwhile, the objective of sensing other white space channels periodically is to find any potential backup channels that the WSDs can use as their new operating channel because of either detecting incumbent users or suffering from performance degradation on their current operating channel for a certain time.

This unique characteristic as previously described, concerning the coexistence between incumbent users and WSDs, requires WSDs that have an ability to adapt to the dynamic changes of wireless environments, and cognitive radio technology is believed to be a right solution to enable them to change their transmission and receiver parameters precisely not to cause interference with incumbent users and/or their neighboring WSDs. In cognitive radio, to manage transmission and reception changes properly, the spectrum management consists of four major functions: spectrum sensing, spectrum decision, spectrum sharing and spectrum mobility [24]. Figure 1 depicts the example of the extent to which four functions work. At label (a), a newly-joining WSD starts transmitting their signals on one white space channel that is marked as

unoccupied according to the results of spectrum sensing. Throughout its activation time, it continues to conduct spectrum sensing to prepare any chance of switching their operating channel like the case as depicted in label (b). In the case of a sudden presence of incumbent users, it will conduct spectrum decision for the optimal decision of its new operating channel among candidates, and spectrum mobility for seamless channel migration. Then, it restarts transmitting their signals on its new operating channel as depicted in label (c) or (e). As illustrated in (d) label, it continues to perform spectrum sensing to monitor which white space channels are unoccupied and then to register them as candidate channels for spectrum mobility. However, if another newly-joining WSD can not find vacant channels, through spectrum sharing methods such as transmit power control, the new one can share one channel with the WSD have been operating on the channel as depicted in label (f). Figure 1 clearly illustrates that all operations of the spectrum management basically rely on spectrum sensing.

As described previously about the extend to which spectrum sensing is important, the throughput of WSDs depends on whether they have highly accurate and efficient spectrum sensing methods and other supplemental techniques designed for assisting WSDs to find spare channels quickly and efficiently.

### ***1.1 Technical Trends***

To increase the accuracy of spectrum sensing methods, the sacrifice such as a further resource consumption, particularly power consumption, which is undesirable for portable WSDs, might be inevitable. Thus, concerning the balance between the accuracy and the energy efficiency results in the need of inventing supplemental methods that can reduce a burden of spectrum sensing methods or new spectrum sensing methods that can improve the probability of detection. The burden of spectrum sensing

methods is related to the fact that WSDs need to conduct spectrum sensing periodically against all white space channels without the priori knowledge of a channel occupancy, either *occupied* or *unoccupied*. Even this overhead becomes worsen when the WSDs do not know which white space channels are really open for the unlicensed use of WSDs. To resolve these overheads, various supplemental proposals from IEEE 802.22 and other standard groups such as ETSI, IEEE and ECMA, suggest that WSDs have to have any features to figure out their current location and a list of affordable white space channels for unlicensed use at their current location. For the retrieval of the list, the WSDs shall provide their current location to a database of white spaces, a so-called “spectrum map server,” which they can connect to through the Internet. From the spectrum map server, they will retrieve a location-based list of available white space channels, a so-called “spectrum map.” at their current location. Based on the retrieved spectrum map, they can conduct spectrum sensing against only white channels included in the list and classified as open for unlicensed use of WSDs. With the results of spectrum sensing stating the occupancy status, they can determine which channels are unused. As they move to other areas, they might connect to the spectrum map server in advance to retrieve the spectrum map of new locations. Although the spectrum map solution resolves the concern of unnecessary spectrum sensing against white space channels not allowed for the unlicensed use, the solution does not present what is the current occupancy status of white space channels. If the WSDs know the channel occupancy, they can save and energy for spectrum sensing. To the WSDs, that improvement means that they can launch their service earlier on more reliable channel than the case that hey have rather a low accuracy of spectrum sensing. In addition, since they can release their operating channel earlier, other potential WSDs that will fail to find their operating channel can have a chance to occupy the early-released channel. More accommodations of WSDs after all can contribute to increase in the utilization of white space channels. Thus, the

**Table 1:** Comparison of Feature Detection and Energy Detection.

	Feature detection	energy detection
Method	identify unique signature features (preamble, PN sequence)	measure the power within a certain frequency bandwidth
Sensitivity	high	low
Processing Time	long	short
Hardware Complexity	high	low
Usage	accurate, final sensing in a small bandwidth	fast, initial sensing in a wide bandwidth

new spectrum map that can offer the channel occupancy will be a key contribution for the efficient spectrum management.

While, as the supplemental solution, the spectrum map contributes to decrease in the load of spectrum sensing, we need a fundamental approach to achieve increase in the probability of detection on spectrum sensing. In addition, the new approach should arrange a trade-off between the acceptable accuracy of spectrum sensing methods and resource consumption. In general, spectrum sensing methods are classified into two categories: feature detection and energy detection. Feature detection identifies the unique signature features of a signal modulation scheme such as a pseudo-random noise (PN) sequence in a U.S. digital television (DTV) signal. Energy detection estimates the total power over a certain bandwidth (e.g. 6 MHz of TV channel) and compares it with a pre-defined threshold value to determine the validity of the signals of other devices. As shown in Table 1 and [15], although energy detection is more unreliable against noise uncertainty than feature detection, energy detection is faster in spectrum sensing and simpler in implementation than feature detection. However, since both detection methods cannot alone solve imposed challenges in spectrum sensing, IEEE 802.22 suggests a dual-stage spectrum sensing approach. First, WSDs execute energy detection on all available white space channels according to the spectrum map. Then, they execute feature detection on unoccupied channels according to the spectrum sensing results of energy detection.

Thus, they using the dual-stage approach can reduce total spectrum sensing time and spend fewer resources for feature detection. However, since they with both sensing methods that rely on only radio signals can still cause false alarms that identify occupied channels as unoccupied ones, they cannot still avoid generating interference to incumbent users or other WSDs. To minimize uncertainty with one energy or feature detector, cooperation detection collaborates with other WSDs to collect measured spectrum sensing results to increase the accuracy of spectrum sensing. However, this approach can cause further resource consumption because of overhead traffic required for cooperation.

As the supplemental method, the spectrum map can contribute to avoiding unnecessary spectrum sensing against channels that are not open for unlicensed use. However, the WSDs should conduct spectrum sensing against all white space channels regardless of their occupancy status, which means they still conduct further unnecessary spectrum sensing against any channels that are occupied by other incumbent users or WSDs. As the fundamental method, typical methods are not qualified in a matter of balancing well a trade-off between the accuracy of spectrum sensing and resource consumption.

## ***1.2 Motivation of Dissertation***

The fact that WSDs should coexist with incumbent users originates the following challenges: decrease in the overhead of conducting spectrum sensing and the design of precise spectrum sensing methods. Beside the coexistence between WSDs and incumbent users, the coexistence between WSDs is another challenge, and this challenge becomes the critical one for supporting spectrum sharing between heterogenous WSDs. As illustrated in Figure 2, the coexistence issue that is generally triggered between vertically heterogeneous licensed or unlicensed systems operating on different frequency bands will be generated between multiple horizontally heterogeneous

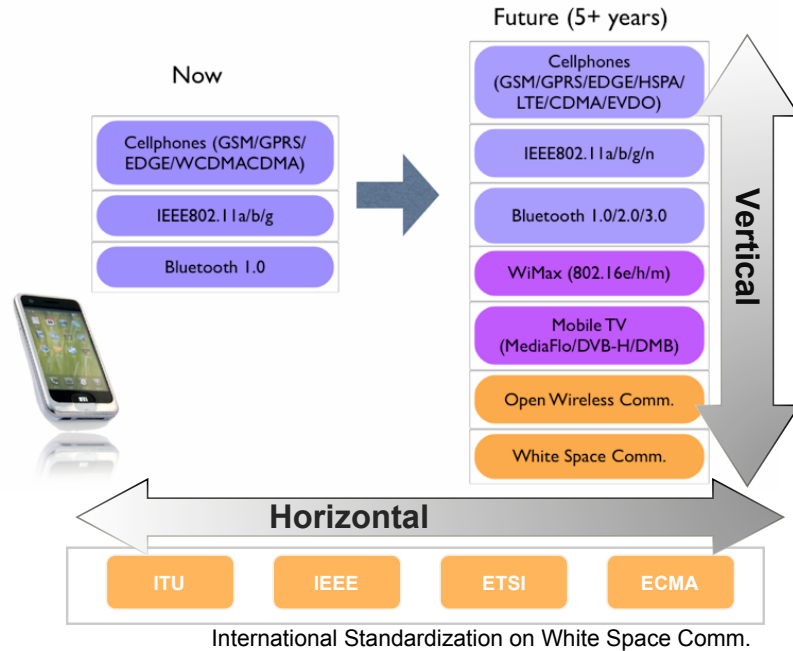


**Figure 2:** The coexistence of heterogeneity

standards for white space. In addition, typical coexistence schemes as depicted in Figure 45 on Chapter A implemented in physical and/or medium access control layers are inadequate to support spectrum sharing between heterogenous WSDs. Thus, the solutions to resolve coexistence-related challenges should be implemented over multiple layers vertically from a physical layer to an application layer. For instance, while the design of precise spectrum sensing methods is a challenge to physical and medium access layers, decreasing the load of spectrum sensing is a challenge to all layers. Thus, along with researching an individual optimal solution of the challenges, the spectrum management for white space applications requires a cross-layer architecture that is capable of deploying all solutions properly over all layers. For instance, as the solution of spectrum sharing, conventional transmit power control (TPC)-based coexistence mechanisms are non-collaborative mechanisms, where WSDs adjust their transmit power not to interfere with their neighboring WSDs without any negotiation of their new transmit power. Although we can consider to adapt new schemes, introduced in [2] and [39], WSDs roughly adjust their transmit power because of the

absence of a collaborative negotiation. For the effective control, they prefer a collaborative TPC mechanism, which requires the involvement of multiple protocol layers over white space network devices. Thus, they need the cross-layer architecture for the support of the collaboration-based TPC.

The first objective of the dissertation is to propose a cross-layer spectrum management framework that enables all network equipments for white space application to handle the uncertainty of white space channels in a cooperative way and to implement collaboration-based spectrum management schemes. The proposal lets the spectrum map server and other network management systems keep track of the occupancy-status change of white space channels by collecting the spectrum sensing results of WSDs as the return of providing a spectrum map. With the extended spectrum map offering the occupancy status of white space channels, newly-joining WSDs could perform faster spectrum sensing by building a target list of spectrum sensing with only channels that are marked as open and unoccupied according to the retrieved spectrum map. Based on the cross-layer cooperation between WSDs and the spectrum map server, the second objective of this dissertation is to propose a collaboration-based spectrum sharing framework, a so-called “inter-cell transmit power adaptation (ITPA),” that provides a way of sharing one channel between two homogenous and/or heterogenous WSDs by adjusting their transmit power with the assistance of the spectrum map server. The ITPA-based spectrum sharing provides the algorithm that assists a newly-joining WSD to determine which channels that belong to neighboring WSDs are affordable for spectrum sharing. The newly-joining WSDs can initiate the negotiation of adjusting their transmit power toward the neighboring WSD operating on the channel that the ITPA algorithm declares the availability of spectrum sharing. Both WSDs conduct the ITPA negotiation indirectly through the spectrum map as an intermediary to support spectrum sharing between heterogenous WSDs. The third objective of this dissertation is to propose a new transceiver

framework, a so-called “frequency-domain coexistence beacon (FCB),” that aims to increase the probability of detection. In a matter of increase in the probability of detection, conventional spectrum sensing methods require resource consumption with a dedicated hardware for transmission and reception of the signals of WSDs. Instead of the dedicated hardware, this proposal is to allot a beacon frequency at the same location of the DTV pilot in white space channels that enables a receiver to reuse a DTV pilot detector and WSD equipped with the new receiver to detect neighboring WSDs at a higher probability of detection as a result of a higher signal-to-noise ratio (SNR). The increase in SNR is due to the fact that the narrow bandwidth of the DTV pilot contributes to a higher SNR compared to that of the 6 MHz.

This dissertation contributes to the followings:

- the cross-layer spectrum management framework enables WSDs and the spectrum server to cooperate in building and managing the extended spectrum map.
- the extended spectrum map contributes to decreasing the number of channels targeted for spectrum sensing, which results in decreasing not only the overhead of conducting spectrum sensing but also the probability of false detection, which marks occupied channels as unoccupied ones.
- the cross-layer spectrum management framework provides a backhaul network for the collaboration-based spectrum sharing.
- the transceiver framework based on the FCB contributes to increase in the probability of detection, which results in achieving a higher utilization of white space channels with less interference and more accommodation of newly-joining WSDs.
- the collaboration-based spectrum sharing based on the ITPA contributes to allowing homogeneous and/or heterogeneous WSDs to share their operating channel with adjusting their transmit power in the not arbitrary but calculated

amount.

### ***1.3 Organization of Dissertation***

This dissertation consists of the following chapters.

Chapter 2 presents the cross-layer framework for the dynamic spectrum map management that builds and manages the extended spectrum map with the cooperation between WSDs and the spectrum map server. In this chapter, we also describe the extent to which the extended spectrum map assists newly-joining WSDs to not only shorten the total spectrum sensing time but also decrease interference to neighboring WSDs by reducing the possibility of miss detection. We demonstrate the extent to which the cross-layer architecture contributes to increase in the utilization of white space channels through performance evaluation.

Chapter 3 describes another cooperation that aims to shorten the retrieval time from the spectrum map server to WSDs with the assistance of the Dynamic Host Configuration Protocol (DHCP) server. Instead of retrieving the spectrum map from the spectrum map server, we propose the DHCP server could embed the spectrum map retrieved from the spectrum map server into DHCP messages. We demonstrate the extent to which this fast retrieval of the spectrum map contributes to increase in the capacity of white space applications.

Chapter 4 presents the extent to which the new transceiver architecture using the FCB improves the probability of detection on spectrum sensing. This chapter also describes the extent to which the proposed scheme improves the probability of detection compared to that of a typical energy detection. In addition, we demonstrate the extent to which the detection improvement increases the total capacity of white space channels through numerical evaluation.

Chapter 5 describes the collaboration-based spectrum sharing framework that provides the decision algorithm of selecting the channels for the ITPA-based spectrum

sharing. In addition, we present the extent to which two heterogeneous WSDs conduct the procedures of the ITPA negotiation using the backhaul network presented by the cross-layer architecture of the spectrum management. In this chapter, we analyze the performance of the ITPA-based spectrum sharing with numerical results of performance evaluation and simulation results.

Chapter 6 summarizes this dissertation.

This chapter introduces the cross-layer design of the spectrum management for white space channels to enrich the usage of the spectrum map.

### *2.1 Motivation of Cross-layer Architecture*

After retrieving the location-based spectrum map of a current location, newly-joining WSDs conduct spectrum sensing. With the results of spectrum sensing, they select their operating channel among channels marked as unoccupied. Inside spectrum decision, they comply with spectrum etiquette that defines the basic rules in spectrum sharing among unlicensed neighboring WSDs. However, this spectrum etiquette has no authority to force selfish WSDs, which at least follow the FCC rules, to yield their operating channel. According to [51], [34], [29], [24] and [30], WSDs can find their operating channel in non-cooperative ways such as dynamic frequency selection or dynamic frequency sharing without the assistance of neighboring WSDs. To increase the efficiency of channel selection, WSDs can find their operating channel using spectrum auction or leasing mechanisms that are managed by a spectrum management controller. For instance, a decentralized controller can conduct the spectrum map management of a local area while a centralized controller can provide spectrum map management over all areas. Regardless of the spectrum management techniques that WSAs depend on, we prefer the method that one WSD exclusively operates on one

white space channel at one location. This exclusiveness is different to spectrum management of other unlicensed access networks such as WiFi<sup>TM</sup>, which permits multiple devices to operate on the same channel without concerning for the collision or the service degradation with neighboring WiFi<sup>TM</sup> devices.

As a coordinated method of above two approaches, multiple WSDs can share one channel using message-based spectrum contention [37] that schedules exclusive access in a promised set of data frames within a super frame. In addition, using transmit power control, WSDs can adjust their transmit power after negotiating with neighboring WSDs to generate less interference to neighboring WSDs. Newly-joining WSDs will be pleased if anyone can inform which channels are unused at the current location of the WSDs. Based on this preference, we suggest extending the role of a spectrum server that provides not only a spectrum map but also the channel occupancy status, either *occupied* or *unoccupied*, with extra information. Using an extended spectrum map having the occupancy status, newly-joining WSDs can reduce the scope of spectrum sensing from all white space channels to a small number of channels that are believed to be unoccupied. As the return of the retrieved spectrum map, newly-joining WSDs could send the results of spectrum sensing to the spectrum server to assist it in building and dynamically updating the spectrum map with the occupancy status extracted from the results of spectrum sensing. Throughout this dissertation, the radio resource management (RRM) server represents the spectrum server that provides the extended spectrum map. To provide the spectrum map and to retrieve the results of spectrum sensing, the cooperation between WSDs and the RRM server is essential, and the implementation of that cooperation should involve all protocol layers of WSDs with the assistance of the RRM server. Thus, the cross-layer architecture is suitable for the dynamic spectrum management of white space channels.

As a result of cross-layer cooperation between WSDs and the RRM server, newly-joining WSDs using the extended spectrum map have the benefit of not only shortening the total spectrum sensing time but also causing less interference to neighboring WSAs by decreasing the possibility of miss detection. This chapter consists of the following sections: Section 2.2 describes the architecture of the dynamic spectrum map management, technical challenges, and solutions. Section 2.3 presents the extent to which the RRM server manages the extended spectrum map and the newly-joining WSDs exploit the extended spectrum map in a channel selection. Section 2.4 describes what we conduct in theoretical analysis.

## ***2.2 Dynamic Spectrum Map Architecture***

WSDs and the RRM server act as the main system components on the cross-layer architecture for the dynamic spectrum map management.

### **2.2.1 Network Reference Model**

Figure 3 depicts a network reference model of dynamic spectrum management that does not support WSDs operating in ad-hoc mode. Client-based white space portable devices (WSPDs) that may have multiple licensed and/or unlicensed wireless interfaces can associate with one or multiple infrastructure-based white space access points (WSAPs). Depending on the purpose of WSPDs, we can have three types of client-based WSPDs: Type 1, Type 2, and Type 3, as depicted in Figure 3. A Type 1 WSPD has licensed and unlicensed wireless interfaces while a Type 2 WSPD and a Type 3 WSPD have only white space interfaces. Thus, two heterogenous WSPDs cannot communicate as depicted in a stop mark of Figure 3. However, if neighboring WSAPs can support interoperation interfaces such as RRM - SU1, RRM - SU2, and RRM - SU3 in Figure 3, two WSAPs can indirectly communicate through the RRM server. The RRM server that retrieves the results of spectrum sensing from registered WSAPs builds a location-based spectrum map. As the best information

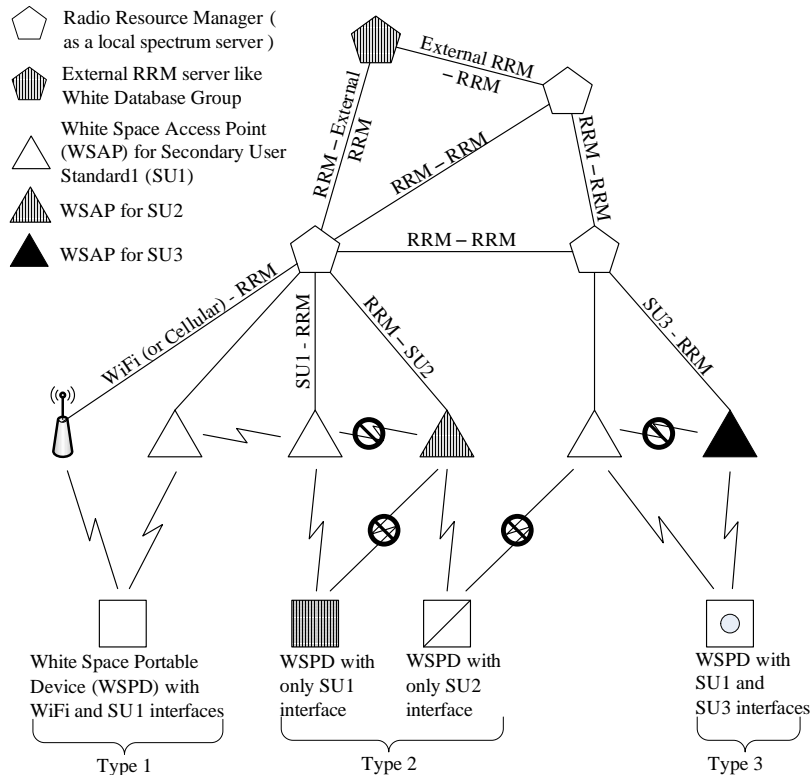


**Figure 3:** A network reference model for the spectrum map management.

providers, WSAPs can transmit their spectrum sensing results and other spectrum sensing results they collected from associated WSPDs. Meanwhile, newly-joining WSAPs retrieved the extended spectrum map of their current location conduct spectrum sensing on the channels marked as unoccupied according to the retrieved spectrum map. If they cannot find their operating channel, the RRM server can assist them to execute coexistence mechanisms such as transmit power control.

### 2.2.2 Structure of Spectrum Map

The RRM server builds the spectrum map of every location, and let denote  $T = \{t_1, t_2, \dots, t_N\}$  a list of white space channels when  $N$  is the total number of white space channels, and  $t_i$  contains channel information,  $\langle S, W, C, \gamma \rangle$ , of the  $i^{th}$  channel.  $S = \{0, 1\}$  indicates whether the  $i^{th}$  channel is occupied, one, or unoccupied, zero, and

$W$  presents what kind of standard or service the WSAP operating on  $i^{th}$  channel support. Since WSAPs should protect incumbent users and neighboring homogeneous and/or heterogeneous WSAPs, supporting the coexistence between diverse types of WSAPs and/or WSDs become a major issue. In this dissertation, we consider transmit power control (TPC) as the only coexistence mechanism.  $W$  of the  $i^{th}$  channel represents a service type of a WSAP operating on the  $i^{th}$  channel, and  $C$  of  $i^{th}$  channel indicates coexistence mechanisms permitted by the WSAP operating on the  $i^{th}$  channel.  $\gamma$  is a reliability index that indicates whether the channel information is reliable. The channel information of the spectrum map depending on the results of spectrum sensing becomes inaccurate due to the inaccuracy of spectrum sensing methods. Thus, WSAPs use  $\gamma$  as a barometer of the accuracy of the spectrum map. If  $\gamma$  is greater than a certain threshold, the WSAPs believe the given channel information as reliable. We present more details how to manage  $\gamma$  on Section 2.3.

Along with the retrieved spectrum map, WSAPs construct and update a list of backup channels,  $B$ , that are not currently occupied by neighboring WSAPs. They can select one of the backup channels included in  $B$  as their recovery channel when they meet inevitable cases like the unexpected appearance of incumbent users on their current operating channel. Thus, the  $S$  field of the channels must have zero, unoccupied. In the selection, the best channel is that its channel occupancy is unoccupied and is not considered as the backup channel of neighboring WSAPs.

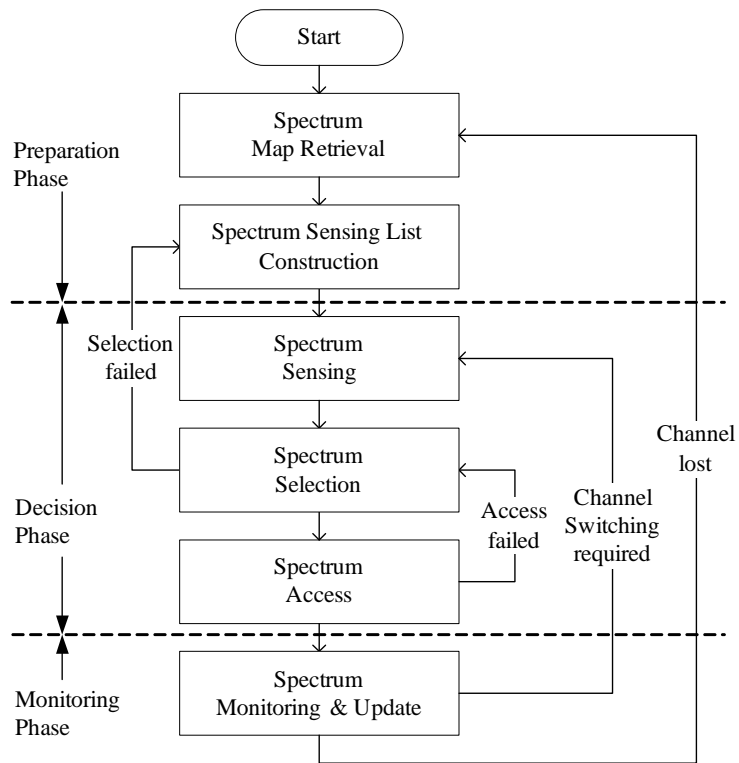
### 2.2.3 Spectrum Map Lifecycle

As described in the previous section, every geo-location has its own spectrum map that stays either in the learning stage or in the serving stage. When the RRM server creates the spectrum map of the new location, the new spectrum map starts from the learning stage. In the learning stage, the RRM server can figure out a usage pattern of white space channels through analyzing the results of spectrum sensing retrieved

from associated WSAPs operating at the new location, and then, the RRM server can update the occupancy status,  $S$ , of white space channels. After the successful first update, the spectrum map moves to the serving state, in which the RRM server can provide it to newly-joining WSAPs. Regardless of which state the spectrum map resides on, the RRM server continues to update the spectrum map with the retrieved spectrum sensing results from associated WSAPs. We have two approaches of retrieving the spectrum map, a centralized approach and a decentralized approach. The centralized approach is to retrieve the spectrum map from the RRM server while the decentralized approach is to retrieve it from the coexistence beacon frames of neighboring WSAP if they broadcast their spectrum map not only collected by themselves but also revised by their associated clients. Thus, the WSAPs retrieving those coexistence beacon frames can update their spectrum map, and they can provide their updated spectrum sensing results to the RRM server periodically and/or in a manual way. The spectrum sensing results merging the spectrum sensing results of neighboring WSAPs can contribute to increase in the accuracy of the spectrum map. However, if the accuracy of the spectrum map becomes less than a certain level, the spectrum map restarts from the learning stage.

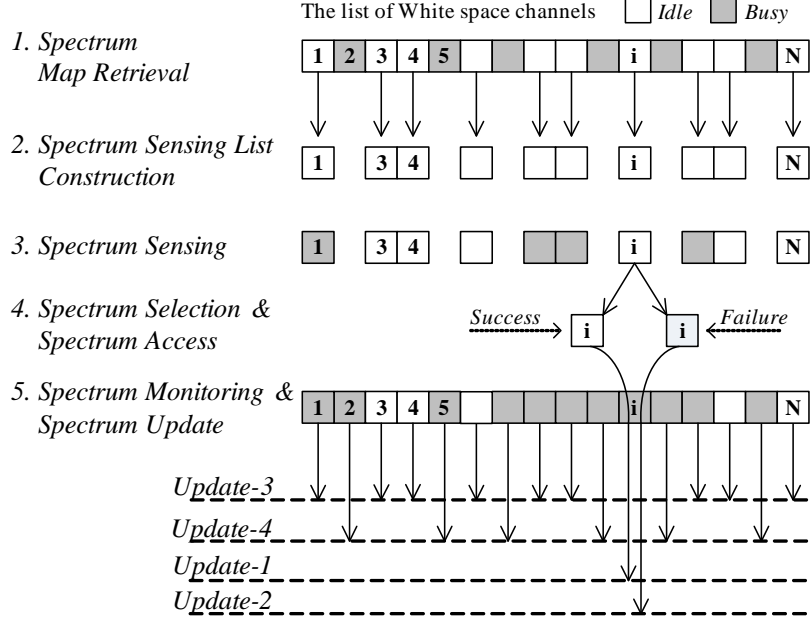
#### **2.2.4 General Flow of Spectrum Selection with Extended Spectrum Map**

Figure 4 illustrates the general flow of channel selection that consists of three operation phases: the preparation phase, the decision phase, and the monitoring phase. In the preparation phase, WSAPs retrieving the extended spectrum map build a list of white space channels targeted for spectrum sensing, and then, they execute spectrum sensing on channels included on the target list as the initial step of the decision phase. If the results of spectrum sensing indicate that one or more unoccupied channels exist, they select their operating channel among unoccupied channels, and if spectrum access on the selected channel is successful, they start their operation in the active



**Figure 4:** A general flow of a channel selection procedure with the extended spectrum map.

state on the channel. Otherwise, they conduct the second spectrum sensing on the channels excluded on the target list for the first spectrum sensing. In fact, since they can fail in spectrum access on their selected operating channel because of the inaccuracy of spectrum sensing, they continue to examine the next available channel among unoccupied ones until they succeed in spectrum access on the channel. However, if they failed in all spectrum access, they start from the preparation phase by redefining the target list for spectrum sensing. On the other hand, if they succeed in spectrum access on their selected operating channel, they immediately move to the monitoring phase and continue to monitor the wireless environments of their operating channel. In the monitoring phase, they must be ready to switch their operating channel if any incumbent users appear on the their operating channel or they suffer from performance degradation. Thus, activated WSAPs must periodically execute spectrum sensing on white space channels and thus, they can also provide the additional spectrum sensing results to the RRM server. Figure 5 illustrates the extent to which newly-joining WSAPs perform a channel selection. Updating the spectrum map with the results of spectrum sensing occurs on both the RRM server and the WSAPs. At the stage of building the target list of spectrum sensing, the WSAPs do not include occupied channels on the target list according to the spectrum map. For instance, they exclude the second channel and the other channels such as the fifth one on the target list as depicted in the second step of Figure 5. After spectrum sensing, they now recognize that the occupancy status of some channels on the target list does not change while the occupancy status of the others does. They update the spectrum map stored in their internal memory, and deliver the updated map to the RRM server whenever they send any message to the RRM server. While the WSAPs relies on their own spectrum sensing results mostly, the RRM server believes the retrieved spectrum sensing results partly since the accuracy of the results is proportional to the accuracy of spectrum sensing methods. Since all WSAPs can



**Figure 5:** An example of a channel selection procedure with the proposed framework

have different spectrum sensing methods, every spectrum sensing result can have a different accuracy. Thus, to handle this instability in the accuracy of the results of spectrum sensing, the RRM server manages the reliability index,  $\gamma$ , that numerically scales the reliability of the occupancy status information of every white space channel on the spectrum map. Since newly-joining WSAPs build a target list of unoccupied channels for spectrum sensing in compliance with the extended spectrum map, the results of spectrum sensing include the current occupancy status of the only channels on the target list. Thus, updating the occupancy status of every channel occurs asynchronously with the results of spectrum sensing retrieved from the diverse accuracy of spectrum sensing methods, and that is the reason why the RRM server maintains  $\gamma$  per channel. The RRM server has multiple ways of calculating the reliability index of a channel if it was included on the target list for spectrum sensing and was selected as the operating channel. As depicted in the bottom of Figure 5, if a newly-joining WSAP selected the  $i^{th}$  channel as its operating channel, calculating the accuracy index of the  $i^{th}$  channel has two ways, *Update-1* and *Update-2*, depending on success in

spectrum access. Otherwise, except the operating channel, for the channels included on the target list such as the first channel in Figure 5, the RRM server calculates the reliability index with *Update-3*. For the rest of channels excluded on the target list, the RRM server calculates the reliability index with *Update-4*. We describes more details of calculating the reliability index on Section 2.3.1.

### 2.2.5 Technical Challenges and Solutions

In the extension of the RRM server, maintaining a radio resource map that matches the real radio environments of white space channels for all locations will constitute multiple technical challenges. For one, the RRM server should have a large number of WSAPs that connect to the RRM server. Depending on the density of activated WSAPs at a location, the change in the channel occupancy status will occur either dynamically or slowly. If the RRM server has only a few WSAPs that inform the server about a change in the channel occupancy in a densely populated area, the RRM server cannot build a reliable radio resource map or the spectrum map that reflects the latest occupancy status of white space channels. Another challenge is that the spectrum map depends on the accuracy of spectrum sensing since all WSAPs determine the channel occupancy based on the results of spectrum sensing. As the accuracy of spectrum sensing methods increases, the accuracy of the spectrum map increases. However, the RRM server cannot always retrieve the results of spectrum sensing from WSAPs having a high accuracy of spectrum sensing methods since heterogeneous WSAPs have their different target applications and/or spectrum sensing methods. Thus, the RRM server obtains diverse spectrum sensing results that contain the rather different radio environment reports in the same location. In addition, although previous researches studied the evaluation metrics of spectrum sensing based on the characteristics of spectrum sensing techniques such as energy detection [47] and feature detection [19], they do not numerically scale the values of evaluation

metrics. For example, Table 2.2 of [30] presents a comparison of multiple spectrum sensing detectors, which summarizes the characteristics of multiple spectrum sensing detectors with three properties: *computational complexity*, *sensitivity to synchronization errors*, and *robustness to noise uncertainty*. They only define evaluation values to be relative comparison to each detector as *High* or *Moderate*, and thus, the RRM server cannot use the evaluation values to update the reliability index of channels on the spectrum map.

To resolve the first challenge, which requires a certain large number of registered WSAPs for a high reliability of the spectrum map, we need to invent a way of analyzing the real environments of white space channels with the assistance of only registered WSAPs until they reach the certain number. Thus, we suggest that the RRM server conducts the analysis of network environments of white space channels based on the retrieved spectrum sensing results from registered WSAPs. Through monitoring the change of the occupancy status of white space channels, the RRM server can estimate the density of WSAPs, and Section 2.3.1 describes the extent to which the RRM server does it. A keyword in the second and third challenges is heterogeneity in spectrum sensing methods, and based on this keyword, we can redefine two challenges into the following problems: the support of spectrum sharing between heterogeneous WSAPs and the accuracy management of the spectrum map. Since heterogeneous WSAPs cannot directly communicate or perform cooperative spectrum sharing mechanisms, we suggest that the RRM server acts as a main coordinator of supporting spectrum sharing and managing the accuracy of the spectrum map with the assistance of registered WSAPs.

### ***2.3 Dynamic Spectrum Map Management***

The RRM server can effectively lead the cross-layer spectrum map management by accommodating any type of WSAPs having different access standards as long as they

can communicate with the RRM server.

### 2.3.1 Spectrum Map Information Management

To support spectrum sharing between heterogeneous WSAPs and to maintain the accuracy of the spectrum map over a certain level, the RRM server should be able to analyze the real network environments of white space channels from the results of spectrum sensing of registered WSAPs. Thus, we suggest that the RRM server collects the following parameters:

- The number of WSAPs that made the report messages of the results of spectrum sensing.
- The number of occupied channels and detected neighboring WSAPs from each report message.
- The number of the activation and the de-activation of WSAPs.
- The duration time of one channel to be occupied with the start and end times.

Once the RRM server finishes the collection of the above parameters, the RRM server can estimate the following parameters:

- The average duration time of one channel to be occupied.
- The average number of occupied channels and detected neighboring WSAPs.
- The average inter-arrival time between two report messages.
- The average number of report messages during a pre-defined duration.

The RRM server will use  $R_{to}$  that represents the average inter-arrival time between two report messages to decide a wait time for a next report message. In addition, by simply dividing the average duration time by the average inter-arrival time, the RRM

server can estimate the average number of simultaneously activated WSAPs that connect to the RRM server ( $N_\alpha$ ). Meanwhile, using the average number of occupied channels and detected neighboring WSAPs, the RRM server can also estimate the average number of neighboring WSAPs,  $N_\beta$ . We define the ratio of the two numbers,  $\nu = N_\alpha / N_\beta$ , that represents the percentage of the total number of WSAPs that connect to the RRM server. Thus, for a high accuracy of spectrum sensing,  $\nu$  should approach 1. With a calculated  $\nu$ , we suppose the network environment of white space channel in the location of WSAPs.

Every location data in the RRM server include the reliability index,  $\gamma$ , that numerically scales the reliability of the occupancy status of all the channels in the spectrum map. Let  $\gamma_i$  denote  $\gamma$  of the  $i^{th}$  channel. When the RRM server creates the spectrum map of all the locations for the first time, it sets  $\gamma$  to zero for all channels. Now, the RRM server, which retrieves the spectrum sensing results of the  $i^{th}$  channel at a location for the first time, initializes  $\gamma_i$  with the probability of detection,  $P_d$ , of spectrum sensing methods of the WSAP that reported the results of spectrum sensing. After the server updates  $\gamma_i$  once, the server updates  $\gamma_i$  in two different situations: before and just after retrieving a report message. Until the server retrieves a next report message from any WSAP at location  $L$  within  $R_{to}$  time, which follows the exponential distribution as depicted in Figure 6(a), the server applies the exponential decrease in  $\gamma_i$  of location  $L$  with the following equation :

$$\gamma_i^x = \gamma_i^0(1 - e^{-\gamma_i^0 x}), i \in \{1, 2, 3, \dots, N\}, \quad (1)$$

where  $\gamma_i^0$  for the  $i^{th}$  channel is initialized with  $\gamma_s$  ( $= P_d$  of spectrum sensing methods used by the WSAP sent the first spectrum sensing results), and  $x$  is given by  $t/R_{to}$  when  $t$  is the duration time of the consecutive expirations of  $R_{to}$  timers. If the server fails to retrieve the expected report message and instead, retrieves a sign of the expiration of the  $R_{to}$  timer, the server restarts the new  $R_{to}$  timer after updating  $\gamma_i$  with (1). However, when the server retrieves the expected report message before

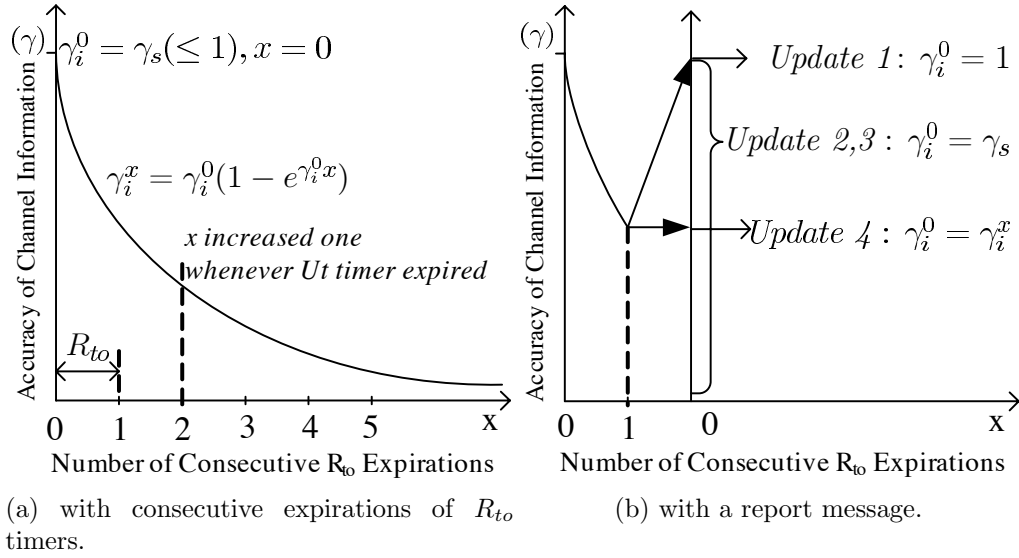


**Figure 6:** Calculation of the accuracy index of the  $i^{th}$  channel

the  $R_{to}$  timer is expired, the server has three choices of updating  $\gamma_i$ : no change as depicted in *Update 1* of Figure 6(b), initialization with a given  $\gamma_s (= P_d)$  as depicted in *Update 2/3*, or initialization with one as depicted in *Update 4*. The first choice is that the RRM server does not update  $\gamma_i$  if the retrieved report message does not have the spectrum sensing results of the  $i^{th}$  channel at location  $L$  since WSAPs did not execute spectrum sensing on the  $i^{th}$  channel. The second choice is that the RRM server updates  $\gamma_i$  with  $P_d$  of spectrum sensing methods used by the WSAP that sent the report message since the WSAP selected the  $i^{th}$  channel as its operating channel, but the WSAP failed in spectrum access on the channel. The second choice also includes the case of updating  $\gamma_i$  of all channels included in the results of spectrum sensing except the operating channel. The third choice is that the RRM server updates  $\gamma_i$  with one, which indicates that the accuracy of spectrum sensing of the WSAP is reliable since spectrum access on the  $i^{th}$  channel is successful. Since the update of  $\gamma$  occurs asynchronously,  $\gamma$  of all channels can differ at any time. Now, we have five ways of updating  $\gamma$  consisting of one way in a case of the expiration of the  $R_{to}$  timer and four ways, *Update-1/2/3/4*, in a case of the retrieval of the report message

---

**Algorithm 1** createSpectrumSensingList

---

```
1: procedure CREATESPECTRUMSENSINGLIST( $T, \chi, W_d$ )
2:    $ST[] \leftarrow 0$ 
3:   for  $i \leftarrow 1$  do  $length(T)$ 
4:     Begin
5:        $\{i, S, W, \gamma\} \leftarrow \{S, W, \gamma\}$  of  $t_i$  in  $T$ 
6:       If  $\gamma \geq \chi$  then
7:         Begin
8:           If  $S = 0$  then
9:              $ST.add(\{i, S, W, \gamma\})$ 
10:          else
11:            If  $W_d = W$  then
12:               $ST.add(\{i, S, W, \gamma\})$ 
13:          End
14:        else
15:          If  $W \neq PrimaryUsers$  then
16:             $ST.add(\{i, S, W, \gamma\})$ 
17:          End
18:        return  $ST$ 
19: end procedure
```

---

containing the results of spectrum sensing.

### 2.3.2 Spectrum Map Creation Procedure

Newly-joining WSAPs retrieved the spectrum map execute Algorithm 1 to build a target list of channels for spectrum sensing, and the algorithm uses  $\gamma_i$  to decide whether it includes the  $i^{th}$  channel, which the spectrum map marked as unoccupied, on the target list. If  $\gamma_i$  is greater than a certain threshold,  $\chi$ , the algorithm believes the occupancy status information,  $S$ , of the  $i^{th}$  channel on the spectrum map as reliable. Thus, the algorithm includes the  $i^{th}$  channel on the target list of spectrum sensing,  $ST$ , if  $S$  is zero. In addition, the algorithm also includes any occupied channels, but if the white space standard,  $W$ , of the newly-joining WSAPs is same as the standard,  $W_d$ , of neighboring WSAPs, which were previously detected by other WSAPs at the same location, operating on the  $i^{th}$  channel. This addition aims to collect the coexistence beacon frames of neighboring WSAPs and prepare the inevitable case of performing coexistence mechanisms because of the absence of

unoccupied channels. In this case, the WSAPs can obtain the coexistence mechanisms supported by neighboring WSAPs from the collected beacon frames. The previous operations as shown in lines 7-13 are only meaningful when  $\gamma$  is greater than or equal to  $\chi$ , and otherwise, the algorithm include the  $i^{th}$  channel on the target list only if the channel is not occupied by incumbent users as shown in lines 15-16.

### 2.3.3 Spectrum Sensing Result Retrieval

Against all channels on the target list,  $ST$ , the newly-joining WSAPs conduct spectrum sensing. Regardless of spectrum sensing methods, they expect the retrieval of the results of spectrum sensing,  $ST_s$ : a set of  $\langle ch, S', W, C \rangle$  of all channels included on  $ST$  with  $P_d$  of the spectrum sensing methods. The  $ch$  field of the  $j^{th}$  element on  $ST_s$  is the channel number of the white space channel that its spectrum sensing results are stored in the  $j^{th}$  element on  $ST_s$ ,  $S'$  indicates the occupancy status according to the results of spectrum sensing, and  $W$  indicates the existence of incumbent users operating on the channel or any detected neighboring WSAPs that support the same access standard of the newly-joining WSAPs. For instance, we can define  $W$  to have one of values,  $PU_1, PU_2, SU_1, SU_2, SU_3$ , and  $UN$ .  $PU_1$  represents TV broadcasting services,  $PU_2$  does wireless microphones, and  $SU_{1/2/3}$  represent different unlicensed white space standards while  $UN$  indicates that the access standard of detected neighboring WSAPs is unknown. If the WSAPs locate in a densely populated area, the WSAPs can detect multiple neighboring WSAPs operating on the same channel. If all detected neighboring WSAPs are homogenous, the WSAPs can build a list of neighboring WSAPs by interpreting retrieved coexistence beacon frames from neighboring WSAPs, and they exploit the list in the coexistence. For instance, depending on the coexistence capability of the WSAPs and the neighboring WSAPs, they can initiate the adjustment negotiation of their transmission power for coexistence. At that moment, the WSAPs can use  $W$  and  $C$  to decide whether the negotiation of

coexistence with the neighboring WSAPs is capable or not.

Let denote  $ST_s = \{r_1, r_2, \dots, r_u\}$ ,  $u = size(ST)$  the spectrum sensing results of channels on  $ST$ , in which  $r_j$  of the  $j^{th}$  element on  $ST_s$  has  $\langle ch, S', W, C \rangle$  of the  $r_j.ch^{th}$  channel with the following extra parameters:

- $A$ : a list of the detected neighboring WSAPs on the  $ch^{th}$  channel. This is optional.
- Backup channel flag ( $BF$ ): the flag that indicates whether the  $ch^{th}$  channel is a potential backup channel for neighboring WSAPs.

In addition, the WSAPs maintain the following list:

- $SS_s$  ( $SS_s \subseteq ST$ ): a list of channels included on  $ST_s$ , which their occupancy status according to  $ST_s$  is unoccupied, but its real occupancy status is occupied according to the spectrum map of neighboring WSAPs.

The WSAPs build  $SS_s$  with  $ST_s$  and  $T$  of the neighboring WSAPs extracted from the retrieved coexistence beacon frames.

### 2.3.4 Spectrum Selection Procedure

Based on the acquired spectrum sensing results, the newly-joining WSAPs perform the selection of their operating channel. Using  $ST_s$  and  $SS_s$ , the WSAPs execute Algorithm 2 for a channel selection, and the algorithm consists of two steps: the collection of unoccupied channels and the selection of the operating channel. In the first step, as shown in lines 3-8, the algorithm searches unoccupied channels on  $ST_s$ . Since the  $j$  index on  $ST$ ,  $ST_s$ , and  $SS_s$  no longer indicates a channel number, instead, we use the  $ch$  field to indicate a channel number. If the occupancy status of the  $r_j.ch^{th}$  channel,  $S'$ , is zero, the algorithm adds  $r_j$  to a list of candidate channels for the operating channel,  $CS$ . The algorithm executes the previous operation on all channels on  $ST_s$ , and then, the algorithm counts the size of  $CS$ . If the size is only

---

**Algorithm 2** channelSelection

---

```
1: procedure CHANNELSELECTION( $ST_s, SS_s, \gamma_s, \chi$ )
2:    $CS[] \leftarrow 0$ 
3:   for  $i \leftarrow 1$  do  $length(ST_s)$ 
4:     Begin
5:        $S' \leftarrow S'$  of  $r_i$  in  $ST_s$ 
6:       If  $S' = 0$  then
7:          $CS.add(r_i)$ 
8:       End
9:       If  $length(CS) = 1$  then
10:        return  $CS[1]$ 
11:      else
12:        Begin
13:          If  $length(CS) > 1$  then
14:            return  $selOneFromMultiples(CS, SS_s)$ 
15:          else
16:            If  $\gamma_s \geq \chi$  then
17:              # return Transmit Power Control
18:            else
19:              return null
20:            End
21:          return null
22:        end procedure

23: procedure SELONEFROMMULTIPLES( $CS, SS_s$ )
24:   for  $i \leftarrow 1$  do  $length(CS)$ 
25:     Begin
26:       If  $r_i.BF = 0$  and  $r_i.ch$  found on  $SS_s$  then
27:         return  $r_i.ch$ 
28:       End
29:    $j \leftarrow rand(length(CS))$ 
30:   return  $CS[j].ch$ 
31: end procedure
```

---

one, the algorithm declares the  $r_0.ch^{th}$  channel on  $CS$  as the operating channel of the WSAPs. However, as shown in lines 16-19, the size of  $CS$  can be a greater than one, which means that we have multiple unoccupied channels. In the second step, the algorithm calls the *selOneFromMultiples* function that selects one channel among multiple ones.

In *selOneFromMultiples*, the algorithm attempts to find any candidate channel that is also detected as the none of the backup channel for neighboring WSAPs. The previous operation can find one or more candidate channels, and in this case, the function simply chooses the first channel as shown in line 27. However, if all unoccupied channels are backup channels for neighboring WSAPs, the function randomly selects one of them as shown in line 29. The WSAPs perform spectrum access on the selected operating channel, and if it is successful, they moves to the active state that provides the broadband Internet access to their customers along with the update of the spectrum map. Otherwise, they repeat the new channel selection procedure, which executes Algorithm 2 and performs spectrum access on a selected operating channel, after deleting the current operating channel from  $ST_s$ . When the size of  $CS$  is less than one, which means that the algorithm failed to search any unoccupied channel, the algorithm can conduct TPC if  $\gamma_s(= P_d)$  is greater than  $\chi$  or the second spectrum sensing on channels that were not included on  $ST$  of the first spectrum sensing. However, If the WSAPs failed in the second spectrum sensing, they can finally decline their activation and wait until some channels are released. Instead of the presented function, our cross-layer architecture permits other spectrum decision algorithms to be adopted. For instance, an alternative decision algorithm could select the channel that its neighboring channels are also unoccupied with respect to interference.

---

**Algorithm 3** spectrumMapUpdate

---

```
1: procedure SPECTRUMMAPUPDATE( $Ind, ac, T, ST_s, P_d, \chi$ )
2:    $UT[] \leftarrow T$ 
3:   for  $j \leftarrow 1$  do  $length(ST_s)$ 
4:     Begin
5:        $c \leftarrow ch$  of  $r_j$  in  $ST_s$ 
6:       If  $c = ac$  then
7:         If  $ind = success$  then
8:            $UT[c].\gamma = 1$ 
9:         else
10:           $UT[c].\gamma = P_d$ 
11:        else
12:          Begin
13:             $UT[c].\gamma = P_d$ 
14:          End
15:          If ( $ind = success$ ) or ( $P_d \geq \chi$ ) then
16:             $UT[c].S = r_j.S', UT[c].W = r_j.W$ 
17:          End
18:    $T = UT;$ 
19: end procedure
```

---

### 2.3.5 Spectrum Map Update Procedure

Regardless of success or failure in spectrum access, the WSAPs execute Algorithm 3 that updates the retrieved spectrum map with the results of spectrum sensing. Along with  $T$  and  $ST_s$ , the algorithm obtains the values of  $ind$  and  $ac$  parameters as the results of the channel selection and spectrum access procedures.  $Ind$  represents the success or the failure of spectrum access, and  $ac$  represents a channel number of the operating channel. The algorithm updates  $\gamma$  of the channels on  $T$  with the above update rules as shown in lines 8-13, and the algorithm also updates the  $S$  and  $W$  fields of the channels on  $T$  if spectrum access was successful and the accuracy of spectrum sensing is greater than or equal to  $\chi$  as shown in lines 15-16. In fact, the algorithm running on the WSAPs do not execute lines 6-14 because the RRM server is only responsible for updating  $\gamma$ . However, as shown in lines 15-16, the algorithm in the WSAPs updates  $S$  and  $W$  fields, which are internally stored in the WSAPs, and the WSAPs use the updated local spectrum map in a further channel selection

or switching until they retrieve the newly-updated spectrum map from the RRM server or the new spectrum map of the new location as the WSAPs move to the new location.

While the WSAPs operate in the active state, they perform a periodic spectrum sensing on their operating channel and another channel regardless of the occupancy status of the other channel as the WiFi<sup>TM</sup> devices do. For example, 802.11 a/g devices scan 11 channels within the default 180 seconds (50 ms scan time on each channel every 16 seconds). The same approach on WSAPs can amend a corrupted spectrum map indicating a particular channel as occupied, but, the channel is in fact unoccupied. This amendment takes a little longer time than the case that the newly-joining WSAPs execute the second spectrum sensing against the channels excluded from the first spectrum sensing. Through a periodic scan, our proposed framework builds more reliable spectrum map as more spectrum sensing on the active state continues. To validate the retrieved spectrum map results, the RRM server will only accept the spectrum sensing results from registered WSAPs. However, this dissertation does not provide specific identification schemes, and that is beyond the scope of this dissertation. In addition, to resolve conflicts that can occur because of the diverse spectrum sensing results from heterogeneous WSAPs having different spectrum sensing methods, the RRM server prefers the most recent spectrum sensing results from the highest accuracy of spectrum sensing methods.

## ***2.4 Theoretical Analysis***

For theoretical analysis of the proposed cross-layer spectrum management framework, we adopt the  $M/G/m/m$  queueing model to define the  $M/B/N/N$  model as the evaluation model of dynamic spectrum management. In our  $M/B/N/N$  queueing model,  $M$  indicates that the activation of newly-joining WSAPs follows a Poisson distribution, and  $B$  indicates that a service duration time follows a bounded Pareto

**Table 2:** Parameters for evaluation of the cross-layer framework.

	Description	Unit	Value
$N$	number of channels		30, 50
$R$	default service radius	m	120, 180
$A$	unit area	$\pi m^2$	25
$m$	number of WSAPs per $A$		[0.025: 0.025: 0.05]
$\rho$	density of WSAPs ( $=m/A$ )		[0.001-0.02]
$\varphi$	duty cycle		1.0
$k$	min session duration time	sec	120
$p$	max session duration time	sec	2400
$E(T_d)$	mean session duration time	sec	333
$\mu$	session termination rate		10.8

distribution. With the  $N$  number of white space channels, the second  $N$  indicates that newly-joining WSAPs will fail to search unoccupied channels if the number of activated neighboring WSAPs is greater than  $N$ . In addition, Table 2 shows the values of parameters for evaluating dynamic spectrum management. We refer to the duration time of speech of 120 seconds as the minimum session duration time [12] and 12 times the duration time to watch web videos [20],  $192 \times 12$  seconds, as the maximum session duration time.

A newly-joining WSAP will send one report message to the RRM server since the WSAP should connect to the RRM server to retrieve the spectrum map. Since the average inter-arrival time of two consecutive report messages follows an exponential distribution, and its average is expressed as  $E(T_{arr}) = 1/\delta = 1/\rho\pi R^2$ , in which  $\delta$  is the average number of active WSAPs,  $\rho$  is the density of the WSAPs, and  $R$  is the average distance of service coverage. The average service duration time, which follows the bounded Pareto distribution, is expressed as

$$E(T_d) = \frac{k^\omega}{\left(1 - \left(\frac{k}{p}\right)^\omega\right)} \left(\frac{\varphi}{\omega - 1}\right) \left(\frac{1}{k^{\omega-1}} - \frac{1}{p^{\omega-1}}\right), \quad (2)$$

where  $\omega$  is 1.2 [49]. With  $k$  and  $p$  in Table 2, we have  $E(T_d) = 333$  seconds, and  $\mu = 10.8$  is calculated by  $\frac{3600}{E(T_d)}$ . We estimate the blocking probability,  $P_B(\delta, \mu)$ , and

the expected number of active WSAPs,  $E_N(\delta, \mu)$ , using the following equations:

$$P_B(\delta, \mu) = \frac{(\delta/\mu)^N/N!}{\sum_{n=0}^N (\delta/\mu)^n/n!}, E_N(\delta, \mu) = \left(\frac{\delta}{\mu}\right) (1 - P_B(\delta, \mu)). \quad (3)$$

In our analysis, instead of  $\delta$ ,  $N_\beta$  represents the average number of WSAPs, which is expressed as

$$N_\beta = \rho \varphi \pi R^2, \quad (4)$$

where  $\varphi$  is a duty cycle of WSAPs, and  $\rho = m/A$  is the density of WSAPs, in which  $m$  is the average number of WSAPs, and  $A$  is the unit area. This dissertation sets  $\varphi$  to one, which means one call per hour for every WSAP. Even though  $\varphi$  is one in theoretical analysis, the activities of spectrum allocation and release are based on one service life cycle. For example,  $E(T_d)$  in Table 2 refers to the mean time of one white space channel occupied by one WSAP. This indicates that one channel will be dynamically allocated to a newly-joining WSAP for  $E(T_d)$  seconds. When the WSAP terminates one session, it may turn into a dormant state, and it will release the channel. Using (2), (3), and (4), we can calculate the expected number of activated WSAPs,  $E(N_\beta)$ , with the following equation:

$$E(N_\beta) = E_N(N_\beta, 1/E(T_d)). \quad (5)$$

In fact, depending on the accuracy of spectrum sensing methods or the probability of detection ( $P_d$ ), newly-joining WSAPs have a possibility to fail to detect the  $E(N_\beta)$  number of neighboring WSAPs. Thus, we define  $E'(N_\beta)$ , which reflects the accuracy of spectrum sensing methods in the calculation of the expected number of detected neighboring WSAPs. We use the following equation to calculate  $E'(N_\beta)$ .

$$E'(N_\beta) = \sum_{i=0}^N \{(P_d)P_i + P_f(1 - P_i)\}, \quad (6)$$

where  $P_i$  is the probability of the occupancy of the  $i^{th}$  channel at any time, and  $P_f$  is the probability of false alarm. If WSAPs attempt to access all channels equally,  $P_i$

becomes equal to  $E(N_\beta)/N$ , and we have a simplified  $E'(N_\beta) = (P_d - P_f)E(N_\beta) + N \times P_f$ . However, spectrum sensing methods can make mistakes such as miss detection, which can detect unoccupied channels as occupied, and false alarm, which can detect occupied channels as unoccupied. Thus, we can calculate the number of channels misjudged by spectrum sensing with the following equation:

$$N_e = \sum_{i=0}^N \{(1 - P_f)P_i + P_f(1 - P_i)\}. \quad (7)$$

Using  $E'(N_\beta)$  and  $N_e$ , we define the spectrum sensing reliability index (SSRI), which is given by

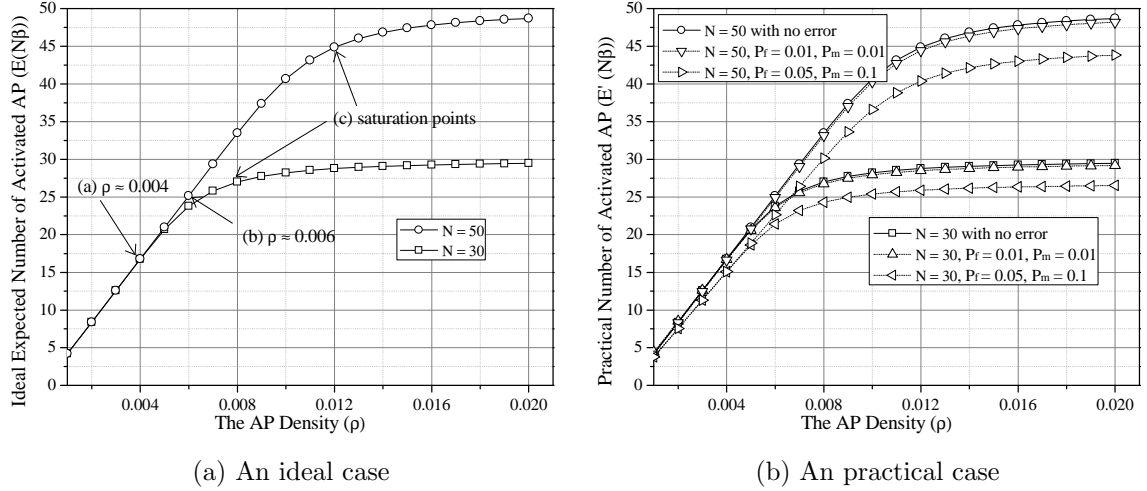
$$R_s = 1 - \frac{N_e}{N - E'(N_\beta)}, \quad (8)$$

and in theoretical analysis, we exploit  $R_s$  as  $\chi$  in the algorithms.

#### 2.4.1 Accuracy of Extended Spectrum Map

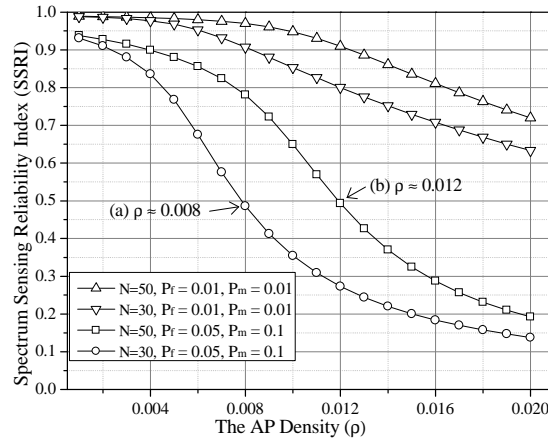
Since the performance of the proposed framework relies on the accuracy of the extended spectrum map, we studied the extend to which  $R_s$  is affected by the environments of white space and the accuracy of spectrum sensing methods. According to (8),  $P_d$ ,  $P_f$ ,  $\rho$ ,  $\mu$ , and  $E(N_\beta)$  are key parameters for evaluating the performance of  $R_s$ . Thus, we define previous five parameters as the evaluation parameters for  $R_s$  and the values of the parameters for the analysis of the performance of  $R_s$ . By applying the values to (8), we evaluate the extend to which our framework performs according to  $R_s$ .

Figure 7(a) illustrates the expected number of occupied channels for  $P_d = 1$  and  $P_f = 0$  when the density of WSAPs ( $\rho$ ), the average rate of service time ( $\mu$ ), and the expected number of simultaneously activated WSAP,  $E(N_\beta)$ , are known. With  $\mu = 10.8$  and  $N = 30$ , the expected number of occupied channels reaches around half of 30 when  $\rho$  reaches approximately 0.004. In the case of  $N = 50$ , the expected number reaches around half of 50 when  $\rho$  reaches approximately 0.006. Based on



(a) An ideal case

(b) An practical case



(c) Spectrum Sensing Reliability Index (SSRI)

**Figure 7:** The expected number of activated WSAPs with  $R = 120 m$  and errorless spectrum sensing methods when the density of WSAPs ( $\rho$ ), the average rate of the service time ( $\mu$ ), and the expected number of activated WSAPs,  $E(N_\beta)$ , are known (Subfigure (a)). vs. the expected number of activated WSAPs with erroneous spectrum sensing methods (Subfigure (b)). Subfigure (c) depicts the extent to which the Spectrum Sensing Reliability Index (SSRI) is affected with the known  $P_m$ ,  $P_f$ ,  $\rho$ ,  $\mu$  and  $E(N_\beta)$ .

these observations, we decide the range of the density of WSAPs for the theoretical analysis of spectrum sensing from 0.002 to 0.02, and we regard  $\rho$  beyond 0.008 as the situation in which most channels are occupied. For  $N = 50$ , we select the range of  $\rho$  from 0.010 to 0.018 in the analysis.

With given  $P_m (= 1 - P_d)$ ,  $P_f$ ,  $\rho$ ,  $\mu$ , and  $E(N_\beta)$ , we analyzed the extent to which they affect  $R_s$ . As depicted in Figure 7(b), with  $P_m = 0.01$  and  $P_f = 0.01$ , the difference of  $E(N_\beta)$  and  $E'(N_\beta)$  is about one channel. Even with a high probability such as  $P_m = 0.1$  and  $P_f = 0.05$ , the difference between  $E(N_\beta)$  and  $E'(N_\beta)$  is less than five for  $N = 30$  and  $N = 50$ . Thus, we disregard the impact of miss detection or false alarm in the calculation of the number of detected neighboring WSAPs in theoretical analysis. Figure 7(c) illustrates the calculated  $R_s$  with  $P_i = E(N_\beta)/N$ . With a low probability of miss detection and a low probability of false alarm,  $R_s$  has a bigger value than  $R_s$  with a high probability. For example, with  $P_m = 0.01$  and  $P_f = 0.01$ ,  $R_s$  is greater than 0.9 for both  $N = 30$  and  $N = 50$  while  $R_s$  for  $P_m = 0.1$  and  $P_f = 0.05$  is less than 0.8 and 0.5 for  $N = 30$  and  $N = 50$  respectively.  $R_s$  with  $\rho = 0.008$ , which approaches 0.5 for  $N = 30$ , approaches 0.5 for  $N = 50$  with  $\rho = 0.012$ . According to the observation of label (c) in Figure 7(a),  $E(N_\beta)$  reaches almost  $N = 30$  and 50 at  $\rho = 0.008$  and 0.012 respectively. Thus, the analysis confirms that the RRM server can provide a reliable spectrum map when  $R_s$  is greater than 0.4, and we can set the threshold,  $\chi$ , used in Algorithm 1/2/3, for  $\gamma$  to 0.4. We do not evaluate the performance of the proposed framework with  $R_s \leq 0.4$ .

### 2.4.2 Probability of Success in Channel Search

With a typical spectrum sensing approach, we can estimate the probability of success in a channel search with the following equation:

$$\begin{aligned}
P_s &= P_d \left\{ \sum_{k=1}^N \sum_{c=1}^{\frac{N!}{k!(N-k)!}} \left\{ \prod_{i \in S_c^k} (1 - P_i) \prod_{i \in S^n - S_c^k} P_i \right\} \right\} \\
&= P_d \left( 1 - \left\{ \sum_{k=0}^1 \sum_{c=1}^1 \left\{ \prod_{i \in S_c^0} (1 - P_i) \prod_{i \in S^n - S_c^0} P_i \right\} \right\} \right) \\
&= P_d \left( 1 - \prod_{i \in S^n} P_i \right),
\end{aligned} \tag{9}$$

where  $S^n$  is a set of channels from 1 to  $N$ , and  $S_c^k$  is a set of  $k$  chosen channels that are marked as unoccupied as the  $c^{th}$  combination among all possible ways of choosing  $k$  channels from  $N$  total channels.  $P_s$  is zero when  $E(N_\beta)$  is greater than or equal to  $N$ , and channel reusability, which can accommodate more WSAPs than the  $E(N_\beta)$  number of WSAPs at one location, is not studied but in Chapter 5. However, with the extended spectrum map, we have two steps of spectrum sensing: the first spectrum sensing and the second spectrum sensing. Thus, we cannot use (9) to calculate the probability of success in a channel search with the extended spectrum map. Let  $P_i(t)$  denote the probability of the occupancy of the  $i^{th}$  channel at time  $t$ , which we refer to as occupied or unoccupied according to the results of spectrum sensing. Thus, at any time  $t$ ,  $P_i(t)$  for occupied channel should be  $P_d$  while  $P_i(t)$  for unoccupied channels should be  $P_f$ . In addition, we can calculate the number of channels on  $ST$  by  $N - E(N_\beta)$ . Between two report messages, over a  $\Delta t$  period, we can estimate the number of the newly-activated neighboring WSAPs by  $\psi(\Delta t) = \Delta t / E(I_\beta)$ , where  $E(I_\beta) (= 1 / N_\beta)$  is the inter-arrival time of the two report messages with  $N_\beta$ . These activations can occur without the notification of the RRM server. In other words, the newly-joining WSAPs that are not registered to the RRM server probably occupy  $\psi(\Delta t)$  channels among  $N - E(N_\beta)$  unused channels. This

unawareness of the activation of unregistered WSAPs can be possible since old-style WSAPs prefer a conventional spectrum map server instead of the RRM server. Now, after  $\Delta t$ , we can estimate  $P_i(t + \Delta t)$  with the following equation.

$$P_i(t + \Delta t) = P_i(t) + \left( \frac{\psi(\Delta t)}{N - E(N_\beta)} \right), E(N_\beta) < N. \quad (10)$$

In (10), we are not concerned with  $E(N_\beta) \geq N$ . In fact, this dissertation assumes that the WSAPs can find at least one or more unoccupied channels after performing spectrum sensing, which means that  $E(N_\beta)$  is always less than  $N$ . Otherwise, as introduced in Chapter 5, newly-joining WSAPs should conduct any spectrum sharing methods. Now, using (9) and (10), we estimate the probability of success in finding unoccupied channels in the first spectrum sensing with the following equation:

$$P_{fs}(t, \Delta t) = P'_d \left( \frac{R_s(t)}{e^{\phi \Delta t}} \right) \left( 1 - \prod_{i \in ST} P_i(t + \Delta t) \right) \quad (11)$$

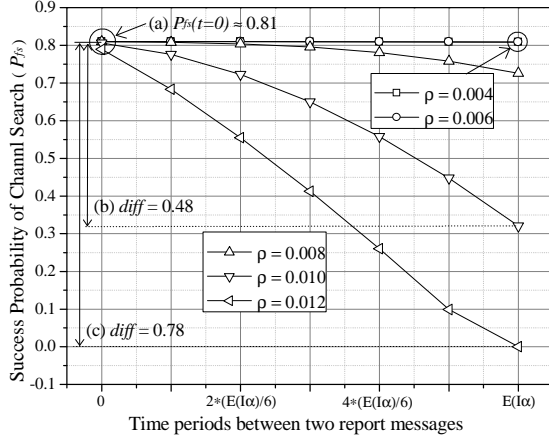
$$\phi = \frac{E(I_\alpha) - E(I_\beta)}{E(I_\alpha)}, i \in ST,$$

where  $e^{\phi \Delta t}$  aims to reflect the degradation of  $R_s$ ,  $P'_d$  is the probability of detection of WSAPs that prefer spectrum sensing with the extended spectrum map, and  $R_s(t)$  is the  $R_s$  of the WSAP sending the report message at time  $t$ . With  $1/N_\alpha$ , we estimate  $E(I_\alpha)$ , which is the inter-arrival time of two report messages with  $N_\alpha$ , which is the average number of WSAPs that connect to the RRM server. In our analysis, we estimate  $N_\alpha$  with a given  $\nu$  ( $\nu = N_\alpha / N_\beta$ ). In addition,  $\phi$  is a scale parameter that controls a degradation range. For example, as  $\phi$  approaches zero,  $R_s(t)/e^{\phi \Delta t}$  decreases more smoothly compared to the case of  $\phi$  approaching one. As registered WSAPs increases,  $E(I_\alpha)$  approaches  $E(I_\beta)$ , and thus,  $\phi$  approaches zero. This coincides in the fact that the RRM server can trust more the spectrum map with a high  $\nu$  than the spectrum map with a low  $\nu$ . With a low  $\nu$ , since  $E(I_\alpha)$  becomes greater than  $E(I_\beta)$ ,  $\phi$  approaches one resulting in a bigger decrease of  $R_s(t)/e^{\phi \Delta t}$ .

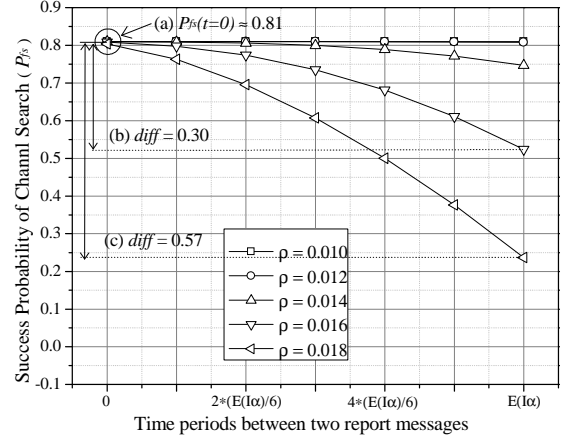
While neighboring WSAPs that do not enroll in the RRM server occupy  $\psi(\Delta t)$  channels among  $N - E(N_\beta)$  unused channels, some activated WSAPs will release their

operating channel during the  $\Delta t$  time, which will increase the probability of success in the second spectrum sensing. In fact, we expect that  $\frac{\Delta t \mu}{3600}$  channels will be released during the  $\Delta t$  time. However, if  $\frac{\Delta t \mu}{3600}$  is greater than  $\psi(\Delta t)$ , newly-joining WSAPs will occupy the channels released during the  $\Delta t$  time, resulting in no change between  $P_i(t + \Delta t)$  and  $P_i(t)$ . While  $P_{fs}(t, \Delta t)$  represents the expected probability of success in the first spectrum sensing,  $P_{fs}(t)$  represents the highest probability of success in spectrum sensing if all the channels on  $ST$  remain in the current occupancy status, occupied.

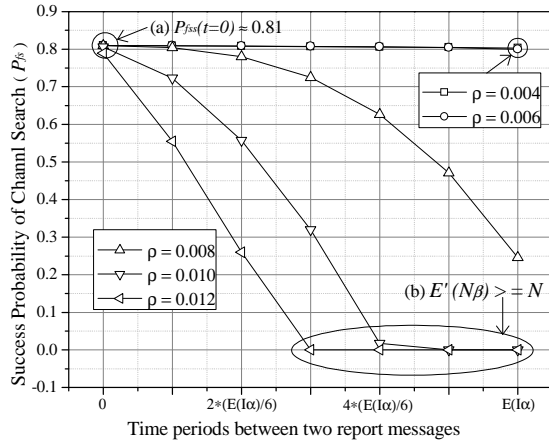
Figure 8(a) and (b) with  $\nu = 0.8$  and  $R_s = 0.9$  illustrate that the probability of success in a channel search approaches 80% when  $\rho$  is less than or equal to 0.008 for  $N = 30$  and 0.014 for  $N = 50$ . Thus, we can have a high probability of success in a channel search in the first spectrum sensing until  $\rho$  becomes greater than the saturation point. In addition, with a low  $R_s$  such as  $\nu = 0.4$  under a low population such as  $\rho = 0.004$  or 0.006, WSAPs with the extended spectrum map can still perform around 80% success in a channel search in the first spectrum sensing. However, the RRM server, which fails to receive the spectrum sensing results of WSAPs within a certain time such as  $R_{to}$ , cannot properly update  $\gamma$ , resulting in a low chance of success in the first spectrum sensing with a rather unreliable spectrum map. When the RRM server has the expiration of the  $R_{to}$  ( $= E(I_\alpha)$ ) timer, the RRM server restarts the timer while  $\gamma$  of all channels in the spectrum map exponentially decreases. Figure 8(d) illustrates the extent to which  $P_{fs}$  decreases if the RRM server fails in retrieving the next expected report message. Nevertheless, the decrease in  $P_{fs}$  with a low  $\rho$  such as 0.002 or 0.004, is insignificant as depicted in label (a) of Figure 8(d) even after the RRM server has the third consecutive expiration of an  $R_{to}$  timer. However, we can observe the drastic decrease in  $P_{fs}$  with a high  $\rho$ . For instance, as depicted in label (c) of Figure 8(d),  $P_{fs}$  with a high  $\rho$  is already less than or equal to 0.3 at the first timer expiration.



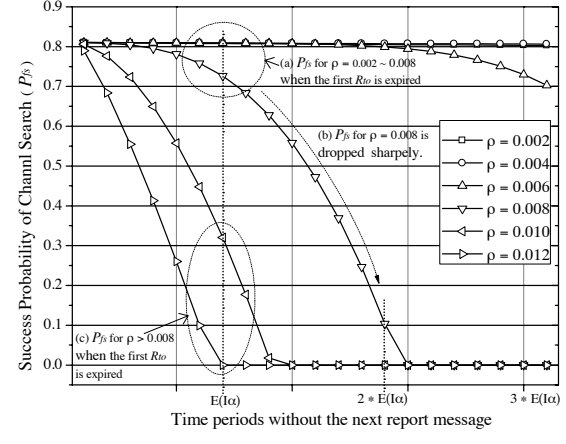
(a)  $P_{fs}(t)$  with  $\nu = 0.8$  for  $N = 30$ .



(b)  $P_{fs}(t)$  with  $\nu = 0.8$  for  $N = 50$ .



(c)  $P_{fs}(t)$  with  $\nu = 0.4$  for  $N = 30$ .



(d)  $P_{fs}(t)$  for  $R_{to}$  expirations with  $\nu = 0.8$  for  $N = 30$ .

**Figure 8:** With the spectrum sensing reliability index,  $R_s = 0.9$ , the analysis results of the expected probability of success in the first spectrum sensing,  $P_{fs}(t)$ , with  $R = 120m$  and  $N = 30$  in (a) and (c) are presented. In subfigure (b), for  $N = 50$ ,  $\rho$  varies from 0.010 to 0.018. Subfigure (a) and (b) illustrate that a higher  $\rho$  contributes to the drastic drop of the probability of success, which we observe in labels (c) of subfigure (a) and (b). In subfigure (c), with a lower  $\nu = 0.4$ ,  $P_{fs}$  still approaches 80% for  $\rho = 0.004$  and  $\rho = 0.006$ . A subfigure (d) depicts the extent to which  $P_{fs}$  will decrease if we have consecutive expiration of  $R_{to}$  timers

When the WSAP fails in the first spectrum sensing, the WSAP launches the second spectrum sensing against either all channels or channels that were not included on  $ST$ . This dissertation assumes that on the second spectrum sensing, the WSAP excludes the channels included on  $ST$  of the first spectrum sensing. During the  $\Delta t$  time,  $P'_i(t + \Delta t)$ ,  $i \in S^n - ST$ , for occupied channels is expressed as

$$P'_i(t + \Delta t) = P_i(t) + \left( \frac{\Delta t \mu}{3600} \right) \frac{1}{E(N_\beta)}, E(N_\beta) > \frac{\Delta t \mu}{3600}. \quad (12)$$

Using (12), the probability of success in a channel search on the second spectrum sensing,  $P_{ss}$ , is expressed as

$$P_{ss}(t, \Delta t) = (1 - P'_m) \left( \frac{R_s(t)}{e^{\phi \Delta t}} \right) \left( 1 - \prod_{i \in S^n - ST} P'_i(t + \Delta t) \right). \quad (13)$$

As shown in Table 3 and 4, as  $\rho$  increases,  $P_{ss}$  increases until  $\rho$  meets the saturation point, for example, 0.008. After the saturation point, since further new arrivals should be denied because of the absence of unoccupied channels, the second spectrum sensing could have a similar performance. With a longer service distance,  $P_{ss}$  of WSAPs, which experienced the failure of the first spectrum sensing at early time compared to the case of WSAPs with a shorter service distance, increases. The previous observation reveals that the proposed framework can provide stable and predictable performance as long as we have proper operation parameters such as  $\rho$  and  $\nu$  for every location through the learning stage of the spectrum map for all locations. In addition, while the enhanced accuracy of spectrum sensing methods can contribute to the improvement of the accuracy of the spectrum map, the proposed framework can also contribute to the improvement as more WSAPs register to the RRM server. The analysis demonstrates that the RRM server requires over 40% of all WSAPs that register to the server and provide their spectrum sensing results.

### 2.4.3 Average Spectrum Sensing Time

We estimate the expected total spectrum sensing time with a conventional spectrum sensing approach, which scans all white space channels, with the following equation:

**Table 3:** The expected success probability of the second spectrum sensing,  $P_{ss}(t)$ , with  $R_s = 0.9$ ,  $R = 120 m$ , and  $N = 30$ .

<i>TimePeriod</i>	$\rho = 0.002$	0.004	0.006	0.008	0.010	0.012
0	0.475	0.671	0.743	0.762	0.768	0.770
$5 \times (E(I_\alpha)/6)$	0.485	0.679	0.749	0.767	0.772	0.775

**Table 4:** The expected success probability of the second spectrum sensing,  $P_{ss}(t)$ , with  $R_s = 0.9$ ,  $R = 180 m$ , and  $N = 30$ .

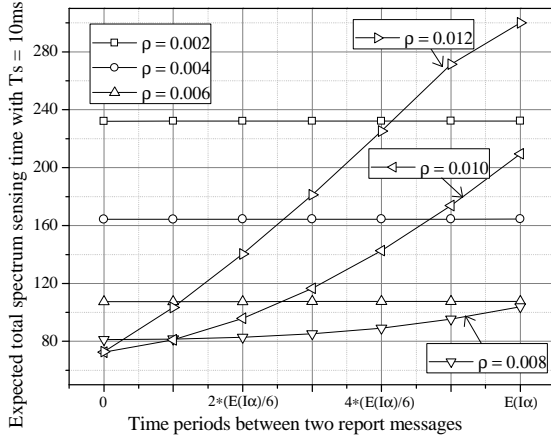
<i>TimePeriod</i>	$\rho = 0.002$	0.004	0.006	0.008	0.010	0.012
0	0.698	0.766	0.771	0.773	0.774	0.774
$5 \times (E(I_\alpha)/6)$	0.705	0.770	0.775	0.777	0.778	0.778

$E(T_{ss}) = N \times t_s$ , where  $t_s$  is a time that takes for sensing one channel. We calculate the expected total spectrum sensing time with the proposed dynamic spectrum management,  $E(T_{ss})(t)$  in (14), as the sum of the expected time in the first spectrum sensing and the expected time of the second spectrum sensing.

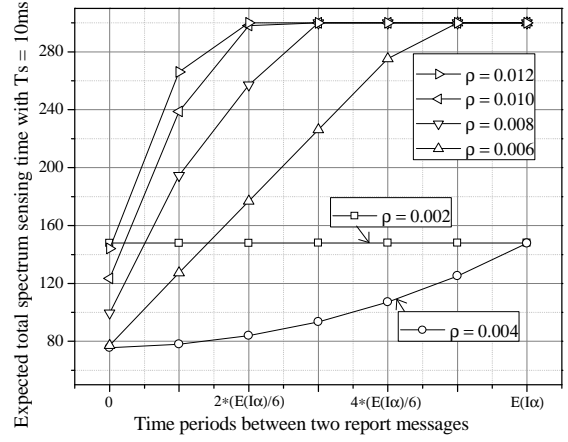
$$E(T_{ss})(t) = (N - E(N_\beta)) t_s + (1 - P_{fs}(t)) E(N_\beta) t_s. \quad (14)$$

In the first spectrum sensing, the number of channels on  $ST$  is  $N - E(N_\beta)$ , and thus, the average time in the first spectrum sensing is calculated by  $(N - E(N_\beta)) t_s$ . Since the number of channels for the second spectrum sensing is  $E(N_\beta)$ , the average time in the second spectrum sensing is calculated by  $E(N_\beta) t_s$ .

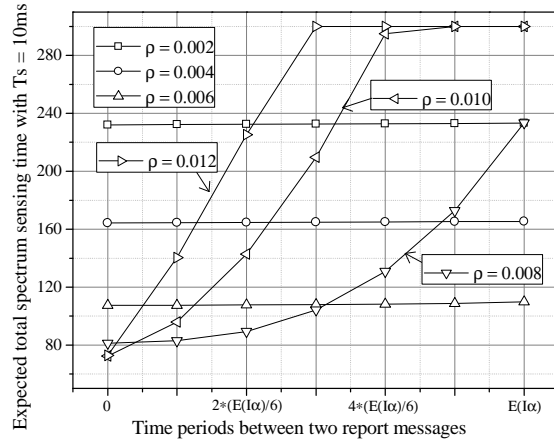
Figure 9(a) and (b) illustrate the expected spectrum sensing time with  $\nu = 8.0$  and  $t_s = 10$  ms [15]. In contrast to 300 ms ( $= 10$  ms  $\times$  30 channels) of the conventional approach, with the extended spectrum map, the expected spectrum sensing time,  $E(T_{ss})(t)$ , is below 300 ms. In addition, as  $\rho$  approaches the saturation point,  $E(T_{ss})(t)$  decreases. For example, in Figure 9(a),  $E(T_{ss})(t)$ , which does not change until  $\rho$  approaches 0.008, decreases after  $\rho$  becomes greater than 0.008, which we can also observe in Figure 9(b). In addition,  $E(T_{ss})(t)$  with  $\nu = 0.4$  is below 200 ms, as depicted in Figure 9(c), with  $\rho = 0.002$  and  $\rho = 0.006$ . However, from  $\rho = 0.008$ , we can observe increase in  $E(T_{ss})(t)$  since a low  $\nu$  results in a low  $P_{fs}$  because the



(a)  $E(T_{ss})(t)$  with  $\nu = 0.8$  for  $R = 120$  m.



(b)  $E(T_{ss})(t)$  with  $\nu = 0.8$  for  $R = 180$  m.



(c)  $E(T_{ss})(t)$  with  $\nu = 0.4$  for  $R = 120$  m.

**Figure 9:** With the spectrum sensing reliability index,  $R_s = 0.9$ , the analysis results of the expected spectrum sensing time,  $E(T_{ss})(t)$ , with  $N = 30$  are presented. Subfigure (b) is the analysis results of  $E(T_{ss})(t)$  for  $R = 180$  m. Three subfigures depict that  $E(T_{ss})(t)$  rather steeply increases when  $\rho$  becomes greater than a saturation point. In subfigure (c), with a lower  $\nu = 0.4$ ,  $E(T_{ss})(t)$  still could be reduced significantly when  $\rho$  is less than or equal to 0.008.

expiration of the  $R_{to}$  timer can highly occur. The previous observations confirm that increase in the number of WSAPs supporting the extended spectrum map can shorten the total spectrum sensing time.

#### 2.4.4 Burden of Updating the Spectrum Map

We expect that the extended spectrum map requires only dozen bytes to be added to a message that WSAPs use to connect to a conventional spectrum map server when they start their operation. The added bytes will be used to indicate the occupancy status of all white space channels, and our proposed framework requires one more connection to the RRM server compared to a conventional approach. The conventional retrieval of the spectrum map occurs once when WSAPs start their service while our proposal requires two retrievals when WSAPs connects and disconnects to the RRM server. Let denote  $bw$  the number of bits in the message for the conventional retrieval of the spectrum map, and then, we can calculate the total bandwidth of retrieving the spectrum map with  $bw \times \rho$ . Our scheme requires  $2 \times \rho \times (bw + (N \times size(S, W, C, \gamma)))$ , where  $N$  is the maximum number of available white space channels,  $size(S, W, C, \gamma)$  is the number of bits for storing channel information for one white space channel, and 2 means that our scheme updates two times related to the activation and the de-activation of WSAPs. In addition, we expect that computational complexity is ignorable since channel information is simply updated using Algorithm 3, and updating the accuracy index,  $\gamma$ , is also not complicated.

### 2.5 Conclusions

In this chapter, we propose the cross-layer spectrum map management framework that can enhance the efficiency of spectrum sensing with the cooperation between white space access points (WSAPs) and the extended spectrum map server, the RRM server. The RRM server that manages a location-based spectrum map can assist WSAPs to shorten the total spectrum sensing time. Since the accuracy of the spectrum

map depends on the accuracy of spectrum sensing methods, the RRM server should acquire the assistance from a certain number of WSAPs that provide their spectrum sensing results of a higher accuracy of spectrum sensing methods. Theoretical analysis demonstrates that for the high accuracy of the spectrum map, the number of WSAPs supporting the proposed framework should be greater than 0.4 times the total number of all WSAPs including registered and unregistered to the RRM server. In addition, the theoretical analysis confirms that the expected total spectrum sensing time can be saved up to 50% as the number of registered WSAPs increases.

The proposed framework assists not only newly-joining WSAPs to improve their starting operation with the shortened total spectrum sensing time, but also already-activated WSAPs to shorten their intermediate spectrum sensing time in the active state. Upon detecting unexpected appearance of incumbent users, all WSAPs perform spectrum sensing while their session is alive. For instance, in [15], WSAPs perform spectrum sensing at least once every 60 seconds, and within two seconds, WSAs is to vacate their operating channel if they detect the appearance of any incumbent users on their operating channel. To minimize the burden of spectrum sensing in every 60 seconds, we expect that WSAPs will scan their operating channel and one more channel, instead of all channels, at each periodic scan as the WiFi<sup>TM</sup> devices do. WSPAs can use the saved time to transmit more user data as a result of decrease in the number of channels for spectrum sensing. With the assistance of the proposed framework, activated WSAPs can recognize the appearance of incumbent users if neighboring WSAPs informed the RRM server of the existence of primary users. This cooperation between WSAPs and the RRM server can contribute to the early vacancies from white space channels. Based on these observations, we expect that the proposed cross-layer framework that integrates WSAPs and the RRM server can enhance the dynamic spectrum map management through the life-cycle of the spectrum map.

This chapter introduces the extent to which Dynamic Host Configuration Protocol (DHCP) operations can assist WSDs to retrieve the spectrum map earlier than the usual way that they retrieve from the spectrum map server after the DHCP operations.

### ***3.1 Motivation of Fast Retrieval of the Spectrum Map***

For the retrieval of the spectrum map, newly-joining WSDs need the Internet connection, which means they have to have the previously connected wireless networks like cellular or WiFi<sup>TM</sup> networks. Thus, after they set up the Internet connection over cellular or WiFi<sup>TM</sup> networks, they connect to the spectrum map or RRM server for the retrieval of the spectrum map of a current location. Using either Global Positioning System (GPS) or network-based location mechanisms, they can determine their current location. In the sequential occurrence of the setup of cellular or WiFi<sup>TM</sup> networks and the retrieval of the spectrum map as depicted in Figure 10, they have a possibility of having the second time of the Dynamic Host Configuration Protocol (DHCP) operations for the IP assignment as depicted in step 9 of Figure 10. The main idea of this chapter is to shorten the interval time between two DHCP operations by embedding the retrieval of spectrum map during the first DHCP operations. For the fast retrieval of spectrum map, we propose extending the DHCP protocol that is able to deliver to the DHCP clients, WSDs, the spectrum map during the setup of cellular

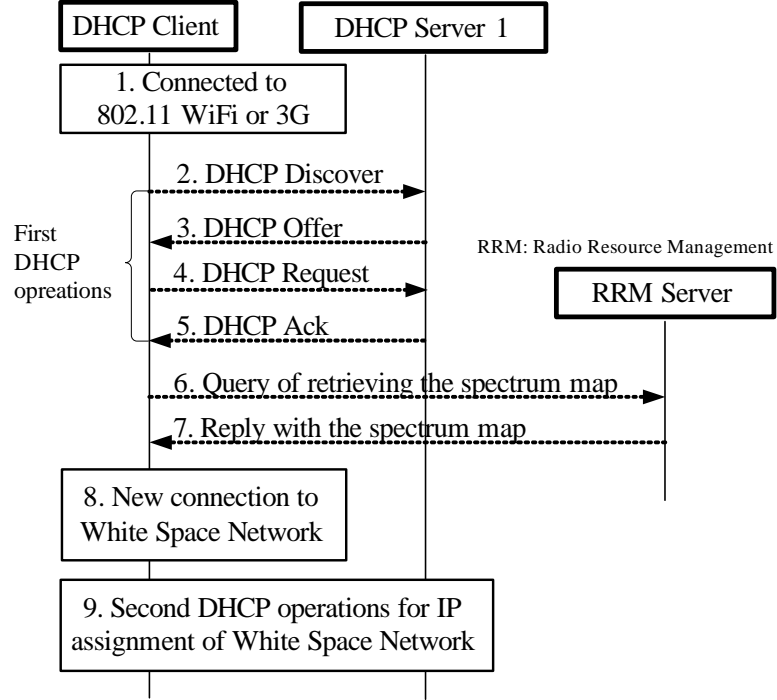


**Figure 10:** The general call flow of the handover from WiFi<sup>TM</sup> to White Space Network

or WiFi<sup>TM</sup> networks. During the DHCP operations for the IP assignment of cellular or WiFi<sup>TM</sup> networks, the DHCP server connects to the RRM servers to retrieve the spectrum map and includes the retrieved spectrum map inside the DHCP messages that will be delivered to the DHCP clients. In our proposal, we also extend the spectrum map providing not only the channel-occupancy information but also the list of available access networks. Similarly to the approach of [44], the extended spectrum map can assist the DHCP clients to select the least traffic load of an access network among multiple networks. The enhanced DHCP server can provide its location information if the DHCP clients can not determine or offer their location as [1] suggests. In addition, as [27] proposes, the enhanced DHCP server can dynamically manipulate the list in accordance with preferable access networks of the DHCP clients. However, in this chapter, we present the modified setup procedures for the fast retrieval of the spectrum map of open white space channels and define the new options that can be included in DHCP messages and used for the fast retrieval of the spectrum map.

The rest of this chapter consists of the following sections: Section 3.2 describes the conventional approach of extending the role of the DHCP server and presents our approach to shorten the total setup time for the retrieval of the spectrum map. Section 3.3 describes the analytical model for the performance evaluation of our proposal, and Section 3.4 presents the analysis results. Section 3.5 describes the conclusions of this chapter.

## **3.2 *Extension of the DHCP***

At [1], the DHCP server only provides its location information not the spectrum map to the DHCP clients although this provision can be useful to the clients when they can not determine their location under certain circumstances such as inside buildings. In other study [4] [9] [14], the DHCP servers are still limited to assist the session continuity, mobility management of mobile devices, or the awareness of secured network location. Our approach is to allow the DHCP server to assist the retrieval of the spectrum map directly from the RRM servers. Thus, compared to previous research, in our approach, the DHCP server acts as the main controller for assisting the DHCP clients to retrieve the spectrum map in advance. We have two approaches on the implementation of our proposal: aggressive and cautious approaches.

### **3.2.1 Aggressive Approach**

According to the message sequence of the typical DHCP operation, since a DHCP Discover is usually the first message, the clients can include a new DHCP field option (*ANMReqInd*) that indicates their desire to retrieve a list of connectable access networks (ANM:Access Network Map) in a current location. For this operation, we define an additional DHCP field for location information (*LocInfo*) in the DHCP Discover message, and the DHCP clients include their location information in the *LocInfo* option. However, when the DHCP clients cannot offer their location information, the DHCP clients include the only *ANMReqInd* in the DHCP Discover, and in this case,

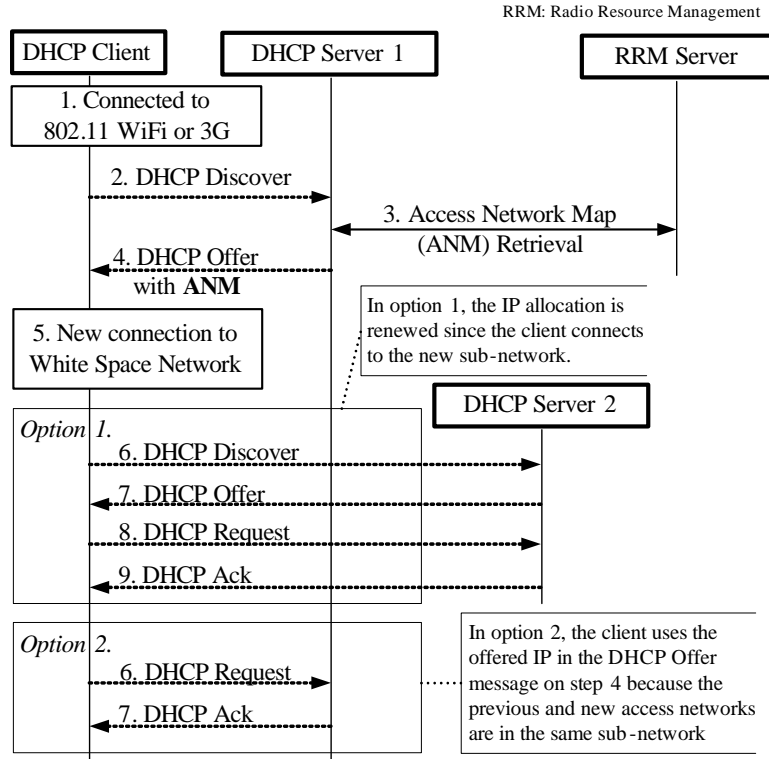


**Figure 11:** The new call flow of the DHCP in the aggressive approach.

the DHCP server uses their location information as the location information of the DHCP clients. Figure 11 depicts the new call flow of the retrieval of the spectrum map with the aggressive approach. The DHCP client that connects to any popular access network such as WiFi<sup>TM</sup> networks includes the *ANMReqInd* option and the *LocInfo* option in the DHCP Discover message as depicted in step 1 of Figure 11, and the DHCP server 1 retrieves a list of connectable access networks, *ANM*, from the RRM server using the *LocInfo* option retrieved from the DHCP Discover message or its own location information. The DHCP server 1 sends the DHCP Offer message with the retrieved *ANM* to the DHCP client, and then, the client performs the handover to the new access network, white space network (WSN), as depicted in step 5 of Figure 11. Afterward, the client has two options: restarting the IP assignment with the new DHCP server, the DHCP server 2, as depicted in steps 6-9 of Option 1, or continuing the remaining procedures with the IP address offered by the DHCP

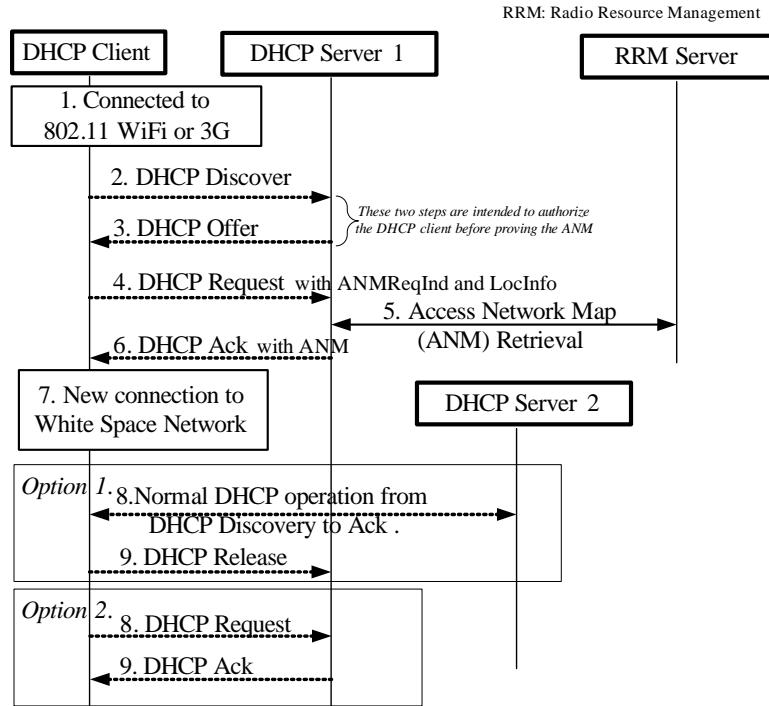


**Figure 12:** The new call flow of the DHCP in the cautious approach.

server 1 as depicted in steps 6-7 of Option 2. However, the DHCP client can have more options like it still remains in the current access network or uses the retrieved ANM later for the mobility management as it moves to neighboring cells.

### 3.2.2 Cautious Approach

Instead of the DHCP Discover message, as depicted in step 4 of Figure 12, the DHCP clients can deliver the *ANMReqInd* in a DHCP Request message. The DHCP server will not send the DHCP Offer, which is the response of the DHCP Discover message, if the DHCP clients are not authorized users or devices. Thus, in this passive approach, they only request the *ANM* when they retrieve the DHCP Offer message that contains the assigned IP address so that they can retrieve the required ANM in a DHCP Ack message. Thus, they wait their settings of the IP address and configuration parameters until they retrieve the DHCP Ack message. In this case, they can switch their working access network to the new one among available access networks in

accordance with the retrieved ANM. Since they use DHCP Request and Ack messages generally for renewing or confirming the current IP address, they can use this defensive approach for the handover after they use a cellular connection for a while rather than an immediate handover from a newly connected WSN.

As the aggressive approach does, they have two options. However, in the first option, they send the DHCP Release message either in parallel during the new IP assignment with the DHCP server 1 or shortly afterward when the new IP assignment is over successfully as depicted in step 9 of Option 1.

### ***3.3 Analytical Model***

To evaluate the performance of the enhanced DHCP, we define the evaluation metric: the probability of the success in call setup and handover with the enhanced DHCP. This metric is to estimate the enhancement in the network utilization of white space networks with our proposal.

#### **3.3.1 Network Model and Evaluations Procedures**

We assume that WSDs connect to cellular or WiFi <sup>TM</sup> networks to retrieve the information of white space channels permitted for the broadband Internet access as depicted Figure 11 and Figure 12 . Thus, in performance analysis, the principle of channel access allows only one white space network to operate on one white space channel, and after all white space channels are occupied, newly-joining WSDs have to wait until any channel is released or conduct spectrum sharing methods. With this occupancy policy, one white space network per channel, not only the evacuation of WSDs from their operating channel proclaimed by incumbent users but also the protection of already-activated WSNs can be effectively supported. Thus, we adopt the  $M/M/n/n$  queuing model as the evaluation model for our proposal since the  $M/M/n/n$  queuing model well matches with the occupancy policy. To evaluate the performance of our proposal, we define three input streams: one stream is for any

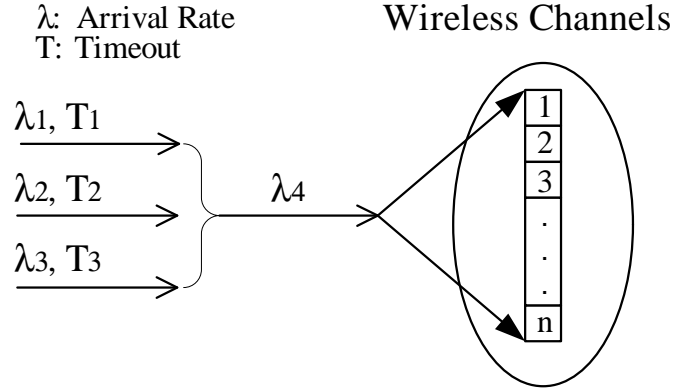


**Figure 13:** Queuing model for the performance evaluation of the extended DHCP arbitrary new and handover calls, one stream is for handover calls with the assistance of the RRM server or the enhanced DHCP, and the last one is for remaining calls that experienced a handover failure.  $T_1$ ,  $T_2$  and  $T_3$  are the timeout parameters for the 1<sup>st</sup> input stream, the 2<sup>nd</sup> input stream, and the 3<sup>rd</sup> input stream respectively [22]. We evaluate the performance of our proposal with the following procedures:

- First, with the queuing model as depicted in Figure 13, we estimate the utilization of white space networks with conventional handover from cellular or WiFi<sup>TM</sup> networks to white space networks.
- Second, we estimate the utilization of white space networks with the handover of our proposal.

After conducting two evaluation procedures, we analyze the extend to which our proposal decreases the setup time with the assistance of the enhanced DHCP.

We define  $T_{sa}$  to stand for the call setup time of arbitrary new or handover calls,  $T_{hr}$  to stand for the call setup and handover times with the assistance of the RRM server,  $T_{hd}$  to stand for the call setup and handover times with the enhanced DHCP server, and  $T_{cr}$  to stand for the spent time on the handover that was failed. Based on the previous definitions, we can assume  $T_{sa} < T_{hd} < T_{hr} < T_{cr}$ . For the first evaluation, we set  $T_1$  to  $T_{sa}$ ,  $T_2$  to  $T_{hr}$  and  $T_3$  to  $T_{cr}$ , and for the second evaluation,

we set  $T_1$  to  $T_{sa}$ ,  $T_2$  to  $T_{hd}$  and  $T_3$  to  $T_{cr}$ . We use (15) to estimate the probability of timeout of the input stream.

$$W^i(t) = \frac{W_E^i(t) - \sum_{k=i}^3 \nu_k W_E^i(T_k)}{1 - \sum_{k=1}^3 \nu_k W_E^i(T_k)}, T_{i-1} < t \leq T_i, \quad (15)$$

where  $W_E^i(t) = \frac{N-\lambda}{N-\Lambda_i} E_{2,N} \theta_{i-1} e^{-(N-\Lambda_i)t}$  is the ordinary Erlang waiting distribution of the  $i^{th}$  input stream,  $N$  is the total number of open white space channels, and  $E_{2,N}$  is Erlang second formula. The parameters  $\nu_i$ ,  $\theta_i$ , and  $\Lambda_i$  are expressed as

$$\Lambda_i = \sum_{k=i}^3 \lambda_k, \theta_i = \sum_{k=1}^i \lambda_k T_k, \nu_i = \frac{\lambda_i}{N - \Lambda_{i+1}}, \theta_0 = 0, \Lambda_4 = 0, \quad (16)$$

where  $\lambda$  is the total arrival rate, which is expressed by  $\lambda = \sum_{k=1}^3 \lambda_k = \Lambda_1$ . With (16), as (2.4) of [22], we use  $P_{to} = \Pi_i(t) = \int_0^t W^i(t) dt, i = 1, 2, 3$  to calculate the probability of timeout for input stream 1, 2 and 3. Thus, we define  $\lambda_4$  as the new arrival rate that is the sum of three arrivals with timeouts, which is expressed as

$$\lambda_4 = \sum_{k=1}^3 \lambda_k (1 - \Pi_i(T_i)). \quad (17)$$

With a calculated  $\lambda_4$ , we estimate the probability of success in all types of new and handover calls using the following equation.

$$P_s = 1 - \frac{(\rho')^N / N!}{1 + \sum_{k=1}^N (\rho')^k / k!}, \rho' = \lambda_4 / \mu, \quad (18)$$

where  $\mu$  is the service rate, and  $\rho' (= \lambda_4 / \mu)$  is a revised traffic intensity.  $\lambda_4$  for the first evaluation, which aims to analyze the performance of the network consisting of conventional new calls with handover calls with the assistance of the RRM server in a conventional way, is expressed by  $\lambda_4^F = \lambda_1(1 - \Pi_1(T_{sa})) + \lambda_2(1 - \Pi_2(T_{hr})) + \lambda_3(1 - \Pi_3(T_{cr}))$ .  $\lambda_4$  for the second evaluation, which aims to analyze the performance of the network consisting of conventional new calls with handover calls with the assistance

of the enhanced DHCP, is expressed by  $\lambda_4^S = \lambda_1(1 - \Pi_1(T_{sa})) + \lambda_2(1 - \Pi_2(T_{hd})) + \lambda_3(1 - \Pi_3(T_{cr}))$ . Thus, we calculate  $P_s$  for the first evaluation with  $\lambda_4^F$  while we do  $P_s$  for the second evaluation with  $\lambda_4^S$ . Before conducting the previous evaluation procedures, we need to figure out how much time we can save from the setup time with our proposal.

### 3.3.2 Setup Time of Network Selection

In our proposal, the DHCP clients conduct the last steps, the connection to the external resource management server and the retrieval of a list of connectable access networks, between the DHCP Discover and the DHCP Offer or between the DHCP Request and the DHCP Ack. Let denote  $T_\alpha$  the setup time of the link layer of WiFi<sup>TM</sup> or cellular network and denote  $T_\beta$  the setup time of the link layer of alternative access network, for instance, white space network. In addition, let denote  $T_\gamma$  the elapsed time between the DHCP Discover and the DHCP Ack and denote  $T_\delta$  the time spent for the retrieval of a list of connectable access networks.

The total time of the call setup and handover with the RRM server in a conventional way is expressed as  $T_{hr} = T_\alpha + T_\beta + 2 \times T_\gamma + T_\delta$ . The conventional mechanism requires two times of the DHCP initial operation while our proposal does one and half or one time of it for the option 1 and the option 2 respectively. Thus, the total of the hand-over with our proposal is expressed as  $T_{hd} = T_\alpha + T_\beta + \phi \times T_\gamma + \psi \times T_\delta$ , where  $\phi$  is 1.5 or 1, and  $\psi$  is the constant value ( $\leq 1$ ) that calculates a reduced time as a result of merging the retrieval of the list of the ANM. If the DHCP server 1 once retrieved the ANM of the location, it can present the retrieved ANM without connecting to the external resource management server. Thus, in this case,  $\psi$  is zero. In performance analysis, we ignore the impact of increase in packet loss because of increase in the packet size to contain proposed options in DHCP messages. According to [48], the packet size in user datagram protocol (UDP), which is a transmission control protocol for DHCP, has the minimum impact on the loss rate such as 0.2 or 0.1%

**Table 5:** Parameters for the performance valuation of the enhanced DHCP.

	Description	Unit	Value
$N$	number of channels		30
$\lambda$	arrival Rate		$[1/17-1/50]$
$k$	min session duration time	sec	120
$p$	max session duration time	sec	2400
$E(T_d)$	mean session duration time	sec	333
$\mu$	session termination rate		$1/333$
$T_\alpha$	L2 setup time of WiFi <sup>TM</sup>	sec	2.5
$T_\beta$	L2 setup time of White Space	sec	3.5
$T_\gamma$	DHCP setup time	sec	1
$T_\delta$	a retrieval time from the RRM	sec	2

with different packet size. Thus, we assume that increase in the DHCP messages has no significant impact on increase in the packet loss rate. The difference of the setup time,  $T_{df} = T_{hr} - T_{hd}$ , has a maximum value when  $\psi$  is zero while it has a minimum value when  $\psi$  is one. Thus, for the option 1, the maximum difference is  $0.5 \times T_\gamma + T_\delta$ , and the minimum difference is  $0.5 \times T_\gamma$ . For the option 2, the maximum is  $T_\gamma + T_\delta$ , and the minimum is  $T_\gamma$ .

### 3.4 Numerical Results

Based on latency budget of WiFi<sup>TM</sup> systems defined in [3], we define the values of parameters in Table 5 for the numerical evaluation. We use the same values of  $k$ ,  $p$ ,  $E(T_d)$ , and  $\mu$  defined at Table 5 and Section 2.4 of Chapter 1. The layer 2(L2) setup of WiFi<sup>TM</sup> consists of 802.11 scan, association and authentication procedures, and from [3], we have  $T_\alpha = 2.5$  seconds that is approximate to the sum of the worst case. We also have  $T_\beta = 3.5$  seconds for the L2 setup of white space devices, and it is one second greater than the L2 setup of WiFi<sup>TM</sup> because of a burden of scanning more channels.

### 3.4.1 Decrease in Setup Time

With given  $T_\alpha = 2.5$ ,  $T_\beta = 3.5$ ,  $T_\gamma = 1$ , and  $T_\delta = 2$ , as the DHCP server can store the retrieved ANM in their local memory or storage, which means  $\psi$  reaches zero,  $T_{df}$  increases up to 3 seconds or 2.5 seconds. The update between the DHCP server and the RRM server in accordance with the update of the ANM causes increase in  $T_{df}$ . However, the frequent update becomes a burden of network traffic between the DHCP server and the RRM server. In this case, since  $\psi$  nears one,  $T_{df}$  decreases to 1 second or 0.5 second. In the selection of an active access network, the DHCP clients with our proposal can expect the fast entry as long as  $\psi$  is less than one.

In fact,  $\psi$  is not greater than one since the extended DHCP server launches the update of the ANM in accordance with the activation of the new clients. If the ANM only provides a list of the available access networks, the list will not be so frequently updated until new access networks are added. In addition, even if the ANM also contains dynamic channel information of wireless environments, the ANM will be updated in proportional to the number of changes occurred in wireless environments of access networks. For instance, with the extended spectrum map defined in Chapter 1, as more WSDs are activated, more changes in a list of unoccupied white space channels occur to match the changed channel occupancy status, which results in more updates in the ANM. However, sometimes, the activation of new clients will not change the ANM if the clients decided not to operate on white space. Thus, we regard that the one update of the ANM between the DHCP server and the RRM server is equal to or less than the one retrieval of the ANM from the RRM server. That is a reason why  $\psi$  is equal to or less than one.

### 3.4.2 Probability of the Success of Call Setup

We set  $T_{sa}$  to  $4.5 = T_\beta + T_\gamma$  with the assumption that WSDs have the cache about a list of available white space channels of a current location, which means that the

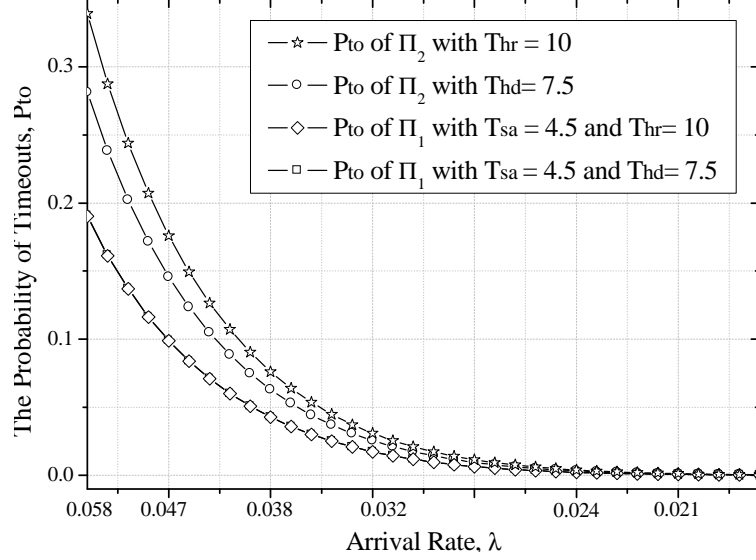
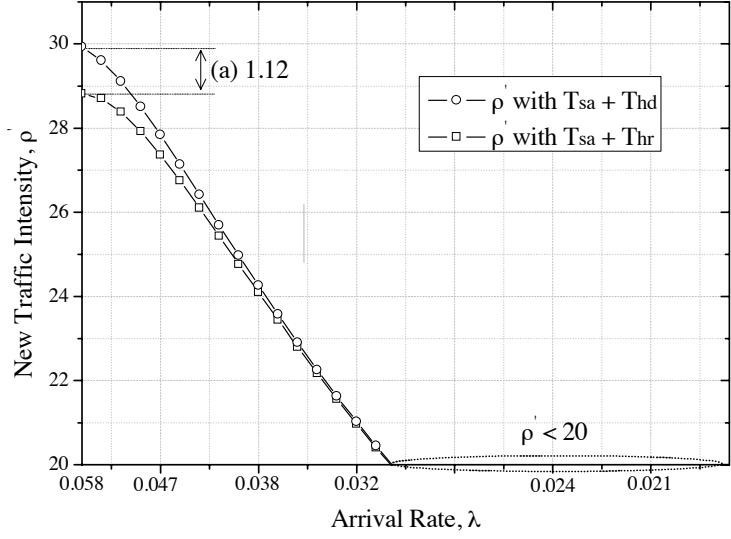


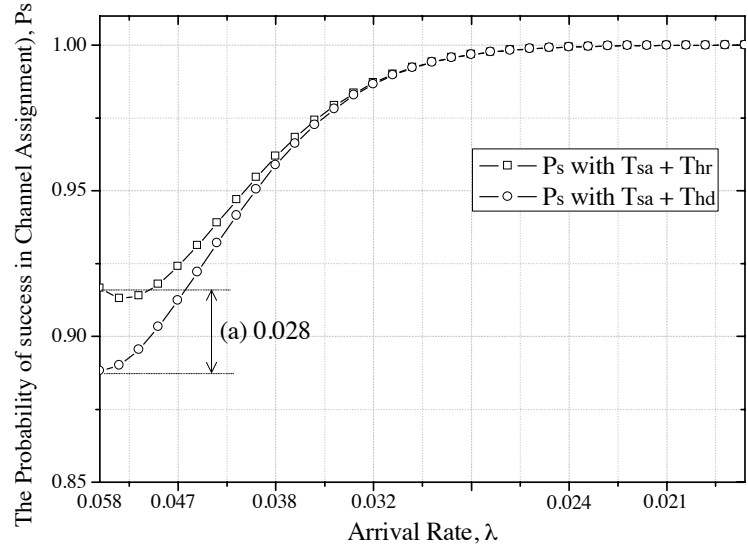
**Figure 14:** The calculated  $P_{to}$  with  $\lambda_1 = \lambda_2 = \lambda_3$

devices can directly execute the layer 2 setup of white space networks. We set  $T_{hr}$  to  $10 = T_{\alpha} + 2 \times T_{\gamma} + T_{\beta} + T_{\delta}$  as the normal call setup and handover with the RRM server, and we set  $T_{hd}$  to  $7.5 = T_{\alpha} + 1.5 \times T_{\gamma} + T_{\beta}$ . The difference, 2.5, between  $T_{hr}$  and  $T_{hd}$  refers to  $T_{df}$  that is described at the previous section. For  $T_{cr}$ , we set it to  $12 = T_{hr} + 2$  as the time in the failure of the handover trial. For the simplicity of analysis, we set  $\lambda_1$ ,  $\lambda_2$ , and  $\lambda_3$  to the same value. At the first evaluation, we have three inputs, normal calls  $(\lambda_1, T_{sa})$ , call setup and handover with the RRM  $(\lambda_2, T_{hr})$ , and calls residing after the handover is failed  $(\lambda_3, T_{cr})$  while at the second evaluation, we have  $(\lambda_1, T_{sa})$ ,  $(\lambda_2, T_{hd})$ , and  $(\lambda_3, T_{cr})$ . We observe that  $P_{to} = \Pi_2$  of  $(\lambda_2, T_{hr})$  is greater than  $P_{to} = \Pi_2$  of  $(\lambda_2, T_{hd})$  as depicted in Figure 14. At  $\lambda_1 = \lambda_2 = \lambda_3 = 0.058$ , the difference is over 0.05, and the difference decreases as  $\lambda_1, \lambda_2$ , and  $\lambda_3$  decrease. Those observations indicate that the handover with the enhanced DHCP has a less probability of timeout compared to the probability of timeout for the conventional handover.

Since our proposal contributes to decrease in the number of new arrivals requiring hand-over to the WSN to be expired, it results in increasing  $\rho'$  that is calculated with



(a) The calculated  $\rho'$



(b) The calculated  $P_s$

**Figure 15:** The  $\rho'$  with  $T_{sa} + T_{hd}$  versus The  $\rho'$  with  $T_{sa} + T_{hr}$  (Subfigure(a)). Probability of the success in handover calls with  $\lambda_1 = \lambda_2 = \lambda_3$  (Subfigure (b))

$\lambda_4$  as depicted in Figure 15(a). Label (a) of Figure 15(a) shows that the difference of traffic intensity between  $\rho'$  of  $\lambda_4^S$  and  $\rho'$  of  $\lambda_4^F$  is about 1.12. This means that among  $N = 30$ , our proposal can accommodate one or more WSDs compared to the conventional approach. As depicted in label (a) of Figure 15(b), with our proposal,  $P_s$  of one wireless device is 0.028 less than  $P_s$  of another device with the conventional approach since the utilization with our approach reaches the limit,  $N = 30$  earlier than the utilization of the conventional approach. With asymmetric arrival rates of  $\lambda_1$ ,  $\lambda_2$ , and  $\lambda_3$ , which  $\lambda_2$  is two times greater than  $\lambda_1$  and  $\lambda_3$ , we observe that the difference between  $\rho'$  of  $\lambda_4^S$  and  $\rho'$  of  $\lambda_4^F$  is about 0.5 at  $\lambda_1 = \lambda_3 = 0.033$  and  $\lambda_2 = 0.066$ . In addition, when  $\lambda_2$  is the half of  $\lambda_1$  such as  $\lambda_1 = 0.07$  and  $\lambda_2 = 0.035$ , the difference is about 0.7. We observe the similar results that  $\rho'$  with our approach reaches the limit ( $N = 30$ ) more closely than  $\rho'$  with the conventional approach with the most cases of asymmetric arrival rates. Previous observations confirm that our proposal with the enhanced DHCP can increase the network utilization compared to the conventional approach with the RRM server.

### 3.4.3 Delay in the Internet access

As a drawback of our proposal, delay in the IP assignment of the WiFi<sup>TM</sup> or 3G network can cause the DHCP clients to experience delay in the Internet access. Through maintaining previously retrieved spectrum maps, the DHCP servers can decrease this delay. Let denote  $D$  the delay in the retrieval of the spectrum map from the RRM server at the DHCP server, which is expressed by

$$D = d_0 + (P_m \times d_1) \times (1 - P_f) + P_f \times d_2, \quad (19)$$

where  $d_0$  is the internal delay of the DHCP server for the IP assignment,  $P_m$  is the miss rate in finding the spectrum map among the stored spectrum maps, and  $d_1$  is the delay time for retrieving the spectrum map from the RRM server.  $P_f$  is the probability of failing to retrieve the spectrum map from the RRM server, and  $d_2$  is the delay time in

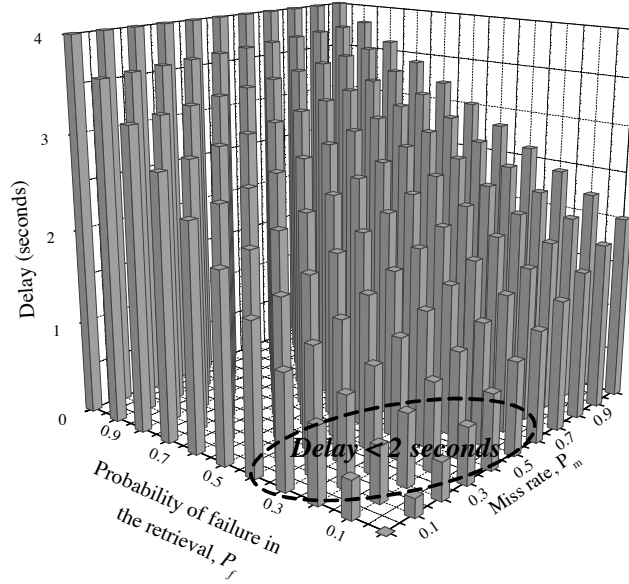


**Figure 16:** Calculated delay in the retrieval of the spectrum map

the case of the retrieval of the spectrum map failed. For the conventional approach,  $D$  is  $d_0$ , and for the simplicity of the analysis, we set  $d_0$  to zero. Thus, compared to the conventional approach, the delay penalty is  $(P_m \times d_1) \times (1 - P_f) + P_f \times d_2$ . We set  $d_1$  to  $T_\delta = 2$  and  $d_2$  to the two times of  $T_\delta$  as the timeout. Figure 16 depicts the results of the calculated delay using (19). When  $P_f$  is less than or equal to 50%, the calculated delay is less than  $T_\delta = 2$  regardless of what  $P_m$  is. With  $T_{df} = 2.5$  presented in the previous section, we can expect that our proposal at least shortens half a second. This observation indicates that the RRM server can offer the spectrum map with a less delay ( $\leq T_\delta$ ) if  $P_f$  and  $P_m$  are less than or equal to 50%. As more spectrum maps are internally stored, decrease in the miss rate will result in decrease in the delay of retrieving the spectrum map. This delay can be deteriorated if we have the DHCP server and the RRM server integrated as one server.

### ***3.5 Conclusions***

In this chapter, we propose the enhanced DHCP that extends DHCP messages to include spectrum map. Our proposal aims to reduce a signaling overhead for handover from the conventional access networks to the alternative networks, white space networks. We propose the retrieval of the spectrum map during the DHCP operation for the first IP assignment and expect that the embedded retrieval of the spectrum map can contribute to increasing the network utilization. In performance analysis, we conduct numerical evaluation with handover cases from cellular or WiFi<sup>TM</sup> networks to white space networks. According to the analysis results, as the arrival rate,  $\lambda$ , reaches a certain level, which means we have no more unoccupied channels, with the enhanced DHCP, we can accommodate up to one or more white space devices, and as a result, the network utilization increases. We expect that we can further use this fast retrieval for any new ranges of open spectrum for the broadband Internet access.

This chapter introduces the frequency-domain coexistence beacon that aims to improve the probability of detection with a low cost hardware.

### ***4.1 Motivation of Frequency-domain Coexistence Beacon***

Conventional spectrum sensing techniques can be classified into feature detection and energy detection as shown in Table 1. According to recent research work evaluated spectrum sensing methods, the evaluation results indicate that pilot detection performs better, particularly at a low SNR under high noise uncertainty [26]. With the narrow bandwidth of the DTV pilot, we can have a higher SNR of the DTV pilot than that of 6 MHz [38]. The increase in SNR contributes to a better detection of DTV signals at a rather low SNR compared to other spectrum sensing methods. For the protection of incumbent users, since all spectrum sensing schemes should detect DTV signals at a low SNR, such as -116 or -107 dBm [25], the DTV pilot detection scheme is a desirable solution for DTV signal detection.

The main idea in this chapter is to adopt the DTV pilot detection scheme to detect the signals of white space devices (WSDs). Like the DTV pilot that has the narrow bandwidth of 10 kHz, we propose assigning a frequency-domain coexistence beacon (FCB) at the same location of the DTV pilot in white space channels for beacon usage. However, since the range of pilot locations can vary, we assign 100 kHz for the FCB while the actual bandwidth for WSDs that transmit their coexistence beacon

frames is 10 kHz. To detect transmitted coexistence beacon frames, we expect that other WSDs will execute a DTV pilot detector that can detect the beacon frames. The rest of this chapter consists of the following sections: Section 4.2 presents a working mechanism of the proposed scheme, and Section 4.3 presents the extent to which the proposed scheme improves the probability of detection in energy detection-based spectrum sensing. In addition, Section 4.3 describes a network model that is defined to evaluate the proposed scheme, the FCB. In addition, this section also presents the extent to which the detection improvement increases the total capacity of white space channels. Section 4.4 presents another network model that is defined to evaluate the additional scheme for supporting channel bonding or aggregation and also demonstrates the extent to which the extended FCB contributes to the savings of the total spectrum sensing time in need of supporting channel or aggregation. Section 4.5 summarizes the proposed and evaluated scheme in this chapter.

## ***4.2 Frequency-domain Coexistence Beacon for White Space Applications***

Figure 17 illustrates the channel structure when WSDs implement the proposed pilot detection scheme. To support the proposed scheme, we have to implement a transceiver for the FCB. We have two ways of implementing the FCB as the followings: the FCB carrying a single tone, a so-called “ $FCB_{v1}$ ”, or the FCB broadcasting coexistence beacon frames, a so-called “ $FCB_{v2}$ .” For one, at the transmitter, we can adopt a simple coexistence beacon generator, and then, its output signal will be combined with data signals at a baseband system. The beacon generator can produce any type of data frame as well as a simple tone such as the DTV pilot tone. This flexibility enables us to define a proper frame structure after we design the coexistence operating scenarios of WSDs with the FCB. At the receiver, we can adopt the DTV pilot detector without hardware increment.

Another one is to extend the FCB to broadcast coexistence beacon frames for

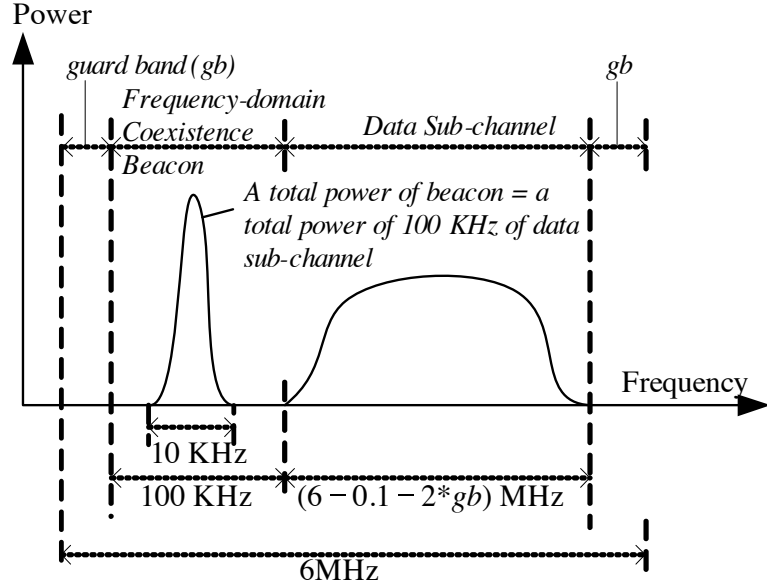


**Figure 17:** A new proposal of white space channel for the proposed pilot detection scheme. The proposed scheme assumes that the total power of 10 kHz of the frequency-domain coexistence beacon is equal to the total power of energy detection of 100 kHz of 6 MHz.

supporting channel bonding or aggregation, which is to allow WSDs to operate on multiple channels when user applications running on the WSDs require more bandwidth than the bandwidth of one channel [5]. The previously proposed FCB ( $FCB_{v1}$ ) aims to increase the probability of detection in spectrum sensing by narrowing the bandwidth for spectrum sensing. Thus, new newly-joining WSDs with the  $FCB_{v1}$  shall still conduct spectrum sensing against all channels one by one regardless of concerning the owner of channels or how many channels one neighboring WSD occupies now. If the newly-joining WSDs can recognize the owner of occupied channels and/or what channels the neighboring WSD operates on in advance, they can save the total spectrum sensing time by sensing only one of the channels assigned to the neighboring WSD. In this chapter, additionally we propose extending the  $FCB_{v1}$  to broadcast coexistence frames about channel information for WSDs, particularly operating on multiple channels. Inside the coexistence beacon frames broadcasted in the FCB of the channels assigned to one WSD, channel information of the channels, which are

assigned to the WSD, shall be included. For instance, if one WSD occupies  $i^{th}$  and  $(i+k)^{th}$  channels, in the FCB coexistence beacon frames of the  $i^{th}$  channel, the WSD can embed the  $(i+k)^{th}$  channel identification. Thus, any newly-joining WSDs nearing the WSD can avoid scanning the  $(i+k)^{th}$  channel when they retrieve the FCB coexistence frames on the  $i^{th}$  channel. The FCB broadcasting coexistence beacon frames ( $FCB_{v2}$ ) is expected to contribute to decrease in the total spectrum sensing time as more WSDs are in need of multiple channels through channel bonding or aggregation.

In the matter of implementation of the  $FCB_{v2}$ , on a transmitter, we can adopt a simple FCB generator that creates the FCB pilot signals from the FCB coexistence beacon frames. The transmitter can combine the pilot frequency converted from the pilot signals with modulated signals of user data, which come out from an analog-to-digital converter (ADC). On a receiver, we can adopt zero or near zero IF receiver architecture [7] for processing the FCB pilot signals without an additional cost. However, the details of the transceiver systems for two versions of the FCB are beyond the scope in this dissertation. The following paragraphs describe the benefits of the FCB for the purpose of improvement in the coexistence of WSDs.

Using the  $FCB_{v1}$  or  $FCB_{v2}$ , we can have a longer service coverage of WSDs than that of conventional energy detection-based WSDs. The transceiver for the proposed scheme assumes that the total power of the FCB( $\leq 10$  kHz) [38] should be equal to the total power of 100 kHz of 6 MHz measured by energy detectors. If the signal power of 6 MHz is evenly distributed, the concentration of the transmit power over 10 kHz assures that the signal strength of 10 kHz is stronger than that of the data sub-channel in the proposed scheme. Because of a strong signal, the coexistence beacon frames of the proposed scheme can cover a longer distance than data frame, and a longer service coverage increases the probability of detecting other active WSDs. In addition, since the total power of 6 MHz with our method might be equal to the total power of 6 MHz of energy detection, which transmits user traffic

on 6 MHz, we can expect WSDs that have only energy detectors can achieve similar performance of detecting the infrastructure-based WSDs implementing our method. This achievement indicates that the proposed scheme can be applied easily, and it can also provide compatibility with other WSDs not supporting the proposed scheme.

Along with extending service coverage and maintaining compatibility with conventional energy detection-based WSDs, the increase in SNR with the proposed scheme also increases the likelihood of detecting other WSDs, and we can estimate the amount of increased SNR by referring to the noise power and the signal power of the FCB. Since the signal power of the FCB is equal to that of energy detection of 100 kHz of 6 MHz, the signal power of the FCB can be expressed as *the total signal power of 6 MHz* ( $T_S$ )  $-10 \log_{10}(6MHz/100kHz) = T_S - 17.8 dB$ . The noise power of the FCB can be also expressed as *the total noise power of 6 MHz* ( $T_N$ )  $-10 \log_{10}(6MHz/10kHz) = T_N - 27.8 dB$ . Thus, the SNR of the FCB can be expressed as  $T_S - T_N + 10 dB$  after extracting the signal power of 10 kHz from the noise power. Since  $T_S - T_N$  is the total SNR of 6 MHz, the proposed scheme can add 10 dB more to the SNR compared to the SNR of a typical energy detection. Section 4.3 presents the analysis of the extent to which WSDs with an enhanced SNR effectively detect other WSDs. The proposed scheme could more effectively assist WSDs if they have only energy detectors.

With the improved detection probability, the proposed scheme can reduce potential interference that WSDs may cause to each other. White space applications can potentially cause interference to their neighbors if they select their operating channel among the channels that are falsely detected as unoccupied. In addition, the improvement with the proposed scheme directly contributes to enhancing the performance of coexistence mechanisms between WSDs since they rely on the accuracy of spectrum sensing. Based on the results of spectrum sensing, if WSDs fail to find unused channels, they perform coexistence mechanisms such as the ITPA-based spectrum sensing

**Table 6:** The threshold,  $\lambda$ , with fixed  $u$  and  $P_f$ .

u	$P_f = 10^0$	$10^{-1}$	$10^{-2}$	$10^{-3}$	$10^{-4}$	$10^{-5}$	$10^{-6}$
1	0.02	4.60	9.21	13.81	18.42	23.02	27.63
2	0.02	7.77	13.27	18.46	23.51	28.47	33.37

proposed defined in Chapter CH5. The increased likelihood of detection with the proposed scheme can support better performance of coexistence mechanisms, and the improvement in coexistence contributes to less interference to neighbors and more accommodation of newly-joining WSDs. Since more active WSDs increase the total network capacity that is the sum of throughput of all active WSDs operating on white space channels, we can expect that the proposed schemes compensate for the loss of throughput experienced by each white space application after the proposed schemes are deployed.

### 4.3 Performance Analysis of FCBv1

#### 4.3.1 Analysis of Detection Probability

To evaluate the performance of the  $FCB_{v1}$ , this section presents the probability of detection,  $P_d$ , which is expressed as  $P_d = Q_u(\sqrt{2\gamma}, \sqrt{\lambda})$ , where  $u$  is the number of samples for energy detection,  $\gamma$  is a SNR, and  $\lambda$  is the threshold of an energy detector [13]. According to (3) from [23],  $P_d$  can be expressed as

$$P_d = \sum_{n=0}^{\infty} \frac{\gamma^n e^{-\gamma}}{n!} \sum_{k=0}^{n+u-1} \frac{e^{-\frac{\lambda}{2}}}{k!} \left(\frac{\lambda}{2}\right)^k. \quad (20)$$

In addition, the probability of false alarm is expressed as  $P_f = \Gamma(u, (\lambda/2)) / \Gamma(u)$ , where  $\Gamma$  is the upper incomplete function. For  $P_f = [10^0 : 10^{-6}]$ , Table 6 shows the values of  $\lambda$  for  $u = 1, 2$ . (Refer to Section 4.6.) If SNR ( $\gamma$ ) follows the Nakagami- $m$  channel, its probability density function (pdf),  $f_{\gamma,nak}(\gamma)$ , is expressed as

$$f_{\gamma,nak}(\gamma) = \frac{1}{\Gamma(m)} \left(\frac{m}{\bar{\gamma}}\right)^m \gamma^{m-1} e^{-\frac{m\gamma}{\bar{\gamma}}}, \gamma > 0, \quad (21)$$

where  $\bar{\gamma}$  is the average of SNR. If  $m$  is one,  $f_{\gamma,nak}$  is the pdf of the Rayleigh distribution. By integrating  $P_d$  to  $f_{\gamma,nak}(\gamma)$ , the average detection probability of Nakagami- $m$  fading

**Table 7:** Parameters for performance evaluation of the  $FCB_{v1}$  in the probability of detection.

	Description	Unit	Value
$u$	the number of samples		[1, 2]
$\bar{\gamma}$	SNR	dB	{10, 20}

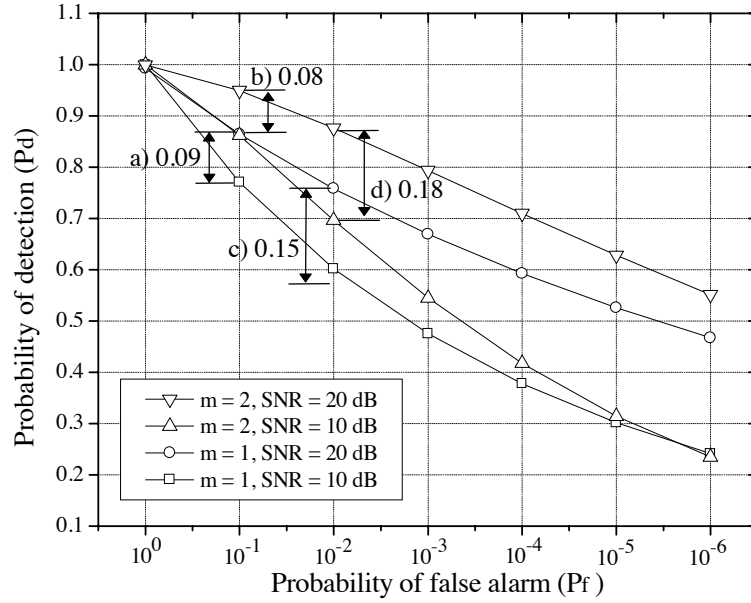
[23] can be expressed as

$$\begin{aligned} \bar{P}_{d,nak} &= \int_0^\infty P_d f_{\gamma,nak}(\gamma) d\gamma \\ &= \frac{e^{-\frac{\lambda}{2}}}{\Gamma(m)} \left( \frac{m}{\bar{\gamma} + m} \right) \sum_{n=0}^{\infty} \left( \frac{\bar{\gamma}}{\bar{\gamma} + m} \right)^n \frac{(n + m - 1)!}{n!} \times \sum_{k=0}^{n+u-1} \frac{\left(\frac{\lambda}{2}\right)^k}{k!}. \end{aligned} \quad (22)$$

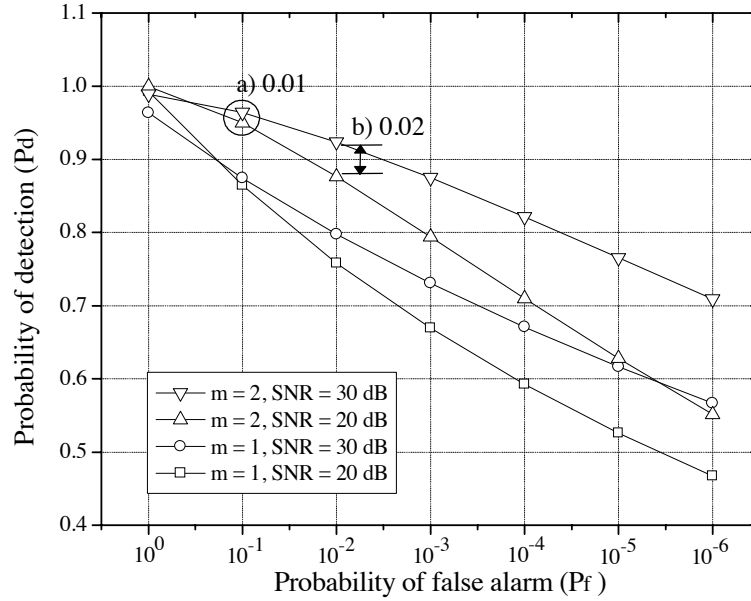
Table 7 shows the values of parameters to calculate  $\bar{P}_{d,nak}$ . With given two tables, Tables 6 and 7, we implement MATLAB<sup>TM</sup> codes to calculate (22), and Figure 18 depicts the results of the numerical calculation of  $\bar{P}_{d,nak}$  for  $u = 2$  and  $\bar{\gamma} = 10, 20$  dB. With  $\bar{\gamma} = 10$  dB, labels a) and b) of Figure 18(a) illustrate that the results of the proposed scheme is greater than over 10% in  $P_d$  with  $P_f = 10^{-1}$  compared to the results of a typical energy detection. As labels c) and d) demonstrates, the difference is about 20% in  $P_d$  with  $P_f = 10^{-2}$ . The difference in  $P_d$  becomes even more as  $P_f$  nears  $10^{-6}$ . With  $\bar{\gamma} = 20$  dB, the improvement of  $\bar{P}_{d,nak}$  is a little as depicted in labels a) and b) of Figure 18(b). In fact, since  $\bar{\gamma} = 20$  dB is a high SNR, energy detection using the  $FCB_{v1}$  can also have a higher probability of detection than that of a typical energy detection. Thus, the proposed scheme can more effectively enhance the performance of spectrum sensing with a low target SNR and a low  $P_f$  than that with a high target SNR and a high  $P_f$ .

#### 4.3.2 Analysis of Network Capacity Increase

To examine the extent to which improvement in the probability of detection affects the network performance of white space channels, in this chapter, we adopt the  $M/G/m/m$  queueing model as done in previous chapters. Table 8 shows the values of parameters for evaluating the aspect of increase in network capacity for the



(a) A comparison of  $\bar{P}_{d,nak}$  for  $\text{SNR}(\bar{\gamma}) = 10$  dB



(b) A comparison of  $\bar{P}_{d,nak}$  for  $\text{SNR}(\bar{\gamma}) = 20$  dB

**Figure 18:** The average probability,  $\bar{P}_{d,nak}$ , of detection in a typical energy detection and the proposed pilot detection scheme. The SNR of the proposed scheme is 10 dB greater than the SNR of energy detection.

**Table 8:** Parameters for performance evaluation of the  $FCB_{v1}$  in network capacity.

	Description	Unit	Value
N	number of channels		30
R	default service radius	m	120
$\rho$	the density		[0.001-0.02]
$k$	min session duration time	sec	120
$p$	max session duration time	sec	2400
$E(T_{arr})$	mean session duration time	sec	333
$\mu$	session termination rate		10.8

**Table 9:** the difference of the expected number of detected WSDs between energy detection using the  $FCB_{v1}$  and a typical energy detection.

	$\rho = 0.004$	0.008	0.012	0.016	0.02
difference	1.5079	2.4307	2.5895	2.6333	2.6525

proposed pilot detection on the  $M/B/N/N$  model. In addition, we exploit this model in the performance analysis of the  $FCB_{v2}$ .

#### 4.3.2.1 Analytical Model

Using (3), we calculate the expected number of active WSDs,  $E(N_b)$ . In fact, depending on spectrum sensing accuracy, newly-joining WSDs cannot successfully detect the  $E(N_b)$  number of other WSDs. Thus, we define  $E'(N_b)$  as representing the expected number of detected active neighboring WSDs according to  $P_d$  and  $P_f$ , and  $E'(N_b)$  is expressed as

$$E'(N_b) = \sum_{i=0}^N \{(P_d)P_i + P_f(1 - P_i)\}, \quad (23)$$

where  $P_i$  is the occupancy probability of the  $i^{th}$  channel at any time. If all channels have the equal probability of being occupied by WSDs,  $P_i$  becomes equal to  $E(N_b)/N$ , and we have a simplified  $E'(N_b) = (P_d - P_f)E(N_b) + N \times P_f$ .

#### 4.3.2.2 Analysis of Network Capacity Increase

To evaluate the improvement of network capacity, we require estimating the expected probability of detection in a typical energy detection and the expected probability of

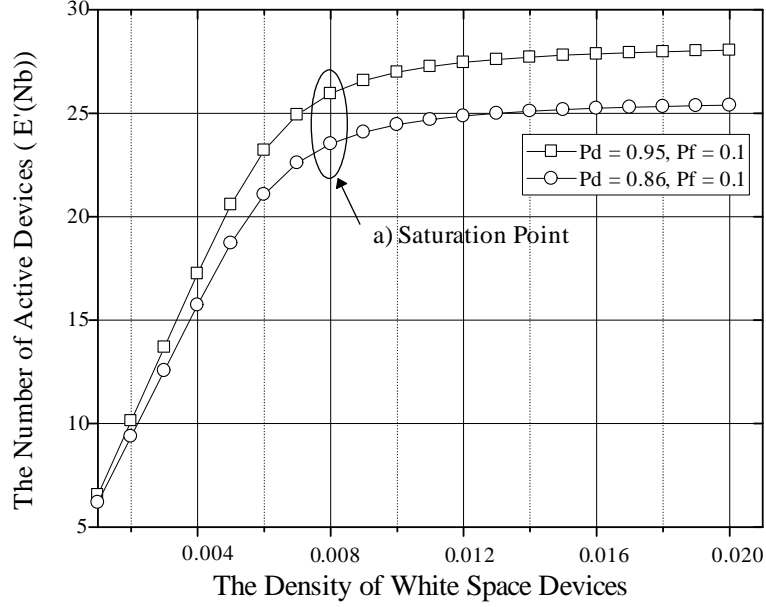


**Figure 19:** The expected number,  $E'(N_b)$ , of occupied channels with  $R = 120 m$ . Symbols for  $P_d \approx 0.95$  represent  $E'(N_b)$  of  $FCB_{v1}$ -based energy detection while symbols for  $P_d \approx 0.86$  represent  $E'(N_b)$  of a typical energy detection with  $\text{SNR}(\bar{\gamma}) = 10 \text{ dB}$  and  $u = 2$ .

detection in energy detection using the  $FCB_{v1}$ . With a fixed  $P_f = 10^{-1}$ ,  $\bar{\gamma} = 10 \text{ dB}$ , and  $u = 2$ , as depicted in label b) of Figure 18(a), energy detection using the  $FCB_{v1}$  has  $P_d \approx 0.95$  while a typical energy detection has  $P_d \approx 0.86$ . Using the simplified  $E'(N_b)$  defined in the previous section and the values of parameters in Table 8, we can calculate  $E'(N_b)$  of energy detection using the  $FCB_{v1}$  with  $P_d \approx 0.95$  and  $E'(N_b)$  of a typical energy detection with  $P_d \approx 0.86$  as depicted in Figure 19. When the density,  $\rho$ , increases,  $E'(N_b)$  of  $FCB_{v1}$ -based energy detection becomes greater than  $E'(N_b)$  of a typical energy detection over two, which indicates that the proposed scheme can contribute to accommodating two more newly-joining WSDs, as shown in Table 9. Using  $E'(N_b)$  of  $FCB_{v1}$ -based energy detection, we can estimate the expected total capacity,  $T_{tot}$ , of white space channels. We define  $T_{tot}$  as the total throughput of the medium access control (MAC) of all activated WSDs, and thus,  $T_{tot}$  is expressed as  $T_{tot} = E'(N_b) \times T_{mac}$ , where  $T_{mac}$  is the average MAC throughput. The data rate or the MAC throughput,  $T_{mac}$ , on WSDs using  $FCB_{v1}$ -based energy detection decreases

**Table 10:** The increase of a total MAC throughput of white space channels.

	$\rho = 0.004$	0.008	0.012	0.016	0.02
increase	42.09 Mbps	67.11	71.42	72.60	73.12

since the bandwidth for delivering user data decreases, and the exacerbation of the MAC throughput is proportional to a loss of 100 kHz for user data transmission. For instance, with the data rate mode of 23.74 Mbps [15] and the ratio of 5.9MHz / 6 MHz, we can estimate the degradation of the MAC throughput at around 0.40 Mbps (=23.74 - 23.34 Mbps). Although the proposed scheme has to abandon 0.40 Mbps, the total capacity of white space channels increases when WSDs support the proposed scheme as shown in Table 9. In the calculation of  $T_{tot}$ , we adopt 23.74 Mbps as  $T_{mac}$  that the WSDs using a typical energy detection can achieve and 23.34 Mbps as  $T_{mac}$  that the WSDs using  $FCB_{v1}$ -based energy detection can achieve. In addition, we adopt  $E'(N_b)$  values for two detection schemes from  $E'(N_b)$  of Figure 19. After the density = 0.008 as the saturation point that is depicted in label (a) of Figure 19, the difference of between two cases becomes greater than two. Table 10 shows that after the saturation point, using  $FCB_{v1}$ -based energy detection, we can expect increase in the total network capacity over 70 Mbps compared to that of a typical energy detection. The previous two subsections reveal that the proposed scheme can improve the performance of energy detection by increasing the probability of detection, and this improvement increases the total network capacity of white space channels. We expect that energy detection using  $FCB_{v1}$  works effectively in any wireless environment especially when the measured SNR with energy detection is rather low. Regardless of the physical distance between WSDs, a low SNR occurs if many obstacles exist between WSDs, and this situation can be highly possible if WSDs are inside buildings. In this case, WSDs using conventional energy detectors cannot easily have a high SNR; however, if they adopt the proposed scheme, we expect that they can have a high SNR.

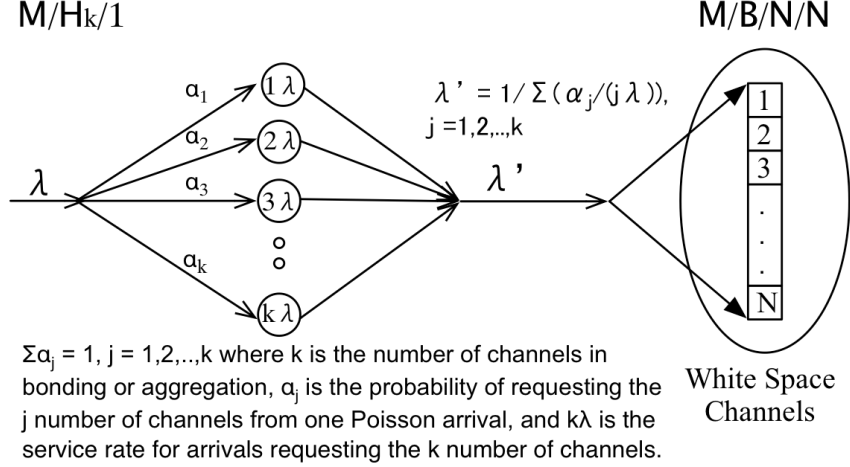


**Figure 20:** Queuing networks for performance evaluation

## 4.4 Performance Analysis of FCBv2

### 4.4.1 Queuing Network for Evaluation of FCBv2

Figure 20 illustrates the details of queuing networks that are defined for the performance evaluation of the  $FCB_{v2}$  and consist of two embedded queuing models,  $M/H_k/1$  and  $M/B/N/N$ . On  $M/H_k/1$ , since newly-joining WSDs can request a different number of channels as their operating channels at a different portion of an arrival rate ( $= \lambda$ ), the activation of the newly-joining WSDs requesting the  $k$  channels has an arrival rate  $= k\lambda$ . Thus, we define a new arrival rate, which is expressed as  $\lambda' = 1 / (\sum_{j=1}^k \frac{\alpha_j}{(j\lambda)})$ . In performance evaluation, we have  $k = 3$ , which means every WSD can occupy up to 3 channels. We have the number of channels,  $N = 30$ , a default service coverage,  $R = 120$  m. Also, we exploit all evaluation parameters defined in Table 8.

#### 4.4.1.1 Average Number of Active WSDs

To analyze the extent to which the  $FCB_{v2}$  affects the utilization of white space channels when WSDs have a permission to operate on multiple channels, we define the average number of occupied white space channels,  $E(N_c)$ , that is calculated by

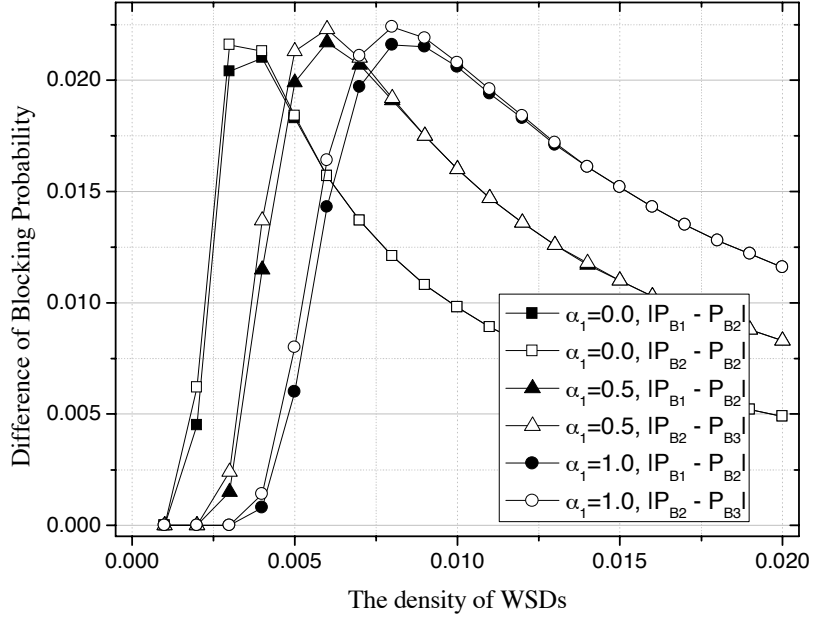


**Figure 21:** Differences between blocking probabilities,  $P_{B1}$ ,  $P_{B2}$ , and  $P_{B3}$

the following equation.

$$E(N_c) = \left( \frac{\lambda'}{\mu} \right) (1 - P_B(\lambda', \mu)). \quad (24)$$

Using  $E(N_c)$ , as the first evaluation metric, we define the average number of activated WSDs,  $E''(N_b) \approx \{\sum_{j=1}^k (1/j)\alpha_j\} \times E(N_c)$ . In the calculation of  $E''(N_b)$ , all activations of WSDs have the same probability of success in the channel assignment, which means that activated WSDs continue to transmit the signals if they have at least one assigned channel regardless of how many channels they originally required. Using  $P_B$ , we calculated three blocking probabilities,  $P_{B1} = P_B$  with  $N$  for blocking probability of  $k = 1$ ,  $P_{B2} = P_B$  with  $N - 1$  for blocking probability of  $k = 2$ , and  $P_{B3} = P_B$  with  $N - 2$  for blocking probability of  $k = 3$ . As depicted in Figure 21, we observed that the difference between  $P_{B1}$  and  $P_{B3}$  is less than or equal to 0.05. Thus, we apply the same probability of success in the channel assignment for  $k = 1, 2, 3$  to the calculation of  $E''(N_b)$ . From Section IV of [50], we adopted  $P_m = 0.14$ , which is the probability of miss detection, for a typical energy detection and  $P_m = 0.05$  for

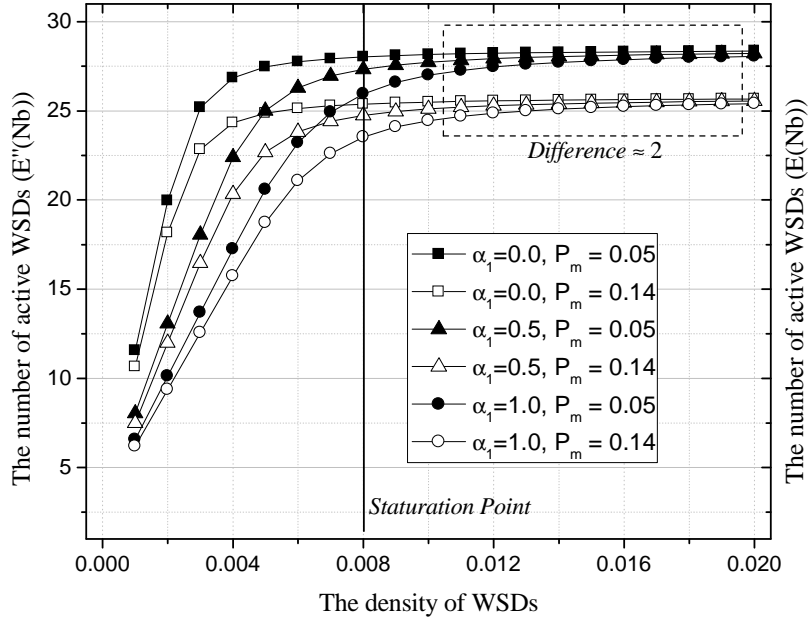


**Figure 22:** The average number of active WSDs ( $E''(N_b)$ ) versus  $E(N_b)$  with  $\alpha_1$ ,  $\alpha_2$ , and  $\alpha_3$

energy detection using the  $FCB_{v2}$ . In addition, we have  $\alpha_2 = \alpha_3 = (1/2)(1 - \alpha_1)$  with  $\alpha_1 = [0.0 \ 0.5 \ 1.0]$ . Figure 22 illustrates that  $E''(N_b)$  of energy detection using the  $FCB_{v2}$ , which is represented by the solid symbols, is two greater than  $E(N_b)$  of a typical energy detection, which is represented by the open symbols, through all cases of  $\alpha_1$  when  $\rho$  reaches a saturation point such as  $\rho = 0.008$ . After the point, which means that we have no more unoccupied channels, the difference between  $E''(N_b)$  of energy detection using the  $FCB_{v2}$  and  $E(N_b)$  of a typical energy detection is steadily maintained over two. This means that we can have two or more newly-joining WSDs to be accommodated using the  $FCB_{v2}$  coexistence beacon frames. Thus, the  $FCB_{v2}$  itself can enhance the capacity of white space channels with channel aggregation or bonding compared to the case only having a typical energy detection.

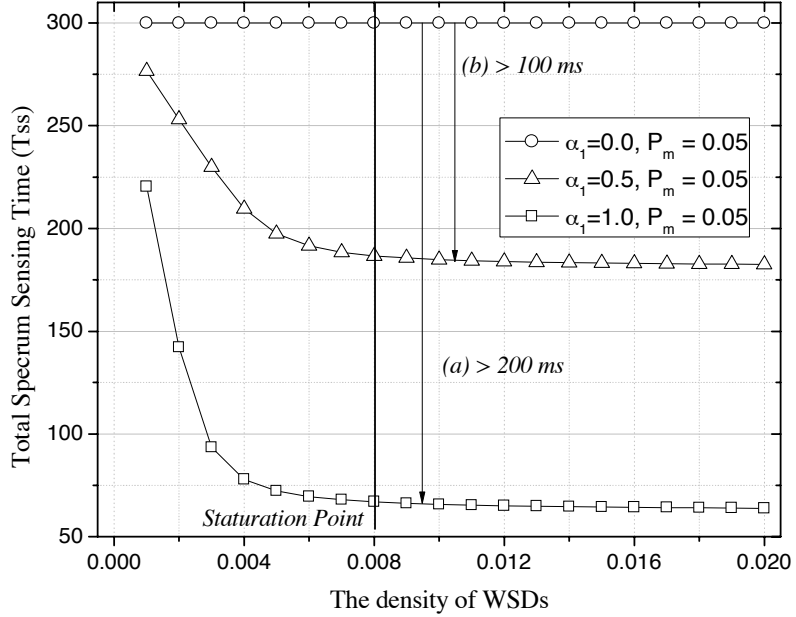


**Figure 23:** The total spectrum sensing time,  $T_{ss}$ , of a WSD conducting  $FCB_{v2}$ -based energy detection

#### 4.4.1.2 Total Spectrum Sensing Time

As the second evaluation metric, we define a total spectrum sensing time, which is expressed as the following equation.

$$T_{ss} = \{N - (1 - P_m)E''(N_b)\left(\sum_{j=1}^k (1/j)\alpha_j\right)\} \times T_s, \quad (25)$$

where  $T_s$  is the spectrum sensing time for scanning one channel. As  $(1 - P_m)$  nears one, we have a better chance to retrieve successfully coexistence beacon frames in the FCB of one channel among channels assigned to a neighboring WSD. This results in only spending  $(1/j) \times T_s$  seconds with the probability,  $\alpha_j$ . With  $T_s = 10$  ms [15], as depicted in labels (a) and (b) of Figure 23, numerical results demonstrate that we can have up to 100 ~ 200 ms decrease in  $T_{ss}$  that a WSD spends to conduct one cycle of spectrum sensing using the  $FCB_{v2}$  compared with  $T_{ss}$  of a typical energy detection, which is equal to  $T_{ss}$  of  $FCB_{v2}$  with  $\alpha_1 = 0.0$ , after a saturation point = 0.008, when  $\alpha_1$  is equal to or less than 0.5. Thus, as the density of WSDs is greater than a certain

level like a saturation point as illustrated in Figure 23, the  $FCB_{v2}$  can contribute to the decrease of the total spectrum sensing time.

## 4.5 Conclusions

In this chapter, we propose a pilot detection scheme for WSDs that assigns a frequency-domain coexistence beacon at the same position of the DTV pilot to transmit a pilot tone or the coexistence beacon frames. Those frames can broadcast channel information of channel bonding or aggregation. We can adopt the DTV pilot detector to detect the pilot signals of WSDs so that we can have a higher SNR as the DTV pilot detection has. With a high SNR, WSDs can have the improved probability of detection, which means that more WSDs can activate themselves with less interference to and better protection of incumbent users and/or neighboring WSDs. In addition, we can implement  $FCB_{v1}$ -based energy detection at a low cost by adopting the DTV pilot detector. The analysis demonstrates that  $FCB_{v1}$ -based energy detection can achieve a better performance at a low target SNR and a low  $P_f$ . In addition, our analysis confirms that the increased in the total network capacity compensates for the exacerbation of the MAC throughput in an individual white space application. Thus, we expect that the  $FCB_{v1}$  can improve the coexistence of WSDs with a little hardware increment. In addition, the performance evaluation of the  $FCB_{v2}$  demonstrates that the  $FCB_{v2}$  broadcasting channel information of channel bonding or aggregation can contribute to not only increase in the capacity of white space channels but also decrease in the total spectrum sensing time of newly-joining WSDs nearing any active WSDs supporting the  $FCB_{v2}$ .

## 4.6 Appendix A.

Using  $\int_v^\infty x^n e^{-tx} dx = e^{-tv} \sum_{k=0}^n \frac{n!}{k!} \frac{v^k}{t^{n-k+1}}$  [36],  $P_f$  can be expressed as  $P_f = \frac{\Gamma(u, (\frac{\lambda}{2}))}{\Gamma(u)} = \frac{1}{(u-1)!} \int_{(\frac{\lambda}{2})}^\infty x^{u-1} e^{-x} dx = \frac{e^{-(\frac{\lambda}{2})}}{(u-1)!} \sum_{k=0}^{u-1} \frac{(u-1)!}{k!} (\frac{\lambda}{2})^k = e^{-(\frac{\lambda}{2})} \sum_{k=0}^{u-1} \frac{1}{k!} (\frac{\lambda}{2})^k$ . From the above equation, the values of  $\lambda$  in Table 6 are calculated.

This chapter introduces the collaboration-based transmit power control that supports spectrum sharing between homogeneous and/or heterogeneous WSDs with the assistance of the RRM server.

### ***5.1 Motivation of Inter-cell Transmit Power Adaptation***

As mentioned in Chapter 1, WSAPs prefer collaborative TPC mechanisms such as that of 3GPP self-organized network (SON), which operates under the rules of licensed service providers. However, since WSAPs operate in an unlicensed mode, they have no tightly centralized controllers as the assistance of the collaborative TPC mechanism. Instead of tightly centralized controllers, we could consider to use other centralized or distributed controllers, suggested in [8] [10] [11] [52] [53] [42] [43], but since those controllers have no authority on channel management, all previous work do not involve the change of channel configuration such as a current transmit power. However, we believe that those controllers can assist heterogeneous WSAPs to negotiate their new transmit power. Based on this perspective, we suggest the collaboration-based TPC, a so called “inter-cell transmit power adaptation (ITPA),” and the ITPA decision algorithm that aims to support the negotiation-based TPC between WSAPs.

The rest of this chapter consists of following sections: Section 5.2 describes the proposed ITPA algorithm and the extent to which the ITPA negotiation proceeds, and Section 5.3 defines the evaluation metrics for theoretical analysis of the ITPA

algorithm. In addition, Section 5.3 presents all equations and conditions applied to evaluate the ITPA algorithm and the evaluation results. Section 5.4 presents the simulation analysis of the ITPA algorithm-based coexistence mechanism, and Section 5.5 summarizes this chapter.

## **5.2 *Inter-cell Transmit Power Adaptation Algorithm***

To estimate the power margin that neighboring WSAPs can afford to adjust, the ITPA algorithm requires three calculation functions: a distance between two WSAPs, the amount of increase in a noise floor, and the expected received signal strength (RSS) of the signals of WSAPs measured at associated clients.

### **5.2.1 Basic Functions**

To calculate a distance between two WSAPs, the algorithm selects a proper path loss model by referring to location and channel configuration information. We assume that WSAPs broadcast not only location information such as an address or a location type – indoor or outdoor – but also channel configuration information such as their current transmit power,  $P_{tx}$ , the worst path loss between them and their associated clients, and their target SNR,  $P_{snr}$ . Let us assume that neighboring WSAPs operate on the  $i^{th}$  channel, and newly-joining WSAPs select the  $i^{th}$  channel as their operating channel. The newly-joining WSAPs can estimate the path loss between them and neighboring WSAPs using  $P_l = P_{tx} - P_{mr}$ , where  $P_{mr}$  is the measured RSS of the signals of neighboring WSAPs at the center of the newly-joining WSAPs. With the location type of neighboring WSAPs, the newly-joining WSAPs can choose a proper propagation model and a fading model and then calculate the distance  $r$  between the newly-joining WSAPs and the neighboring WSAPs using the inverse function of the following equation:  $P_l = P_{loss}(r, f)$ , where  $P_{loss}$  is the function of path loss models, and  $f$  is the center frequency.

The signals of newly-joining WSAPs as interference generators cause the increase

in the noise floor ( $P_N$ ) of neighboring WSAP as interference victims, and the increase can be calculated using the following equation [28]:

$$\Delta P = \Delta P(P_{er}, P_N, d) = 10 \log \left( 10^{\frac{P_{er}}{10}} + 10^{\frac{P_N}{10}} \right) - P_N, \quad (26)$$

where  $P_{er}$  is the expected RSS of the signals of the newly-joining WSAPs at the  $d$  distance from the center of neighboring WSAPs. Contrary to the fact that we can acquire practically measured RSS of the signals of neighboring WSAPs at the center of the newly-joining WSAPs, we can only estimate the expected RSS of the signals of the newly-joining WSAPs at the center of neighboring WSAPs since newly-joining WSAPs do not really transmit their signals. Instead, we can estimate the expected RSS with the following equation:  $P_{er} = P_{tx} - P_{loss}(d, f)$ , where  $P_{tx}$  is the expected transmit power of newly-joining WSAPs.

The expected RSS of the signals of neighboring WSAPs measured by clients associated with the neighboring WSAPs should be greater than or equal to the sum of  $P_{snr}$  of the neighboring WSAPs, the peak-to-average power ratio (PAPR),  $P_{PR}$ , and the expected RSS of the signals of a newly-joining WSAP. Otherwise, the clients cannot catch the signals of their master WSAPs because of the interference caused by the signals of the newly-joining WSAP operating on the same channel. In addition, the ITPA algorithm conduct the same thing against virtual clients associated with the newly-joining WSAP. However, since the newly-joining WSAP has no associated clients yet, the algorithm simply regards that the newly-joining WSAP has the same clients of the neighboring WSAPs. Thus, the expected RSS of the signals of the newly-joining WSAP at the virtual clients, should be greater or equal to the sum of  $P_{snr}$  of the newly-joining WSAP, the PAPR, and the expected RSS of the signals of the neighboring WSAPs. Now, we can define the desired difference,  $P_{diff}$ , with the following equation:

$$P_{diff} = P_{snr} + P_{PR}, \quad (27)$$

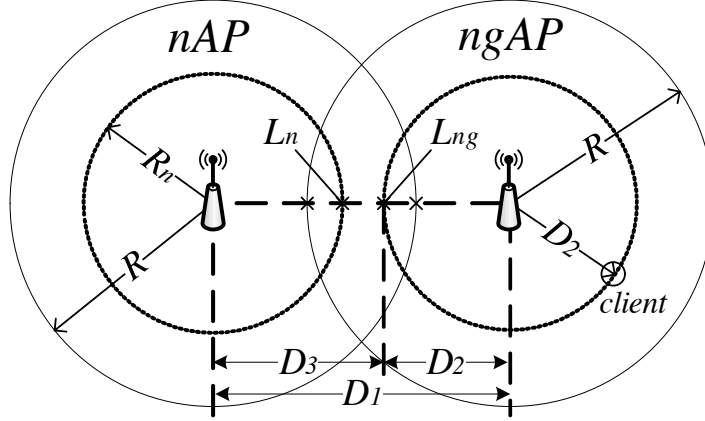


**Figure 24:** Reference model of the ITPA algorithm

where we take the PAPR of 10 dB in this paper, and the ITPA algorithm uses  $P_{diff}$  to check the availability of catching desired signals successfully by filtering out undesired signals.

### 5.2.2 ITPA Algorithm Description

Figure 24 illustrates the reference model of the ITPA algorithm. Let a ngAP denote a neighboring WSAP, and let a nAP denote a newly-joining WSAP. Using  $P_{rx}$  that is the measured RSS of the signals of the ngAP at the nAP and  $P_{tx}$  of the ngAP as the parameters of the inverse function of chosen path loss models, the nAP can estimate the distance,  $D_1$ , between the center of the nAP and the center of the ngAP. In addition, with  $P_{lrx}$  that is the lowest estimated RSS at the clients of the ngAP and  $P_{tx}$  of the ngAP, the nAP can also estimate the active service coverage,  $D_2$ , from the center of the ngAP to its clients that reported  $P_{lrx}$ . Instead of a desired service coverage,  $R$ , the ITPA algorithm regards  $D_2$  as an actual service coverage. Thus, the expected RSS of the signals of the ngAP at the  $D_2$  distance from the center of the ngAP should be greater than or equal to the new  $P_{min}$ , which is the sum of  $P_{snr}$ ,  $P_N$ , and  $\Delta P$ , that should also reflect interference caused by the signals of the nAP. Since  $P_{lrx}$  is the worst path loss between the ngAP and its clients, the algorithm treats the actual distance,  $D_2$ , calculated with  $P_{lrx}$  as the longest distance that the ngAP must

cover.

Thus, as depicted in Figure 24, the strong signals of the ngAP should reach a location,  $L_{ng}$ , where is at the  $D_2$  distance from the center, to provide a better quality-of-service (QoS) to associated clients than a requested QoS at the client that reported the worst path loss. However, since we have to tackle the worst case about the location of the clients, the algorithm assumes that  $L_{ng}$  locates on a straight line between the center of the ngAP and the center of the nAP. Meanwhile, the strong signals of the nAP should reach a location,  $L_n$ , where is at the distance,  $R_n$ , from the center of the nAP. Since the nAP has no real clients, the algorithm adopts  $D_2$  as the desired service coverage,  $R_n$  of the nAP. Using (26), the ITPA algorithm estimates  $\Delta P^{ng}$  at  $L_n$  that is increase, caused by the potential interference from the ngAP, in the noise floor of the nAP and  $P_{diff}$  of the nAP using (27). As depicted in label (a) of Figure 25, the algorithm examines whether the expected RSS of the signals of the nAP,  $P_{rx}^n$ , at  $L_n$  is greater than the new  $P_{min}$  of the nAP, the sum of  $P_{snr}$ ,  $P_{PAPR}$ , and  $\Delta P^{ng}$ , and if not, the algorithm declares that the ITPA negotiation cannot proceed with the ngAP. Otherwise, as depicted in label (b) of Figure 25, the algorithm examines whether the difference between  $P_{rx}^n$  and the expected RSS of the ngAP,  $P_{rx}^{ng}$ , at  $L_n$  is greater than or equal to  $P_{diff}$  of the nAP. If it is, the ITPA algorithm, which regards that the nAP can support its potential clients within a  $R_n$  service coverage, includes the channel where the ngAP operates on into a target list of ITPA negotiation as illustrated in (c) label. Lines 22-29 of Algorithm 4 represents the procedures whether the nAP can accept the ITPA-based spectrum sharing on the channel where the ngAP is operating. If the above operations indicate that the nAP can accept the ITPA-based spectrum sharing, the nAP attempts to investigate whether the ngAP can accept the activation of the nAP with revised channel configuration parameters such as a new or default transmit power of the ngAP on the same channel. At  $L_{ng}$ , the ITPA algorithm estimates  $\Delta P^n$  that is the increase in the noise floor of the ngAP

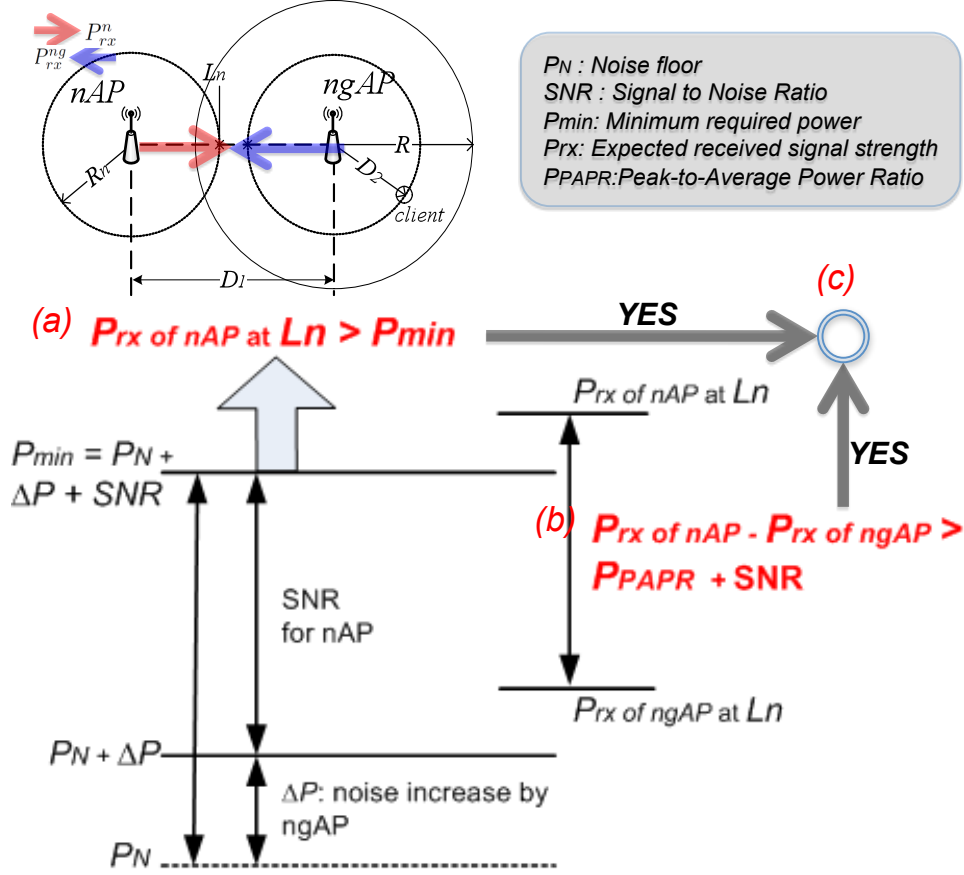


**Figure 25:** Diagram of the extent to which the ITPA algorithm works

and  $P_{diff}$  of the ngAP. With them, the algorithm examines whether the expected RSS of the ngAP,  $P_{rx}^{ng}$ , at  $L_{ng}$  is greater than or equal to the new  $P_{min}$ , the sum of  $P_{snr}$ ,  $P_{PAPR}$ , and  $\Delta P^n$ . If not, the algorithm declares that the ITPA negotiation cannot proceed with the given target channel, where the ngAP is operating on,  $P_{tx}$  of the ngAP, and  $P_{tx}$  of the nAP. Otherwise, the algorithm examines whether the difference between  $P_{rx}^{ng}$  and the expected RSS of the nAP,  $P_{rx}^n$ , at  $L_{ng}$  is greater than or equal to  $P_{diff}$  of the ngAP. If it is, the ITPA algorithm regards that the ngAP can still serve its clients within the  $D_2$  service coverage. Thus, the algorithm concludes that the ngAP and the nAP can coexist on the same channel since both APs can accept ITPA-based coexistence. Lines 30-43 of Algorithm 4 represents the algorithm procedures that decide on whether the ngAP can accept the ITPA-base

spectrum sharing. Before conducting the algorithm, the nAP should have the results of spectrum sensing, which present the received coexistence beacon frames of detected neighboring WSAPs.

The algorithm repeats all above procedures, which examine whether both the nAP and the ngAP can coexist, with all possible changeable channel configuration. If the algorithm finds any affordable channels for the ITPA-based spectrum sharing against all channels listed in the spectrum map, the nAP initiates the ITPA negotiation to the chosen ngAP through the controllers described in Chapter 1. If multiple candidate ngAPs exist, the algorithm might select one of them that requires the least adjustment of its transmit power. However, the proposed ITPA-based spectrum sharing allows other selection approaches to replace the previous mechanism. Figure 25 illustrates the call flow of the ITPA negotiation (refer to the next section). The ngAP has a right to break the coexistence of its operating channel if the ngAP detects decrease in service quality below its minimum SNR. This withdrawal of spectrum sharing can occur when portable clients or the ngAP experiences throughput degradation so they need to increase their transmit power. In this case, the nAP should switch its operating channel to another unused or reusable channels immediately. Thus, the nAP sharing the channel of the ngAP must continue to search unused channels to be able to switch to the new channel immediately.

### **5.2.3 ITPA Negotiation**

As depicted in steps 1-2 of Figure 26, the nAP can extract channel configuration information of neighboring WSAPs, ngAPs, from retrieved beacon frames collected during execution of spectrum sensing. Using them as input parameters of the ITPA algorithm, the nAP is capable of choosing the candidate ngAP for the ITPA negotiation as illustrated in step 3 of Figure 26. Through the Internet connection already established, the nAP can conduct the ITPA negotiation for power adjustment with

---

**Algorithm 4** ITPADecision

---

```
1: procedure ITPADecision( $M, U, V, R_n$ )
2:    $S[] \leftarrow 0$ 
3:   for each channel  $m \in M$  do
4:     Begin
5:       If the number of ngAPs in the channel  $m > 1$  then
6:         go to line 3;
7:       for each TX pwr,  $u \in U$ , for the new AP do
8:         for each TX pwr,  $v \in V$ , for the neighbor AP do
9:           Begin
10:             $w \leftarrow$  FindITPACandidate( $m, u, v, R_n$ )
11:            If  $w \neq Null$  then
12:               $S \leftarrow S \cup (m, u, v, w)$ 
13:            End
14:          End
15:        return  $S$ 
16:   end procedure

17: procedure FindITPACandidate( $m, u, v, R_n$ )
18:   set  $ngAP$  to link to the neighbor AP in the channel  $m$ 
19:   set  $nAP$  to link to the new AP running this algorithm
20:   get  $D_1, D_2$  and  $D_3$ 
21:   If two APs are too close, ( $D_1 < D_2$ ) then
22:     return  $Null$ 
23:   get the desired difference,  $P_{diff}$ , for  $nAP$ 
24:   get  $P_{rx}^n$  from  $nAP$ 's center to  $L_n$  at  $R_n$  distance
25:   get  $P_{rx}^{ng}$  from  $ngAP$ 's center to  $L_n$ 
26:   If  $P_{rx}^{ng} \geq (P_{rx}^n - P_{diff})$  then
27:     return  $Null$ 
28:   get  $\Delta P^{ng}$  caused by  $ngAP$  at  $L_n$ 
29:   If  $P_{rx}^n \geq (P_{min}$  of  $nAP + \Delta P^{ng})$  then
30:     Begin
31:       get the desired difference,  $P_{diff}$ , for  $ngAP$ 
32:       get  $P_{rx}^{ng}$  from  $ngAP$ 's center to  $L_{ng}$  at  $D_2$  distance
33:       get  $P_{rx}^n$  from  $nAP$ 's center to  $L_{ng}$ 
34:       If  $P_{rx}^n \geq (P_{rx}^{ng} - P_{diff})$  then
35:         return  $Null$ 
36:       get  $\Delta P^n$  caused by  $nAP$  at  $L_{ng}$ 
37:       If  $P_{rx}^{ng} \geq (P_{min}$  of  $ngAP + \Delta P^n)$  then
38:         Begin
39:           get ITPA success probability for  $nAP, nP$ 
40:           get ITPA success probability for  $ngAP, ngP$ 
41:           return ( $D_3, nP, ngP$ )
42:         End
43:       End
44:     return  $Null$ 
45:   end procedure
```

---

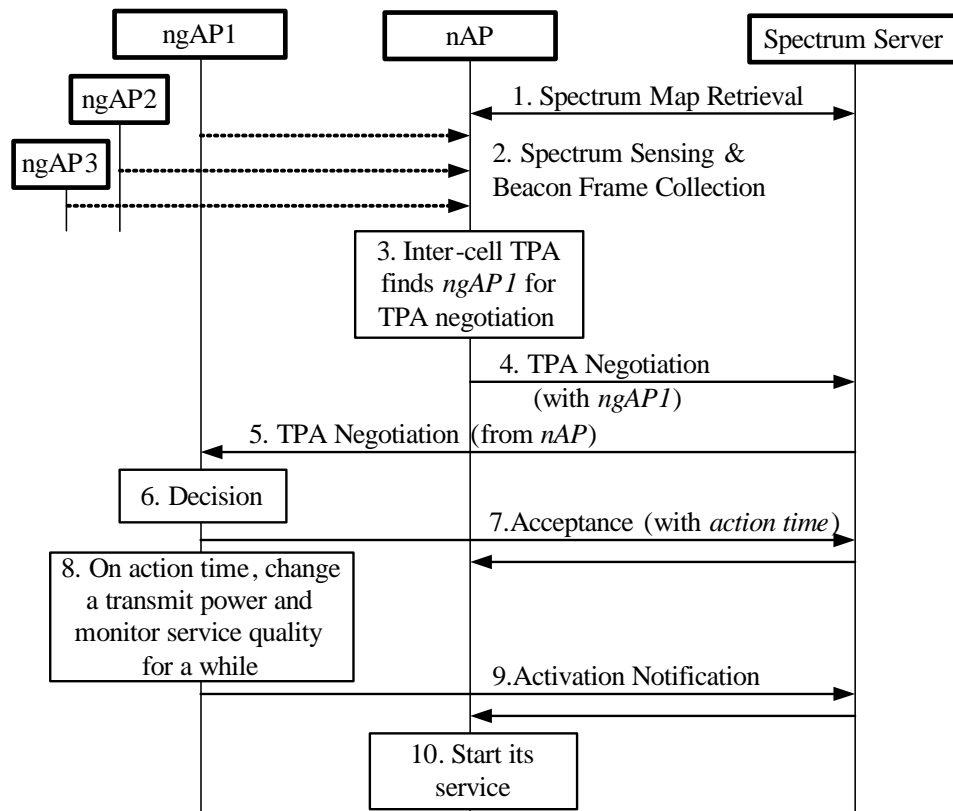


**Figure 26:** A message flow for the ITPA negotiation.

the ngAP directly or indirectly through the RRM server (refer to steps 4-5 of Figure 26). The indirect method allows the ITPA algorithm to be operable between heterogeneous WSAPs. As depicted in steps 6-9, the ngAP replies the acceptance or rejection message to the nAP, and in a case of the acceptance, the reply message shall include two time values, a starting time and a duration time, that is used to monitor new transmit power settings. When the starting time begins, the ngAP first sets its transmit power to the new value. Then, for the duration time, it continues to monitor channel conditions about whether all associated clients do not experience a severe performance degradation with the new transmit power. This grace time aims to let the ngAP have a confidence with the new transmit power. If the ngAP determines to accept the new transmit power as their transmit power, the ngAP informs the nAP of the acceptance through the RRM server as depicted in step 9, and the nAP after all sets its transmitter to the negotiated transmit power value.

### ***5.3 Theoretical Analysis***

For theoretical analysis, we define two evaluation metrics for evaluating the performance of the proposed ITPA algorithm. We only consider the forward link of white space channels since the majority of data transmission occurs in the forward link.

#### **5.3.1 Network and Channel Models**

We adopt the combinations of indoor and outdoor wireless environments and media traffic as the respective reference network model and target application. In addition, we adopt the random waypoint model as the mobility model of the white space clients, WSDs, associated with neighboring WSAPs. Beside the success of spectrum sharing through the ITPA, since the clients of neighboring WSAPs could move around the coverage of the neighboring WSAPs, we need the mobility model to evaluate the extent to two WSAPs operating on the same channel can be affected.

### 5.3.1.1 Outdoor Channel Model

As the channel model for outdoor wireless environments, we adopt Log-normal shadowing [35] and exponential Rayleigh multi-path fading model [32] to calculate the expected mean path loss of an outdoor path,  $P_{loss}^{out}$ , and the expected RSS (ERSS),  $P_{rx}$ , which are expressed as

$$\begin{aligned} P_{loss}^{out}(r, f, d_0) &= L_0 + 10\eta \log(r/d_0) + X \\ P_{rx}(P_{tx}, P_{loss}^{out}) &= -(P_{tx} - P_{loss}^{out}(r, f, d_0)) \ln(1 - \tau), \end{aligned} \quad (28)$$

where  $r$  is the distance of the outdoor path, and  $L_0$ , which is equal to  $10 \log(c/4\pi f)^2$ , is the path loss to the reference distance  $d_0$  ( $= 1$  m).  $f$  is the channel frequency,  $c$  is the light speed, and  $P_{tx}$  is the transmit power of the AP.  $\eta$  ( $= 3$ ) is the log-normal path exponent,  $X$  is a zero-mean Gaussian distribution with standard deviation,  $\sigma$ , and  $\tau$  is a random value between 0 to 1. In the theoretical analysis and the simulation, the reverse function of (28) is used as the function to calculate the distance between two locations. According to the characteristics of outdoor radio propagation loss,  $P_N$  is  $6 - 174 + 10 \log(6 \text{ MHz})$ ,  $\rho$  is from 0.001 to 0.004, and  $\sigma$  has 12 dB [21].  $R_c$  is the distance of sensing coverage, and in this chapter, we assume that the nAP can detect ngAPs within  $R_c$  ( $= 500$  m, which is over three times longer than  $6 \text{ clusters} \times 30 \text{ m}$  average wall distance on IEEE 802.11n Model F [31]).

### 5.3.1.2 Indoor Channel Model

As the channel model for indoor network environments, we adopt a modified Keenan-Motley model [46] as outdoor propagation loss, which is expressed as

$$P_{loss}^{in} = 38.46 + 20 \log_{10} r + qW + Fn^{(n_f+2)/(n_f+1)-0.46}, \quad (29)$$

where  $r$  is the distance of the indoor path, and  $W$  is the wall partition loss (assumed 5 dB), and  $F$  is the floor partition loss (assumed 18.3 dB).  $q$  is number of walls between two locations, and  $n_f$  is the number of floors between two indoor locations. Since

the signals of one WSAP could travel over indoor-to-outdoor or outdoor-to-indoor multiple times to its neighboring WSAPs, in theoretical analysis, we have the need of modeling the ratio of indoor and outdoor paths between two APs. However, in this dissertation, numerical evaluation randomly chooses one among [0.1:0.9, 0.3:0.7, 0.5:0.5, 0.7:0.3, 0.9:0.1] as the ratio of outdoor and indoor parts of a given distance, which is the distance between two WSAPs.

### 5.3.2 Performance Evaluation Metrics

As the evaluation metric, we define an evaluation metric that calculates the probability whether two WSAPs sharing the same channel can continue their service during their overlapped activation time. We have three versions of the evaluation metric according to the different movement models: the model with clients moving at a constant speed and toward uniformly distributed destination, the model with the time-stationary clients, and the model with the portable clients moving randomly. Those metrics aim to assess whether during the overlapped activation time of two WSAPs, they can successfully operate on the sharing channel without performance degradation or with less performance degradation that does not affect the service quality offered to their associated clients. Before three evaluation metrics, we need the basic formulas required for defining the evaluation metrics.

#### 5.3.2.1 Basic Formulas

According to the ITPA algorithm, the nAP declares the acceptance of the ITPA-based spectrum sharing when the expected RSS of the nAP is greater than or equal to the new minimum power  $P_{min}^n = P_{snr} + P_{PAPR} + \Delta P^{ng}$  at the  $L_n$  location. In addition, the nAP declares the acceptance of the ITPA-based spectrum sharing when the expected RSS of the ngAP is greater than or equal to the new minimum power  $P_{min}^{ng} = P_{snr} + P_{PAPR} + \Delta P^n$  at the  $L_{ng}$  location. For the numerical evaluation, we define the probability of interference free (PIF) that calculates the probability

that portable WSDs can successfully retrieve the signals of their desirable WSAPs by overcoming interference caused by their neighboring WSAP sharing the same channel. Thus, we derive the PIF of the nAP at  $L_n$  that is the probability that the following two conditions are met. The first condition is that the expected RSS of the signals of the nAP,  $P_{rx}^n$ , at  $L_n$  is greater than or equal to  $P_{min}'$ . The second condition is that the difference between  $P_{rx}^n$  and  $P_{rx}^{ng}$ , which is the expected RSS of the ngAP at  $L_n$ , is greater than or equal to  $P_{diff}$ . Based on the definition of the PIF for the nAP described previously, the PIF for nAP at the  $L_n$  location is expressed as

$$\begin{aligned} PIF_n &= P(P_{rx}^n > P_{min}') \times P((P_{rx}^n - P_{diff}) > P_{rx}^{ng}) \\ &= P_A(R_n, P_{tx}^{ng}, P_{tx}^n, D_1) \times P'_A(R_n, P_{tx}^{ng}, P_{tx}^n, D_1). \end{aligned} \quad (30)$$

Because the expected RSS follows the Gaussian distribution, we can estimate the  $P_A$  of the PIF using the following equation:  $P_A(d, P_{tx}^a, P_{tx}^v, D) = Q((P_{min}' - P_{rx}(P_{tx}^v, P_{loss}))/\sigma)$ , where  $d$  is the distance to the center of a victim WSAP,  $P_{tx}^a$  is the current transmit power of the aggressor WSAP,  $P_{tx}^v$  is the current transmit power of a victim WSAP, and  $D$  is the distance between two APs.  $Q(x) = (1/\sqrt{2\pi}) \int_x^\infty e^{-\frac{t^2}{2}} dt$  is the Q-function of the normalized Gaussian distribution with standard deviation,  $\sigma$ .  $P'_A$  is expressed as  $P'_A = Q((P_N + P_{diff} + \Delta P) - P_{rx}(P_{tx}, P_{loss}))/\sigma$ .

Like  $PIF_n$ , the PIF for ngAP at the  $L_{ng}$  location is expressed as

$$\begin{aligned} PIF_{ng} &= P(P_{rx}^{ng} > P_{min}') \times P((P_{rx}^{ng} - P_{diff}) > P_{rx}^n) \\ &= P_A(D_2, P_{tx}^n, P_{tx}^{ng}, D_1) \times P'_A(D_2, P_{tx}^n, P_{tx}^{ng}, D_1), \end{aligned} \quad (31)$$

where  $P_{rx}^{ng}$  is the expected RSS of the signals of the ngAP at  $L_{ng}$ , and  $P_{rx}^n$  is the expected RSS of the signals of the nAP at  $L_{ng}$  as noise to the ngAP. Using (30) and (31), we define a general formula for the probability of success in the ITPA negotiation with the following equation.

$$P_s(P_{tx}^n, P_{tx}^{ng}, R_n, D_1, D_2) = PIF_n \times PIF_{ng}. \quad (32)$$

According to (32), we recognize that the success of the ITPA depends on parameters,  $D_1$ ,  $D_2$ ,  $P_{tx}^n$ ,  $P_{tx}^{ng}$ , and  $R_n$ . In general, except  $D_1$  and  $D_2$ ,  $P_{tx}^n$ ,  $P_{tx}^{ng}$  and  $R_n$  are static parameters and given as the input parameters to the algorithm. Thus, we assume that the probability of the success in the ITPA negotiation varies only by  $D_1$  and  $D_2$ . To calculate the expected value,  $E(D_1^l)$ , of  $D_1$  with the  $l^{th}$  neighboring ngAP uses the probability density function (pdf) of the  $l_{th}$  nearest neighbor defined in [45], which is expressed as

$$E(D_1^l) = \int_0^\infty r f_l(r) dr = \int_0^\infty r \frac{2\pi^l \rho^l r^{2l-1}}{(l-1)!} e^{-\pi\rho r^2} dr = \left( \frac{1}{\sqrt{\rho}} \right) \left( \frac{(2l)! l}{(2^l l!)^2} \right), \quad (33)$$

where  $f_l(r)$  is the pdf of the  $l^{th}$  nearest ngAP within a given radius,  $r$ , and  $\rho$  is the density of the WSAPs. Since  $D_2$  is the distance between associated clients and the neighboring WSAPs, if the movement of the clients follows the random waypoint model with a constant movement, the pdf of  $D_2$  is expressed as

$$f_{RP1}(r, R) = f_{RP1}(r, \phi) = f(r) = - \left( \frac{2}{R^4 \pi} \right) r^2 + \frac{2}{R^2 \pi}, \quad (34)$$

where  $R$  is the maximum radius distance. For the analysis of evaluation metrics for different configurations of the movement models, we adopt the pdf,  $f_{RP2}(r, \phi)$ , of the time-stationary distribution of a client location as the pdf of  $D_2$  for the time-stationary clients and the pdf,  $f_{RP3}(r, \phi)$ , of the next waypoint as pdf of  $D_2$  for the next point [6], which are expressed as

$$\begin{aligned} f_{RP2}(r_n, \phi) = f_{RP2}(x, y) &= \frac{45r_n}{32\pi} (1 - r_n) E(r_n^2) \\ f_{RP3}(r_n, \phi) = f_{RP3}(x, y) &= \frac{45}{32\pi} (2r_n^2 \sqrt{B} + 2r_n \arcsin(r_n) - (B) E(r_n^2)), \quad B = 1 - r_n^2, \end{aligned} \quad (35)$$

where  $r_n$  is the radius from the center to  $(x, y)$  and divided by  $R$ , which its value is the converted radius on the unit disk, and  $E(r_n^2) = \int_0^{\pi/2} \sqrt{1 - r^2 \sin^2(\phi)} d\phi$  is the complete elliptic integral of the second kind.

### 5.3.2.2 The Probability of Continuity in the ITPA-based Spectrum Sharing with a Constant Movement

Using (33) and (34), we define the expected probability of success in the ITPA negotiation,  $E(P_{s1}(E(D_1^l), D_2))$ , which is expressed as

$$E(P_{s1}(E(D_1^l), D_2)) = \int_0^R f_{RP1(r,R)} P_s(P_{tx}^n, P_{tx}^{ng}, R_n, E(D_1^l), r) dr. \quad (36)$$

Using (36), we define the probability of continuity in the ITPA-based spectrum sharing,  $S_{ITPA}^{pr}$ , with portable clients constantly moving over a circular area of a neighboring AP, which is expressed as

$$S_{ITPA}^{pr} = \frac{1}{R} \sum_{r=1}^R \{ \{ 1 - \prod_{l=1}^{\alpha N} (1 - E(P_{s1}(E(D_1^l), D_2)) \} \times f_p(r, R) \} \quad (37)$$

$$f_p(r_0, r_m) = f_p(r_0 \leq r_m) = \int_0^{r_0} \int_0^{2\pi} f_{RP1}(r, \phi) r dr d\phi = \frac{r_0^2(2r_m^2 - r_0^2)}{r_m^4},$$

where  $f_p(r_0, r_m)$  is the probability that the client (its distance is  $r_0$ ) stays within  $r_m$  during its movement time, and  $\alpha N$  is the expected number of detected neighboring APs. In the calculation, for all possible values of  $D_2$  from 1 to  $R$ , we calculate the expected probability of continuity in the ITPA-based spectrum sharing with every  $D_2$  value, which is calculated by the probability of success in the ITPA negotiation multiplied by  $f_p(r, R)$  as the weighted factor, and then calculate the average of all calculated expected probability of continuity for all  $D_2$  values. In Section 5.3.4, we investigate  $\alpha N$  with respect to the fact that wireless channels can be reused if two or more WSAPs have a significant distance from each other, and when one AP realizes that all channels are occupied, the number of detected neighboring APs is usually greater than the total number of white space channels.

### 5.3.2.3 The Probability of Continuity in the ITPA-based Spectrum Sharing with a Time-stationary Location of Clients

While  $S_{ITPA}^{pr}$  aims to analyze the probability of continuity in the ITPA-based spectrum sharing when the clients associated with the ngAP moves constantly, in this section,

we analyze the probability of continuity in the ITPA when the clients are time-stationary over a circular coverage of the ngAP. For performance evaluation of the probability of continuity in the ITPA-based spectrum sharing with the time-stationary clients, using (35) and (33), we define the expected probability of success in the ITPA negotiation,  $E(P_{s2}(E(D_1^l), D_2))$ , which is expressed as

$$\begin{aligned}
E(P_{s2}(E(D_1^l), D_2)) &= \int_0^R \int_0^{2\pi} f_{RP2}(r, \phi) P'_s(P_{tx}^n, P_{tx}^{ng}, R_n, E(D_1^l), r) dr d\phi \\
P'_s(P_{tx}^n, P_{tx}^{ng}, R_n, D_1, D_2) &= PIF'_n \times PIF'_{ng} \\
PIF'_{ng} &= P(P_{rx}^{ng} > P''_{min}) \times P((P_{rx}^{ng} - P_{diff}) > P_{rx}^n) \\
P''_{min} &= P_{min} + \Delta P(P_{tx}^a, P_N, f_{d3}(r, \phi)),
\end{aligned} \tag{38}$$

where  $r$  is the distance from the center of the ngAP to their clients, and  $f_{d3}(r, \phi) = \sqrt{(D_1 + r \cos(\beta))^2 + (r \sin(\beta))^2}$  is the distance between the nAP and the clients associated with the ngAP. In the calculation of  $S_{ITPA}^{pr}$ , we assume that associated clients moves around between a straight line between two APs as the ITPA algorithm does. However, in reality, the clients can move to around the coverage of the ngAP as depicted in Figure 27, which means that  $P_s$ ,  $PIF_{ng}$ , and  $P_{min}$  should be redefined to use  $f_{d3}(x, y)$  to calculate  $D_3$ . Using  $f_p(r, R)$  and (38), we define the probability of continuity in the ITPA-based spectrum sharing,  $S_{ITPA}^{sr}$ , with the time-stationary clients locating a circular area of a neighboring AP, which is expressed as

$$S_{ITPA}^{sr} = \frac{1}{R} \sum_{r=1}^R \left\{ \left\{ 1 - \prod_{l=1}^{\alpha N} (1 - E(P_{s2}(E(D_1^l), D_2)) \right\} \times f_p(r, R) \right\}. \tag{39}$$

As the calculation of  $S_{ITPA}^{pr}$  does,  $S_{ITPA}^{sr}$  calculates the average of the probability of success in the ITPA negotiation that is weighted with  $f_p(r, R)$  for all  $D_2$  values from 1 to  $R$ .

#### 5.3.2.4 The Probability of Continuity in the ITPA-based Spectrum sharing with the Next Waypoint

While  $S_{ITPA}^{sr}$  aims to analyze the probability of continuity in the ITPA-based spectrum sharing when the clients associated with the ngAP are time-stationary around a

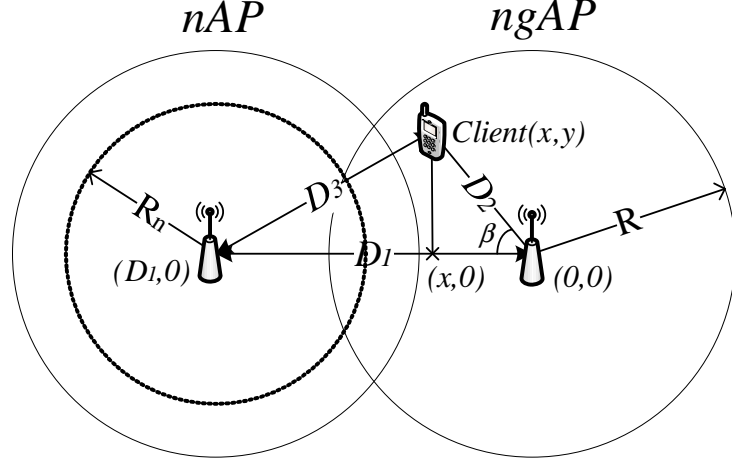


**Figure 27:** A reference model for the analysis of the probability of continuity in the ITPA-based spectrum sharing with a time-stationary location of clients.

circular area, in this section, we define the probability of continuity in the ITPA-based spectrum sharing with the next waypoint. For performance evaluation of the probability of continuity in the ITPA-based spectrum sharing with the next waypoint, we define  $E(P_{s3}(E(D_1^l), D_2))$  that calculates the probability of success in the ITPA negotiation at the next waypoint using the following equation.

$$E[T] = \frac{\bar{l} \ln(v_{max}/v_{min})}{v_{max} - v_{min}}, \quad E[W_n] = E[T_d]/E[T] \quad (40)$$

$$E(P_{s3}(E(D_1^l), D_2)) = \int_0^R \int_0^{2\pi} f_{RP3}(x, y) P'_s(P_{tx}^n, P_{tx}^{ng}, R_n, E(D_1^l), r) dr d\phi,$$

where  $E[T]$  is the mean speed of portable clients when  $v_{max}$  and  $v_{min}$  are the maximum speed and the minimum speed respectively. In our analysis, we adopt  $\bar{l} = 0.905 \times R$ ,  $v_{max} = 0.01m/s$ , and  $v_{min} = 2m/s$ .  $E[T_d]$  is the average activation time of the WSAPs, and we calculate it with the minimum activation time, one hour, and the maximum activation time, three hours, using a bounded Pareto distribution. Based on the equations defined in (40), we define the probability of continuity in the ITPA-based spectrum sharing with the next waypoint,  $S_{ITPA}^{pc}$ , using the average of  $E(P_{s2}(E(D_1^l), D_2))$  and all  $E(P_{s3}(E(D_1^l), D_2))$  during the overlapped activation time of

**Table 11:** Parameters for the numerical evaluation of the ITPA-based spectrum sharing

	Description	Unit	Value
$\rho$	density of WSAPs		[0.001 ~ 0.004]
$R_{io}$	indoor versus outdoor		0.1:0.9 0.3:0.7 0.5:0.5 0.7:0.3 0.9:0.1
$U_i$	unit length of indoor space	m	10+5*rand
N	number of channels		10 30 50 or 30
R	default service radius	m	120
$R_c$	service coverage	m	500
$P_{tx}$	transmit power	dBm	20 15 10
$P_{snr}$	target SNR	dB	10 20 30
$S_{min}$	minimum activation time	sec	1 hour
$S_{max}$	maximum activation time	sec	3 hours

two WSAPs.

$$S_{ITPA}^{pc} = \frac{1}{R} \sum_{r=1}^R \left\{ \left\{ 1 - \prod_{l=1}^{\alpha N} \left( 1 - \frac{E(P_{s2}(D_1, D_2)) + \sum^{E[W_n]} E(P_{s3}(D_1, D_2))}{E[W_n] + 1} \right) \right\} \times f_p(r, R) \right\}. \quad (41)$$

### 5.3.3 Parameters for Numerical Evaluation

Table 11 presents the parameters for calculating the numerical results of three evaluation metrics. As the previous chapters adopt, we adopt the media traffic as the target application. Thus, we choose the values of evaluation parameters according to the characteristics of indoor and outdoor channel environments and media traffic service. To support the target bit error rate (BER) of  $10^{-4}$  for media traffic service, we adopt target SNRs of 10, 20 and 30 dB for QPSK, 16/32 QAM and 256 QAM modulations, respectively [16]. As described in Section 5.3.1.2, the numerical evaluation randomly chooses one among [0.1:0.9, 0.3:0.7, 0.5:0.5, 0.7:0.3, 0.9:0.1] as the ratio between outdoor and indoor paths of a given distance between two APs. In addition, since we assume that the unit of one apartment is  $10\text{m} \times 10\text{m}$ , the unit length of indoor space is around [10 ~ 15] m. We assume that the WSAPs occupy their operating channel from one hour to three hours, which will be enough time for associated white space devices to process streaming or download media traffic.

### 5.3.4 Calculation of Expected Number of Detected Neighboring WSAPs

To evaluate three metrics, we need to calculate the expected number of detected neighboring WSAPs. Thus, we define the ratio of two numbers, called channel occupancy rate (COR), which is expressed as

$$COR = \alpha = N_{ng}/N, \quad (42)$$

where  $N_{ng}$  is the number of detected neighboring WSAPs. To calculate the COR, we conduct the simulation that distributes all inactive WSAPs within an area,  $\pi \times R_c^2$ , where  $R_c = 500\text{ m}$  is the maximum distance, and activates them one by one. Then, the simulation counts the number of detected neighboring WSAPs of every activated WSAP for all cases of the combination of  $N$  ( $= 10, 30, \text{ and } 50$ ) and  $P_{snr}$  (10, 20, and 30 dB), and calculates the average number of detected neighboring WSAPs for all cases. In the calculation of the path loss, the simulation chooses randomly the ratio of indoor and outdoor spaces between two WSAPs,  $R_{io}$ , the number of floors, and the number of walls which the signals of the neighboring WSAP travel toward the center of the newly-joining WSAP. To investigate the extent to which spectrum search with the ITPA-based spectrum sharing or not, the simulation conducts two cases of the channel assignment: one enables the ITPA-based spectrum sharing, and another disables the ITPA-based spectrum sharing. The simulation enabling the ITPA-based spectrum sharing estimates the calculated average number of detected neighboring WSAPs as the COR with ITPA while the simulation disabling the ITPA does the calculated one as the COR without the ITPA. The simulation as the numerical evaluation does randomly chooses one among [0.1:0.9, 0.3:0.7, 0.5:0.5, 0.7:0.3, 0.9:0.1] as the ratio between outdoor and indoor paths of a given distance between two WSAPs.

Tables 12 and 13 present calculated COR values of all cases with the ITPA and without the ITPA respectively. We observed that the COR with the ITPA is greater

---

<sup>1</sup> With  $N = 50$  and  $\rho = 0.001$ , all activate APs succeeded in finding their operating channel. They are excluded in the calculation of  $\alpha n$ .

**Table 12:** COR( $\alpha$ ) without the ITPA for  $P_{snr} = 10, 20$  and 30 dB

	$P_{snr} = 10$ dB			$P_{snr} = 20$ dB			$P_{snr} = 30$ dB		
Density	N = 10	30	50	N = 10	30	50	N = 10	30	50
0.001	2.603	2.763	3.011	2.831	2.908	2.686	2.739	2.840	2.788
0.002	2.935	3.446	3.367	3.040	2.781	3.029	2.746	2.816	2.730
0.003	3.272	2.941	2.979	3.016	3.064	3.02	2.922	2.894	2.929
0.004	3.556	3.020	3.163	2.864	3.126	2.925	2.921	2.957	2.752
Avg.	3.092	3.043	3.130	2.938	2.970	2.916	2.832	2.877	2.799

**Table 13:** COR( $\alpha$ ) with the ITPA for  $P_{snr} = 10, 20$  and 30 dB

	$P_{snr} = 10$ dB			$P_{snr} = 20$ dB			$P_{snr} = 30$ dB		
Density	N = 10	30	50	N = 10	30	50	N = 10	30	50
0.001	3.467	3.365	3.742	3.575	2.937	2.916	0 <sup>1</sup>	0	0
0.002	3.421	3.867	3.319	3.325	3.282	3.335	0	2.860	3.094
0.003	3.516	3.344	3.078	3.427	3.095	3.325	0	2.817	3.156
0.004	3.973	3.423	3.822	3.290	3.434	3.575	2.910	3.457	3.414
Avg.	3.594	3.500	3.490	3.405	3.187	3.288	2.910	3.044	3.191

than the COR without the ITPA over approximately 0.5. In addition, as the  $P_{snr}$  increases, the COR value decreases since WSAPs require a more margin to meet a higher SNR. For instance, in a case of the COR without the ITPA for a target SNR = 10 dB and  $N=10$ , the COR is 3.092 while the COR is 2.832 for a target SNR = 30 dB. Based on all values on two tables, we calculate the average of  $\alpha$  for  $N = 10, 30$  and 50 as shown in Table 14. We have the mean of  $\alpha$ , approximately 2.9, as the mean of the COR without the ITPA and the mean of  $\alpha$ , approximately 3.3, as the mean of the COR with the ITPA. With  $\alpha \approx 2.9$  and 3.3, we have  $\alpha N \approx 87$  and 100

**Table 14:** Average of COR( $\alpha$ ) with the ITPA vs. without ITPA for  $P_{snr} = 10, 20$  and 30 dB

Average COR w.o. the ITPA			Average COR w. the ITPA		
$\alpha$	N	$\alpha N$	$\alpha$	N	$\alpha n$
2.954	10	31	3.303	10	34
2.963	30	90	3.243	30	98
2.936	50	141	3.323	50	152
mean of $\alpha \approx 2.9$			mean of $\alpha \approx 3.3$		

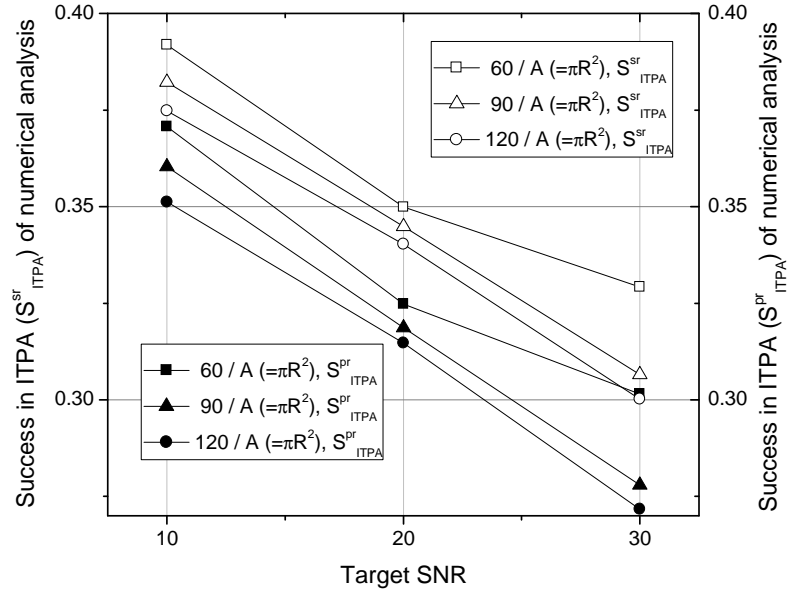
respectively, and based on previous observations, we define three values,  $60/A$ ,  $90/A$ , and  $120/A$ , which  $A$  is the unit area ( $500\text{m} \times 500\text{m}$ ), as the density of WSAPs for the numerical evaluation of three evaluation metrics,  $S_{ITPA}^{pr}$ ,  $S_{ITPA}^{sr}$ , and  $S_{ITPA}^{pc}$ .  $60/A$  means that the expected number of detected active neighboring WSAPs is about 60, and we adopt 60, 90, and 120 to consider a variance in the number of detected neighboring WSAPs.

### 5.3.5 Numerical Results

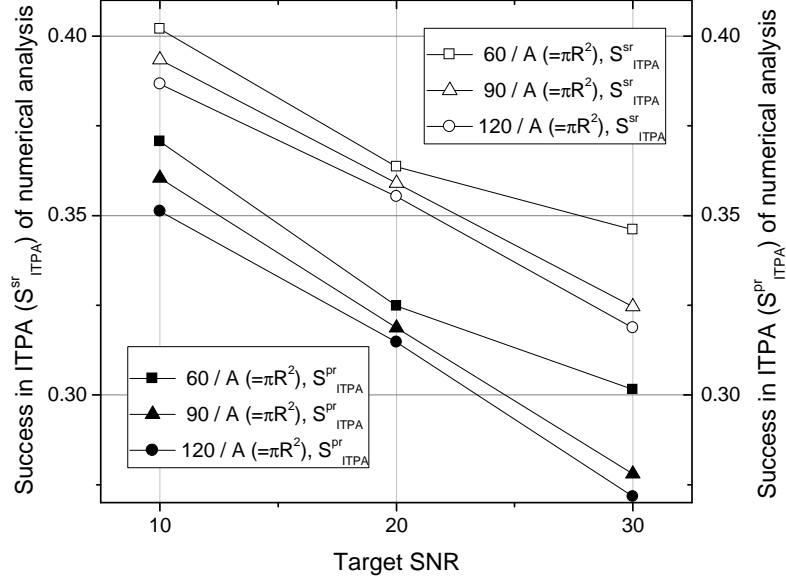
For our numerical evaluation, we select  $N = 30$  as the total number of available channels based on two reports of New American Foundation, Tech. Rep [33] [40].

#### 5.3.5.1 $S_{ITPA}^{pr}$ versus $S_{ITPA}^{sr}$

Figure 28 depicts the numerical results of the probability of continuity with the ITPA-based spectrum sharing for constant moving clients,  $S_{ITPA}^{pr}$ , and the probability of continuity with the ITPA-based spectrum sharing for time-stationary clients,  $S_{ITPA}^{sr}$  in a case of  $\alpha \approx 2.9$  and the maximum floors (MF) = 2. The open symbols represent  $S_{ITPA}^{sr}$  while the solid symbols do  $S_{ITPA}^{pr}$  in Figure 28. For all cases of  $P_{snr} = 10$  and 20 dB, we can expect over 30% in  $S_{ITPA}^{pr}$  and  $S_{ITPA}^{sr}$ , which means that 30% of WSAPs failed to find their operating channel, can find their operating channel through the ITPA-based spectrum sharing. In addition, as depicted in Figure 28(a) and 28(b), when clients are time-stationary, for  $P_{snr} = 30$  dB, we can also expect over 30% in  $S_{ITPA}^{sr}$ . Compared to  $S_{ITPA}^{pr}$ ,  $S_{ITPA}^{sr}$  shows increase over 2~3% as depicted in Figure 28(a) and 28(b). Thus, we expect that the ITPA-based spectrum sharing with the time-stationary clients associated with neighboring WSAPs can achieve a better success in the ITPA negotiation and continuity in service than the ITPA-based spectrum sharing with a constant movement of clients. In a matter of the maximum number of floors, at MF = 10,  $S_{ITPA}^{pr}$  and  $S_{ITPA}^{sr}$  in general are greater than  $S_{ITPA}^{pr}$  and  $S_{ITPA}^{sr}$  at MF = 2 as illustrated in two subfigures of Figure 28. The results are



(a) The mean of  $S_{ITPA}^{sr}$  versus the mean of  $S_{ITPA}^{pr}$



(b) The highest  $S_{ITPA}^{sr}$  versus the highest  $S_{ITPA}^{pr}$

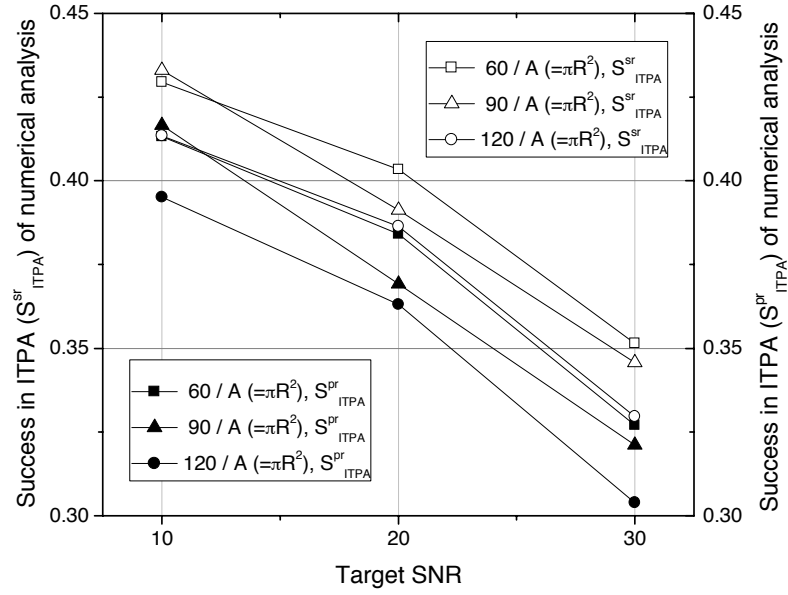
Figure 28:  $S_{ITPA}^{pr}$  versus  $S_{ITPA}^{sr}$  with  $\alpha \approx 2.9$  and MF = 2.

opposite to a fact that with the same density of WSAPs, a lower path loss occurs at the area of higher stories so that it can contribute less chances in the success the ITPA-based spectrum sensing, and in Section 5.4.4, we present the detailed analysis about this awkward results by comparing to the simulation results.

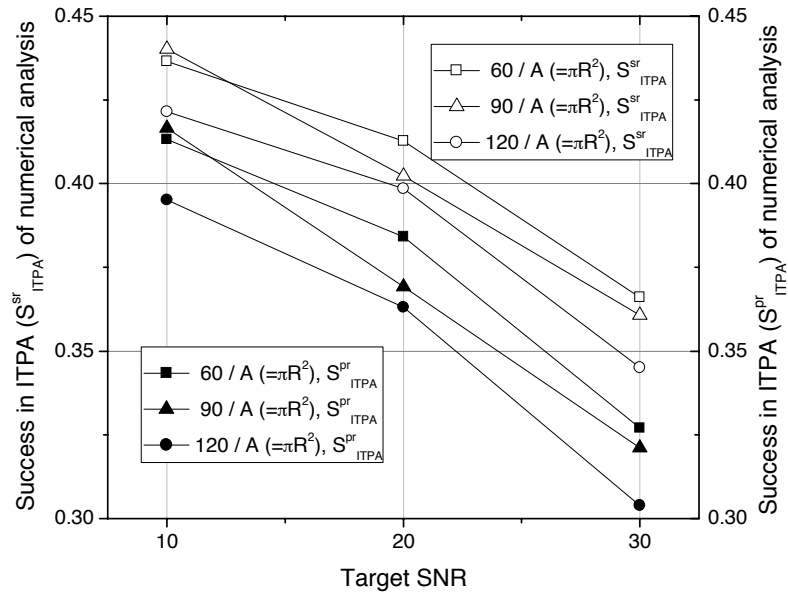
We observe similar numerical results for the case of  $\alpha \approx 2.9$  and MF = 10 as depicted in Figure 29, which  $S_{ITPA}^{sr}$  is greater than over 1~2.5%. For the case of  $\alpha \approx 3.3$ , the difference between  $S_{ITPA}^{pr}$  and  $S_{ITPA}^{sr}$  is around 2% as depicted in Figure 30. Although both  $S_{ITPA}^{pr}$  and  $S_{ITPA}^{sr}$  have the least values at  $P_{snr} = 30$  dB, either with MF = 10 or with  $\alpha \approx 3.3$ ,  $S_{ITPA}^{pr}$  and  $S_{ITPA}^{sr}$  have over 30%. Thus, within less than 3% in variance, the numerical results of  $S_{ITPA}^{pr}$  and  $S_{ITPA}^{sr}$  demonstrate that the ITPA-based spectrum sharing can contribute to supporting over 30% of WSAPs, which have failed to search their operating channel with spectrum sensing methods, to share the channel owned by the neighboring WSAPs at rather low target SNRs such as  $P_{snr} = 10$  and 20 dB.

### 5.3.5.2 $S_{ITPA}^{sr}$ versus $S_{ITPA}^{pc}$

Figure 31 depicts the numerical results of the probability of continuity with the ITPA-based spectrum sharing for the time-stationary clients,  $S_{ITPA}^{sr}$ , and the probability of continuity with the ITPA-based spectrum sharing for the next waypoint,  $S_{ITPA}^{pc}$  in the cases of  $\alpha \approx 2.9$  and  $\alpha \approx 3.3$  when MF is 2. Compared to  $S_{ITPA}^{sr}$ ,  $S_{ITPA}^{pc}$  shows increase in 2~3% for  $\alpha \approx 2.9$  and MF = 2, and we observe the similar pattern on the comparison results for the cases of  $\alpha \approx 3.3$ . The increase is around 1% as depicted in Figure 32. Based on observed numerical results, the comparison of  $S_{ITPA}^{pc}$  and  $S_{ITPA}^{sr}$ , the ITPA-based spectrum sharing can contribute to increase in the success of channel assignment by assisting around 30% of WSAPs failed in the first search of their operating channel to share the channel of the neighboring WSAP whatever configuration of the movement models we adopt for the theoretical analysis.

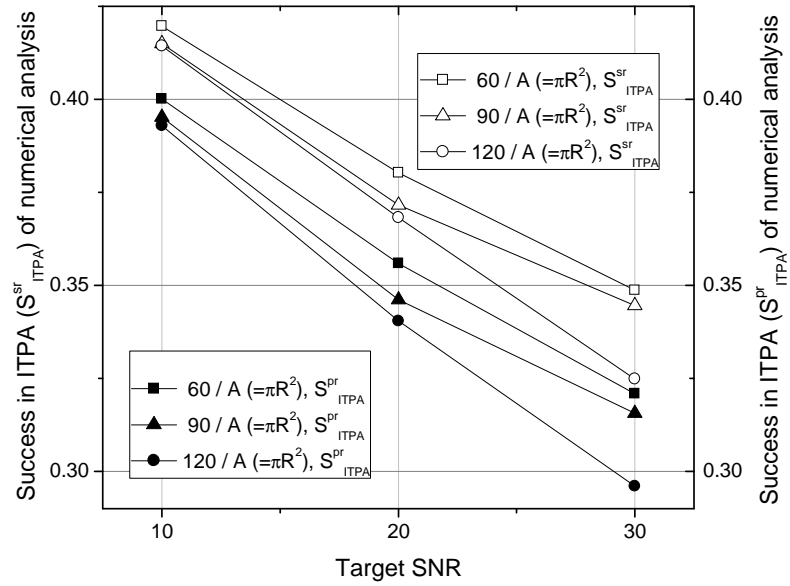


(a) The mean of  $S_{ITPA}^{sr}$  versus the mean of  $S_{ITPA}^{pr}$

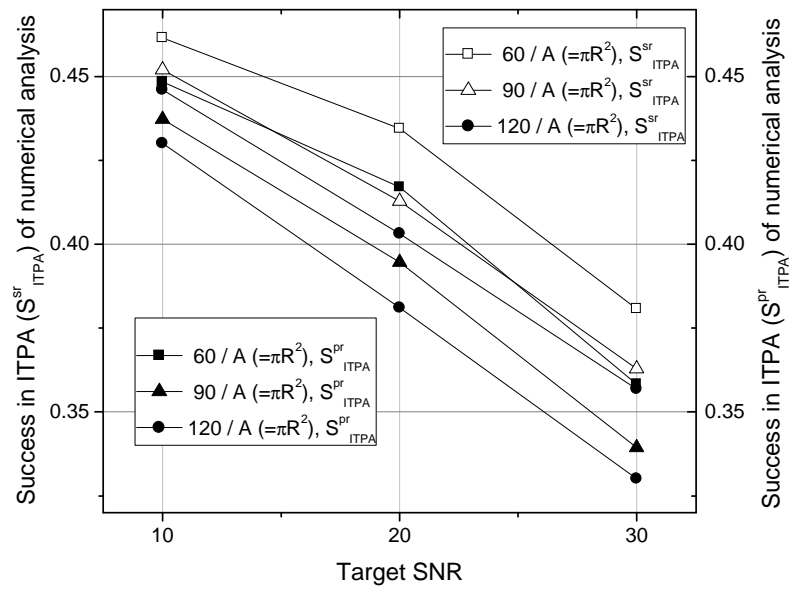


(b) The highest  $S_{ITPA}^{sr}$  versus the highest  $S_{ITPA}^{pr}$

Figure 29:  $S_{ITPA}^{pr}$  versus  $S_{ITPA}^{sr}$  with  $\alpha \approx 2.9$  and MF = 10.

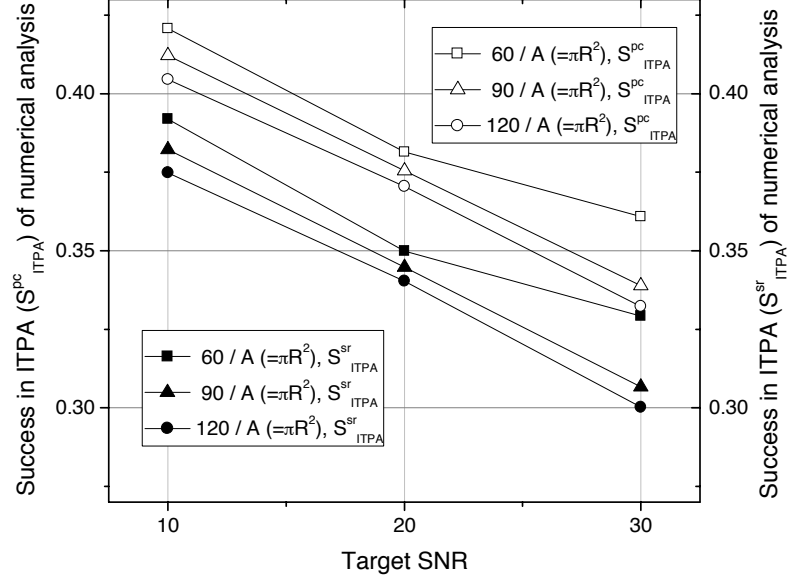


(a)  $S_{ITPA}^{sr}$  versus  $S_{ITPA}^{pr}$  for MF = 2

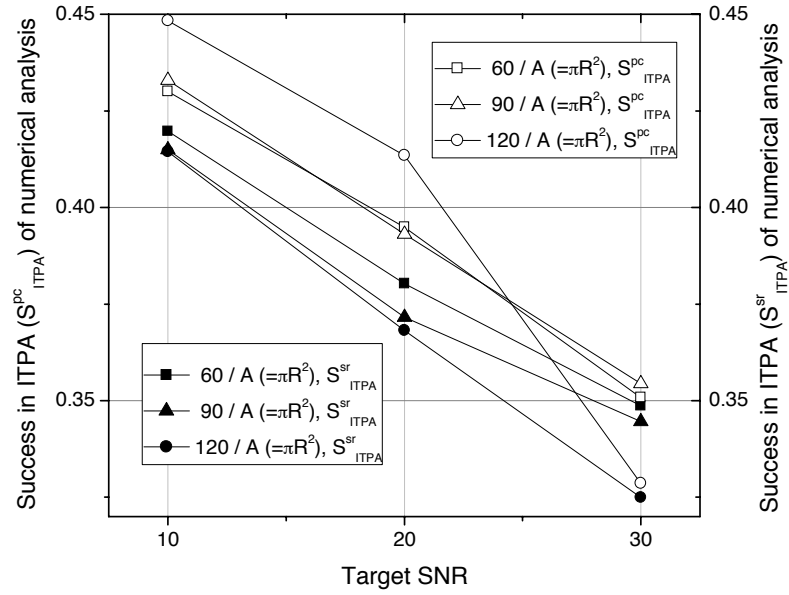


(b)  $S_{ITPA}^{sr}$  versus  $S_{ITPA}^{pr}$  for MF = 10

Figure 30:  $S_{ITPA}^{pr}$  versus  $S_{ITPA}^{sr}$  with  $\alpha \approx 3.3$  and MF = 2 and 10.



(a)  $S_{ITPA}^{pc}$  versus  $S_{ITPA}^{sr}$  for  $\alpha \approx 2.9$



(b)  $S_{ITPA}^{pc}$  versus  $S_{ITPA}^{sr}$  for  $\alpha \approx 3.3$

Figure 31:  $S_{ITPA}^{pc}$  versus  $S_{ITPA}^{sr}$  with  $\alpha \approx 2.9$  and  $3.3$  for  $MF = 2$ .

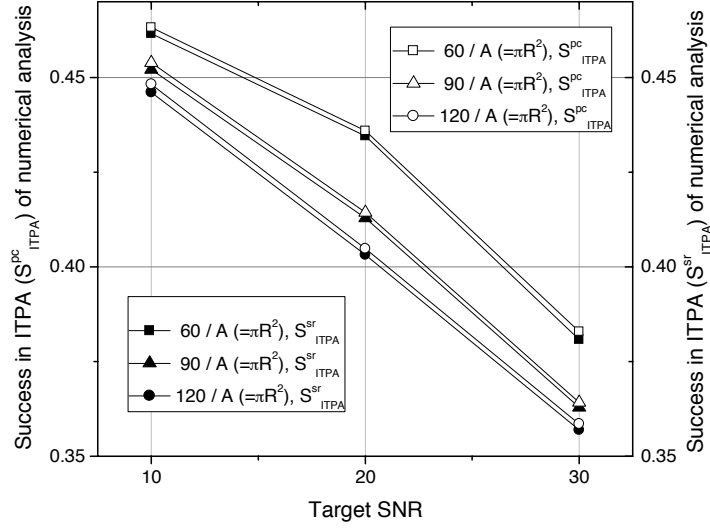


Figure 32:  $S_{ITPA}^{pc}$  versus  $S_{ITPA}^{sr}$  with  $\alpha \approx 3.3$  for MF = 10.

### 5.3.6 Summary of Theoretical Analysis

As the density of WSAPs increases, the values of three probability parameters,  $S_{IPTA}^{sr}$ ,  $S_{IPTA}^{sr}$  and  $S_{IPTA}^{pc}$ , also decrease. The numerical evaluation demonstrates that the ITPA-based spectrum sharing with clients moving randomly has the highest probability of success in spectrum sharing compared to the ITPA-spectrum sharing with the other cases. However, since the differences between them having different configurations of the movement models are a few percentages, we can expect the ITPA-based spectrum sharing can contribute to increase in the success of channel assignment of 20~40% of newly-joining WSAPs that have failed in the first channel assignment with spectrum sensing.

## 5.4 Analysis of Simulation

For the realistic performance evaluation of the ITPA-based spectrum sharing, we conduct the simulation that adopts the urban model as the simulation model.

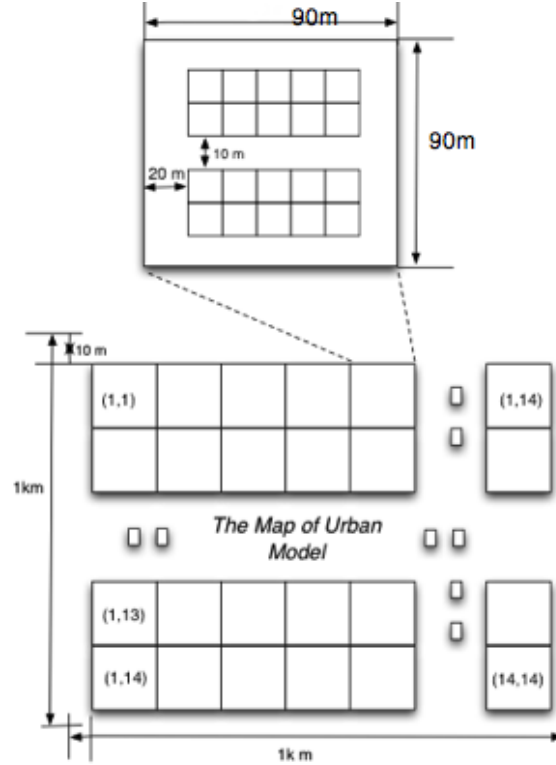


**Figure 33:** The simulation model for the ITPA performance evaluation

#### 5.4.1 The Simulation Model

In our simulation model, within  $1\text{km} \times 1\text{km}$  inter-site distance as [46] did, the simulation distributes 2000 apartments randomly among apartment blocks consisting of two buildings, where one building has up to 20 apartment units when the number of floors is 2 while it has up to 200 units when the maximum number of floors is 10. Each unit is  $10\text{m} \times 10\text{m} \times 10\text{m}$  (width  $\times$  length  $\times$  height), and between two apartment blocks, a street (width=20m) exists. As illustrated in Figure 33, this model has  $14 \times 14$  blocks with a guard distance, 10m, in the border of the simulation area. For the distribution of the WSAPs, the simulation randomly selects one block and the number of floors between 2 and 10. Then, by multiplying 20 by the selected number of floors, the simulation determines the number of assigned apartments to the previously selected block. The simulation continues to conduct previous procedures

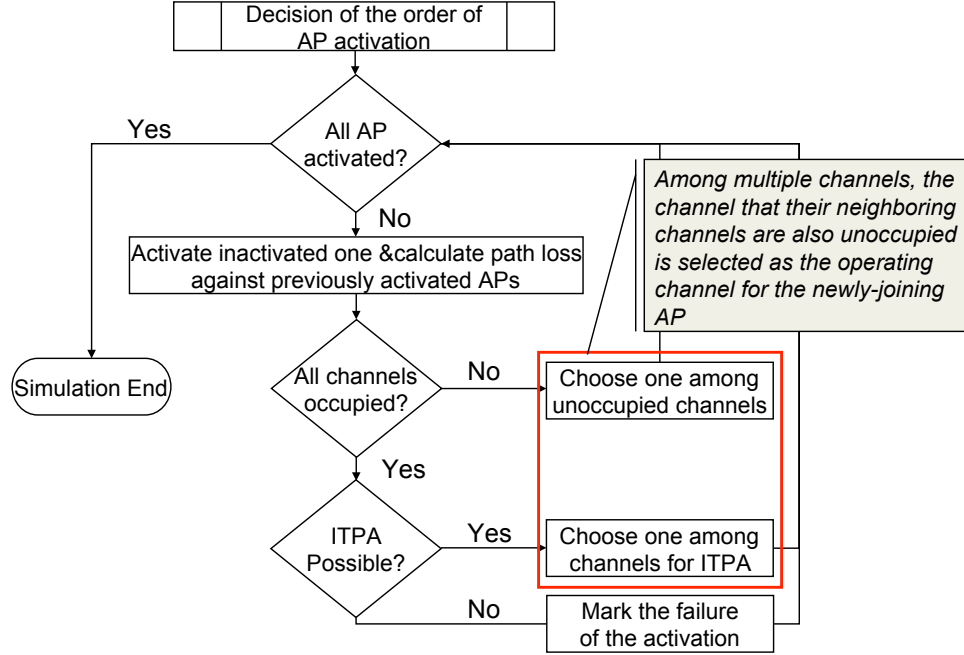


**Figure 34:** The procedures for activating WSAPs in the simulation

for distributing apartments until the simulation finishes the allocation of 2000 apartments. After allotting all apartments, we also assign WSAPs to allocated apartments and conduct the procedures of activating assigned WSAPs that execute the search of their operating channel. Figure 34 illustrates the procedures of the WSAP activation in the simulation. The simulation conducts the same procedures for the activations of all WSAPs. Whenever any WSAPs discover no more spare channels, they conduct the ITPA algorithm implemented in the simulation.

#### 5.4.2 Parameters for Simulation

Table 15 shows the parameters for the simulation. The activation rate of WSAPs (AR) is the rate of the activated WSAPs among 2000 WSAPs that will be potentially activated. For instance,  $AR=0.448$  means that  $0.448 \times 2000$  apartments have the WSAPs that will attempt to activate themselves one by one.  $M$  has 0 if clients associated with neighboring WSAPs are nomadic and 1 if the clients move randomly around the coverage of neighboring WSAPs. In fact, throughout the simulation,

**Table 15:** Parameters for the ITPA-based spectrum sharing simulation

	Description	Unit	Value
AR	activation rate of WSAPs		0.448, 0.560, 0.700
N	number of channels		30
R	default service radius	m	120
$R_c$	service coverage	m	500
$P_{tx}$	transmit power	dBm	20 15 10
$P_{snr}$	target signal-to-ratio	dB	10 20 30
$S_{min}$	minimum activation time	sec	1 hour
$S_{max}$	maximum activation time	sec	3 hours
$M$	stationary or random waypoint	sec	0 (Stationary), 1
$MF$	maximum Floors		2, 10

we observed around 100 or 120 detected neighboring WSAPs, which is analogous to  $100/A$  or  $120/A$  of the numerical evaluation as shown in Table 16. Thus, we compare

**Table 16:** Calculated number of detected neighboring WSAPs during the simulation

M = 0	Max Floors = 2				Max Floors = 10			
AR	$P_{snr} = 10$ dB	20	30	Random	10	20	30	Random
0.448	102	102	101	101	111	112	111	111
0.560	109	105	105	106	118	118	115	116
0.700	108	108	107	107	119	117	113	116
M = 1	Max Floors = 2				Max Floors = 10			
AR	$P_{snr} = 10$ dB	20	30	Random	10	20	30	Random
0.448	103	102	99	100	116	116	114	116
0.560	107	105	106	105	117	117	114	117
0.700	108	106	108	106	115	114	115	113

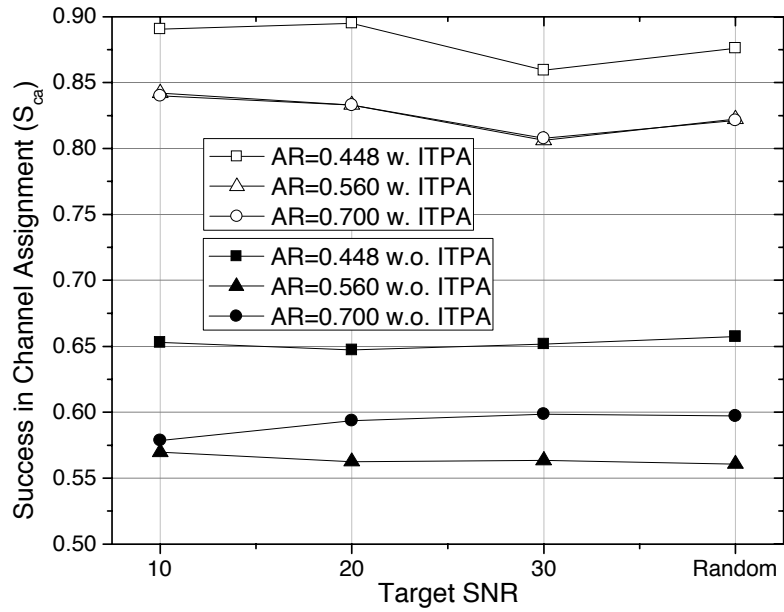
the results of the simulation for  $MF = 2$  to the numerical results of theoretical analysis for  $MF = 2$  and  $\alpha \approx 3.3$ , which its expected number of detected neighboring WSAPs is between 90 and 120.

### 5.4.3 The Probability of Success in Channel Assignment

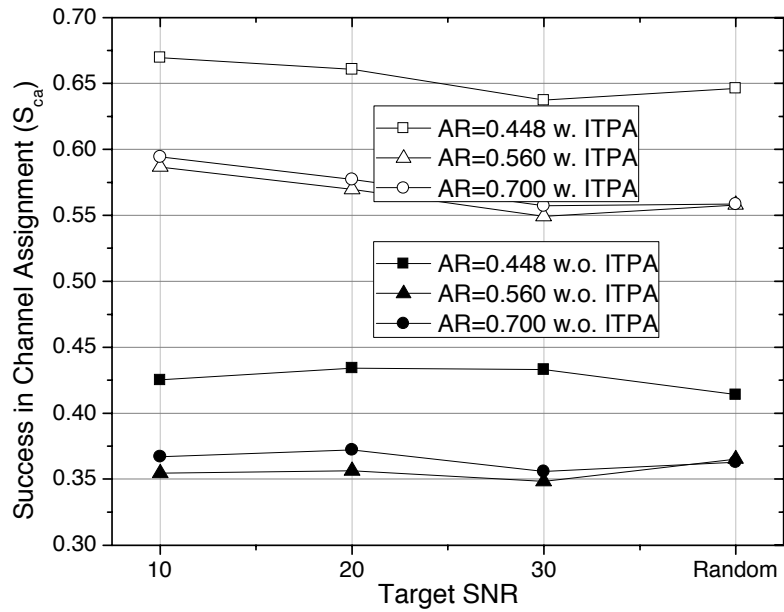
In the simulation, we estimate the probability of success in the channel assignment with the assumption that clients are stationary, which is express as  $S_{wITPA}^{ca} = ((N_{ts} + N_{is})/N_{tot})$ , where  $N_{ts}$  is the number of success in a channel assignment with typical spectrum sensing methods,  $N_{is}$  is the number of success in the channel assignment

with the ITPA-based spectrum sharing and  $N_{tot}$  is the number of all attempts for the channel assignment. For calculating the probability of success in a channel assignment without the ITPA-based spectrum sharing, we define  $S_{woITPA}^{ca} = (N_{ts}/N_{tot})$ .

Figure 35 depicts the simulation results of  $S_{wITPA}^{ca}$  and  $S_{woITPA}^{ca}$  for  $M = 0$ , which means that clients are stationary, and the open symbols represent the results of  $S_{wITPA}^{ca}$  while the solid symbols do the results of  $S_{woITPA}^{ca}$ . At  $MF = 2$  and  $10$ , the difference between  $S_{wITPA}^{ca}$  and  $S_{woITPA}^{ca}$  is over 20% for all target SNRs. In addition, the difference between  $S_{wITPA}^{ca}$  for  $MF = 2$  and  $S_{woITPA}^{ca}$  for  $MF = 10$  is around 20% as the difference between  $S_{wITPA}^{ca}$  for  $MF = 2$  and  $S_{woITPA}^{ca}$  for  $MF = 10$  is over 20%. This difference is based on the fact that WSAPs locating in a densely populated area surrounded by high-story buildings can suffer from interference caused by neighboring WSAPs more seriously than the case that neighboring WSAPs as interference sources locate in the least populated area. As observed in the simulation results of  $S_{wITPA}^{ca}$  and  $S_{woITPA}^{ca}$  for  $M = 0$ , the simulation results of  $S_{wITPA}^{ca}$  and  $S_{woITPA}^{ca}$  for  $M = 1$ , which clients follow the random waypoint mobility model, demonstrate over 20% increase, as illustrated in Figure 36, because of the ITPA-based spectrum sharing. In addition, we observed that the difference between  $S_{wITPA}^{ca}$  and  $S_{woITPA}^{ca}$  for  $M = 1$  is over 20%. The simulation results demonstrate this increase, 20%, even with a higher SNR like 30 dB. Thus, the previous observations confirm that the ITPA-based spectrum sharing contributes to increase around 20% in the success of the channel assignment by allowing WSAPs, which originally failed in a channel search with typical spectrum sensing methods, to find another channel that can be shared with the neighboring WSAP operating on the channel already. Through examining the difference between  $S_{wITPA}^{ca}$  of  $M = 0$  and  $S_{wITPA}^{ca}$  of  $M = 1$ , we observed the difference increases as the target SNR ( $P_{snr}$ ) approaches a higher one like 30 dB when  $MF$  is 10 as depicted in label (a) of Figure 37 although the difference is less than 0.1. In addition, as illustrated in label (b) of Figure 37, the difference of  $S_{ITPA}^{ca}$  increases with

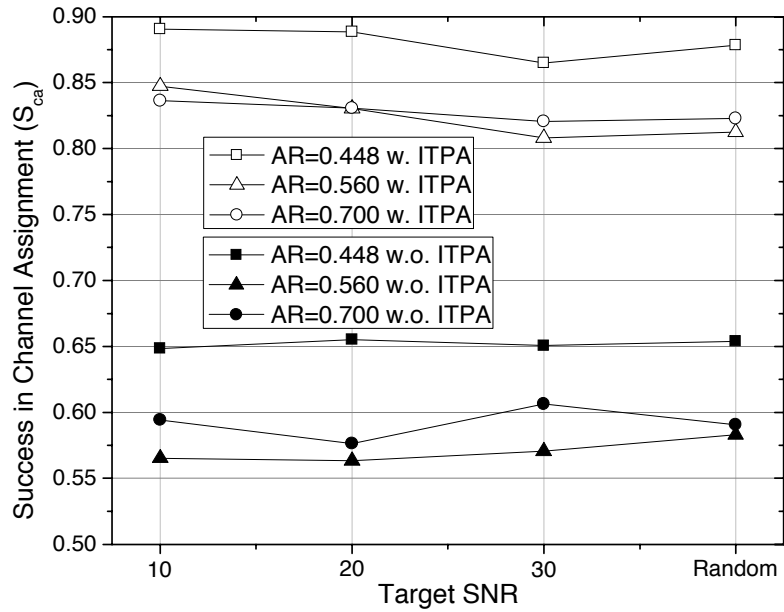


(a)  $S_{wITPA}^{ca}$  versus  $S_{woITPA}^{ca}$  for MF = 2

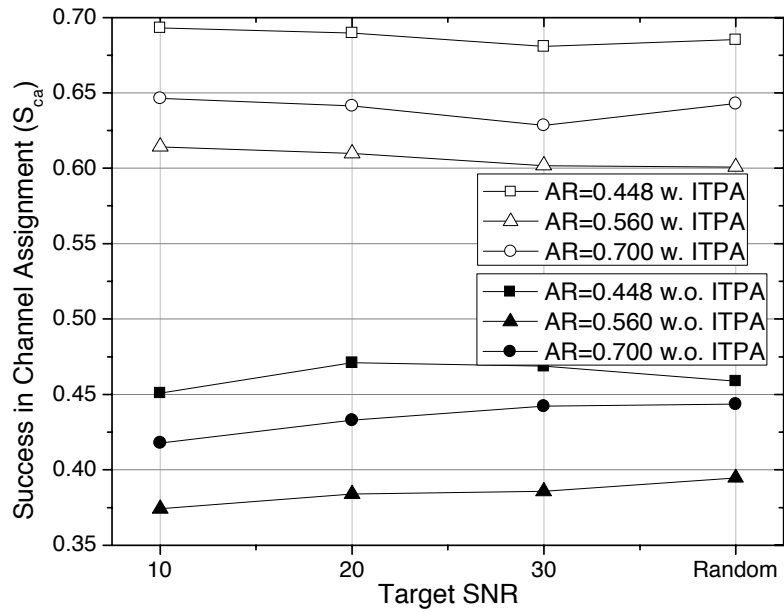


(b)  $S_{wITPA}^{ca}$  versus  $S_{woITPA}^{ca}$  for MF = 10

**Figure 35:**  $S_{wITPA}^{ca}$  versus  $S_{woITPA}^{ca}$  with M = 0.



(a)  $S_{wITPA}^{ca}$  versus  $S_{woITPA}^{ca}$  for MF = 2



(b)  $S_{wITPA}^{ca}$  versus  $S_{woITPA}^{ca}$  for MF = 10

Figure 36:  $S_{wITPA}^{ca}$  versus  $S_{woITPA}^{ca}$  with M = 1.

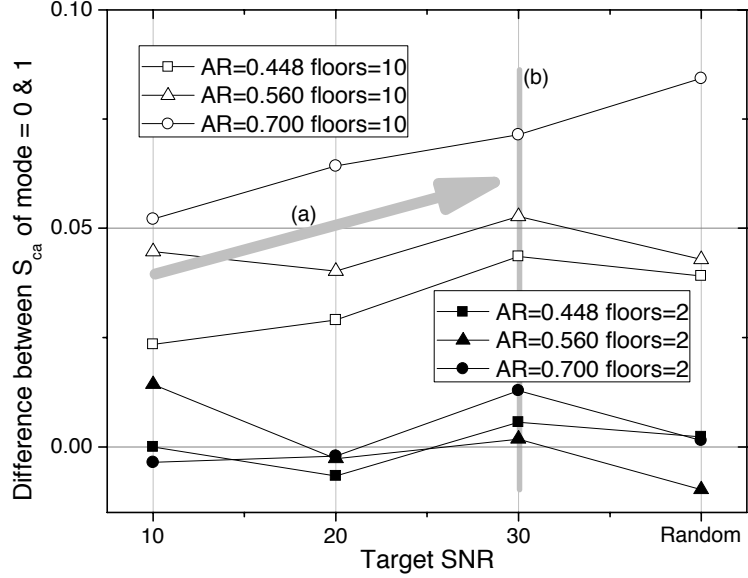


**Figure 37:** The difference between  $S_{wITPA}^{ca}$  for  $M = 0$  and  $S_{wITPA}^{ca}$  for  $M = 1$  at MF = 2 (represented by the solid symbols). The difference between  $S_{wITPA}^{ca}$  for  $M = 0$  and  $S_{wITPA}^{ca}$  for  $M = 1$  at MF = 10 (represented by the open symbols)

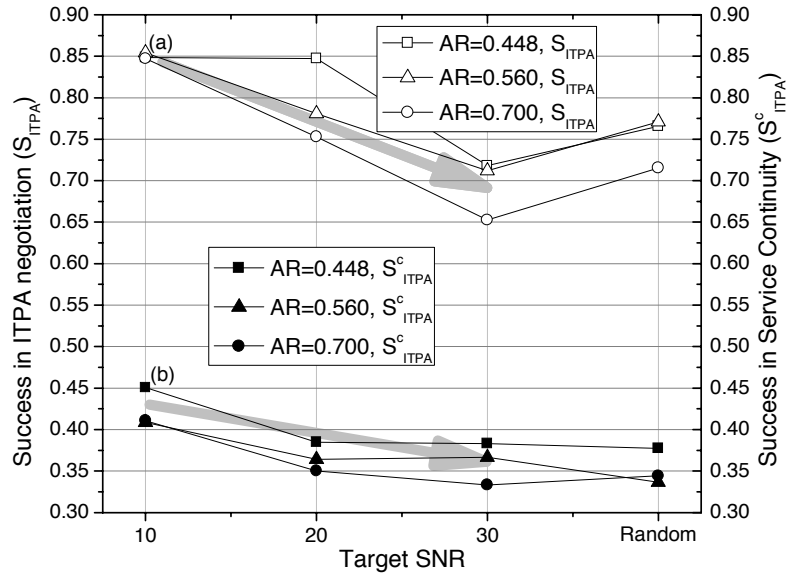
$M = 1$  since the availability of the ITPA-based spectrum sharing with a higher SNR is sensitive to the location of clients. This result is subject to a fact that a higher indoor path loss occurs at the area of higher stories so that it contributes to more chances according to the movement of the WSDs inside buildings [41]. However, the simulation results of the ITPA-based spectrum sharing demonstrate a similar performance between different mobility models within only 10% difference.

#### 5.4.4 The Probability of Success in Service Continuity

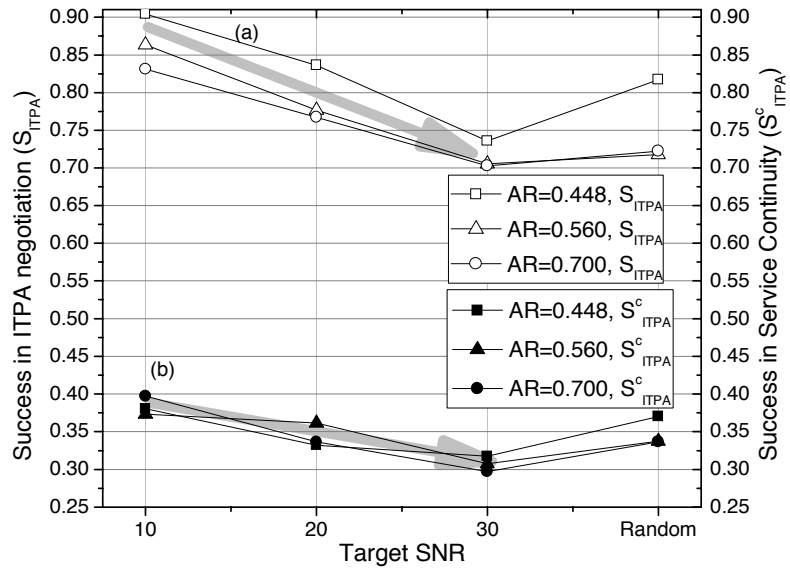
During the simulation, we also estimate the number of success that the ITPA algorithm succeeds in finding an affordable channel for the ITPA negotiation and then calculate the probability of success in the ITPA negotiation, which is expressed as  $S_{ITPA}$  = the number of success / all attempts of conducting the ITAP algorithm. Then, we estimate the probability of service continuity over the overlapped activation time between two WSAPs,  $S_{ITPA}^c$ , by calculating the expected average of  $S_{ITPA}$  during the overlapped time between two WSAPs sharing the same channel. Figure

38 depicts the simulation results of  $S_{ITPA}$  and  $S_{ITPA}^c$  for  $M = 0$ . At  $MF = 2$ ,  $S_{ITPA}$  is between 65% and 85% while  $S_{ITPA}^c$  for  $MF = 10$  is between 0.70 and 0.91 as depicted in labels (a) of Figure 38(a) and Figure 38(b). Those results mean that over 60% of all attempts of the ITPA negotiation can be succeeded, and as depicted in labels (b) of Figure 38(a) and Figure 38(b), over 30% up to 45% WSAPs of WSAPs initially failed in the first channel search can continue to operate on the sharing channel by still providing a reasonable service quality. In addition, as previously observed, the ITPA with a higher SNR like 30 dB can achieve a certain level of  $S_{ITPA}$  and  $S_{ITPA}^c$  like 30% and 65% respectively.

However, we observed that  $S_{ITPA}^c$  with  $MF = 10$  is less than  $S_{ITPA}^c$  with  $MF = 2$ , which is opposite to the results observed in Figure 28 and Figure 30. According to theoretical analysis, all numerical results of  $S_{ITPA}^{pr}$ ,  $S_{ITPA}^{sr}$ , and  $S_{ITPA}^{pc}$  with  $MF = 10$  are greater than the numerical results of them with  $MF = 2$ . We believe that these opposite results are based on the following reason. Since we suspect that the distance of  $l_{th}$  nearest neighboring WSAP will be different according to  $MF$ , we calculate the average distance of all neighboring WSAPs at every activated WSAP during the simulation. As depicted in Figure 39, the average distance of the  $l_{th}$  neighboring WSAP with  $MF = 10$  is less than the average distance with  $MF = 2$ . which means that the path loss with  $MF = 10$  will experience less decrease than the path loss with  $MF = 2$ . These results explain why  $S_{ITPA}^c$  with  $MF = 10$  is greater than  $S_{ITPA}^c$  with  $MF = 2$ . In theoretical analysis, we apply the pdf of the  $l_{th}$  nearest neighbor defined in [45] in the calculation of the formulas used for the numerical evaluation regardless of what  $MF$  is. In addition, we randomly choose the number of floors between two WSAPs. Thus, in our theoretical analysis, the path loss with  $MF = 10$  will be greater than the path loss with  $MF = 2$ , which results in the opposite results compared to the observed results in the simulation about the probability of success in service continuity.

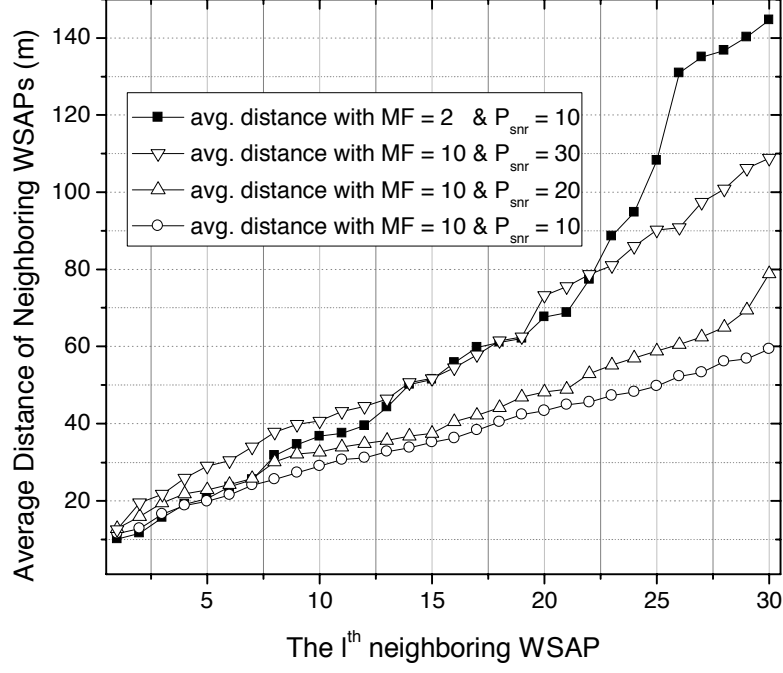


(a)  $S_{ITPA}$  and  $S_{ITPA}^c$  at MF = 2



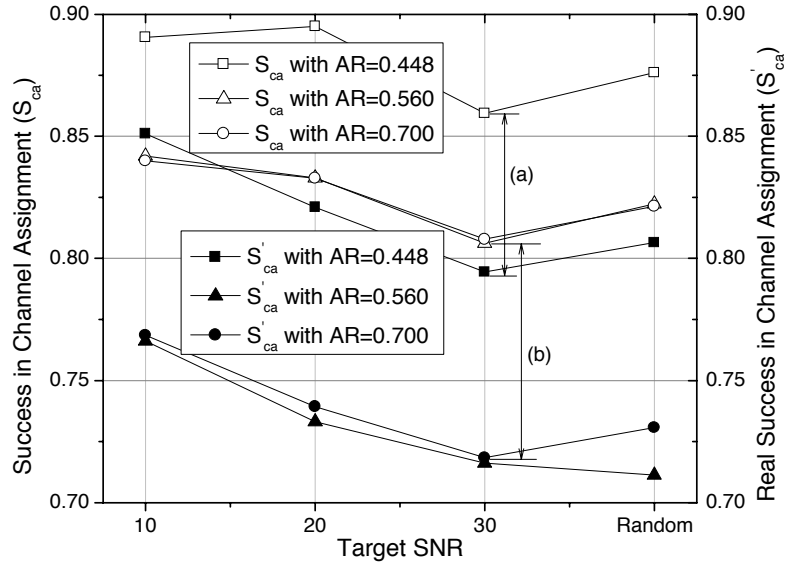
(b)  $S_{ITPA}$  and  $S_{ITPA}^c$  at MF = 10

Figure 38:  $S_{ITPA}$  and  $S_{ITPA}^c$  for M = 0



**Figure 39:** The average distance of neighboring WSAPs with AR = 0.448

Now, with  $S_{ITPA}^c$ , we can calculate the probability of the real success in channel assignment,  $S'_{ca}$ , which is expressed as  $S'_{ca} = (N_{ts} + N_{is} \times S_{ITPA}^c) / N_{tot}$ . Calculating  $S'_{ca}$  aims to the extent to which the ITPA-based spectrum sharing can really contribute to the success of two WSAPs in serving their clients successively over their overlapped activation time. As depicted in labels (a) and (b) of Figure 40, we observed decrease less than 13% in  $S_{ca}$ , but  $S'_{ca}$  is still greater than  $S_{woITPA}^{ca}$ . For instance,  $S_{woITPA}^{ca}$  observed in Figure 35(a) and Figure 36(a) is less than 70% while  $S'_{ca}$  is greater than 70%. As previously we observed that no big difference between  $S_{ca}$  for  $M = 0$  and  $S_{ca}$  for  $M = 1$ , we observed the same result about the difference between  $S_{ITPA}$  for  $M = 0$  and  $S_{ITPA}$  for  $M = 1$  as depicted in labels (a) and (b) of Figure 41. After the AR = 0.560, which is approximately analogous to  $90/A$  of the numerical evaluation, the difference increases less than 0.05. In addition, the maximum difference as depicted in label (b) of Figure 41 is less than 0.10. Thus, the results of the simulation confirm that the ITPA-spectrum sharing can achieve a similar performance on both types of



**Figure 40:** The probability of real success in channel assignment with  $M = 0$  and  $MF = 2$

mobility models adopted in the simulation and the theoretical analysis.

#### 5.4.5 Comparison of $S_{ITPA}^{pc}$ and $S_{ITPA}^c$

As described in the beginning of the simulation, on the results of all simulation cases, we have the calculated average number of detected neighboring WSAPs for  $N = 30$  that is around 100 or 120, which is analogous to the cases of defining three ARs such as  $90/A$  and  $120/A$  in the theoretical analysis. By checking the difference between  $S_{ITPA}^c$  and  $S_{ITPA}^{pc}$ , we observed that the difference is less than 0.10 as depicted in Fig. 42, where the open symbols represent  $S_{ITPA}^{pc}$  while the solid symbols do  $S_{ITPA}^c$ . This means that the simulation and the theoretical analysis confirm that the ITPA-based spectrum sharing can assist over 65% of WSAPs initially failed to find their operating channel using spectrum sensing to find shareable channels and over 30% of the WSAPs to continue serving their associated WSDs.

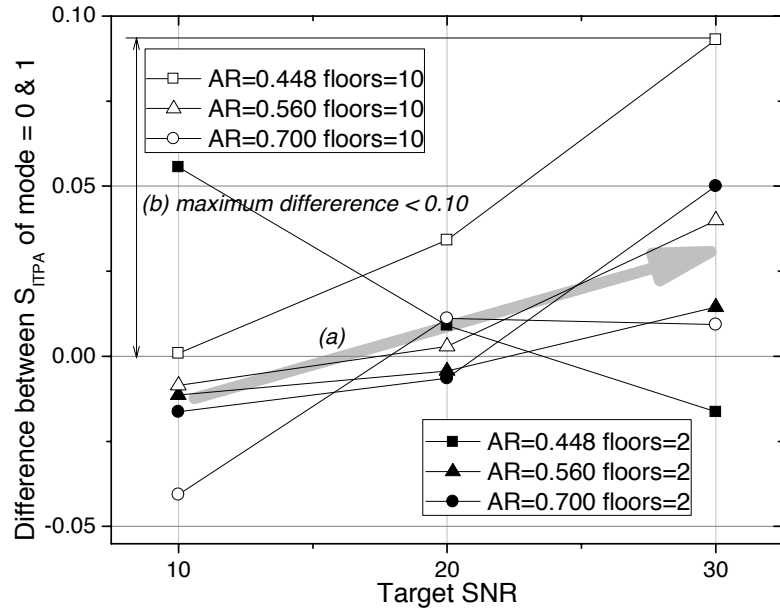


Figure 41: The difference between  $S_{ITPA}$  for  $M = 0$  and  $S_{ITPA}$  for  $M = 1$

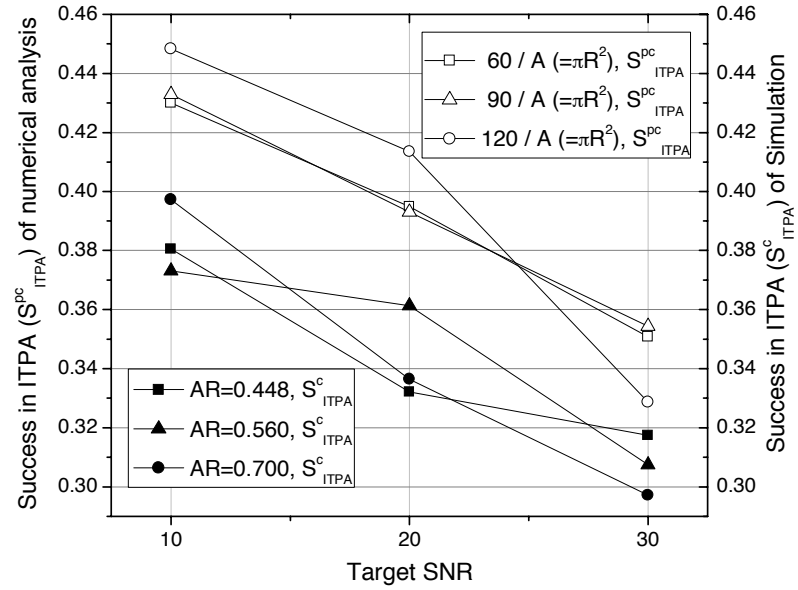


Figure 42: Comparison of  $S_{ITPA}^{pc}$  and  $S_{ITPA}^c$

#### 5.4.6 Summary of Simulation

The simulation results confirm that the ITPA-based spectrum sharing contributes to increase in the success of the channel assignment over 20%, compared to the channel assignment without the ITPA-based spectrum sharing. In addition, the analysis demonstrates that the ITPA-based spectrum sharing can contribute to the another chance to 20% of newly-joining APs failed in the first channel assignment to operate on the sharing channel during the overlapped activation time with their neighboring WSAPs. We observed the similar performance on both types of mobility models, with the stationary clients and with the clients moving randomly.

### 5.5 Conclusions

In this chapter, we propose the ITPA algorithm and ITPA-based spectrum sharing, and for the performance evaluation of the ITPA-based spectrum sharing, we apply random waypoint mobility model with multiple combinations of the indoor-to-outdoor, or the outdoor-to-indoor path loss models between a newly-joining AP and a neighboring AP. We define the formulas for performance evaluation by applying two types of mobility models, a stationary mode and a random movement model, and then conduct the numerical evaluation and the simulation with practical wireless environments as the combination of indoor and outdoor environments. We conduct the comparison between the results of the numerical evaluation and the simulation to verify the performance of the ITPA-based spectrum sharing numerically and practically.

On the analysis of the numerical results and the simulation results, we observed using the ITPA-based spectrum sharing, over 20% of newly-joining WSAPs originally failed in the first channel search can afford to continue their service during their overlapped activation time with the neighboring WSAP sharing the same channel. On whatever wireless environments having a different number of available channels

or a different mean activation time of WSAPs, with the cooperation between WSAPs and the assistance of the RRM server, we expect the ITPA-based spectrum sharing can assist the newly-joining WSAPs to find any shareable channels through the ITPA negotiation when they have no more spare channels.

The objective of this dissertation is to propose the cross-layer spectrum management architecture for white space applications that improves the performance the main functions of the spectrum management.

In the proposed cross-layer architecture, white space network devices such as white space devices and the spectrum map server cooperate to support the extended spectrum map, the inter-cell transmit power adaptation, and the frequency-domain coexistence beacon as illustrated in Figure 43. Upon the cross-layer architecture, firstly, white space devices (WSDs) achieve a faster search and higher accuracy in spectrum sensing with the extended spectrum map, the extended DHCP, and the FCB. Secondly, WSDs achieve the precise selection of their operating channel in spectrum decision with the extended spectrum map and the ITPA. In spectrum sharing, thirdly, the collaboration-based spectrum sharing with the ITPA achieve more accommodation of WSDs by increasing the number of channels shared between WSDs. Finally, WSDs with the FCB and the extended spectrum achieve effective spectrum mobility by obtaining the occupancy-status of channels precisely. Figure 44 illustrates the extent to which proposed schemes work during the activation time of one WSD. This dissertation has the followings contributions.

- the proposed cross-layer architecture for the spectrum management of white space provides the open interface that enables white space network devices to

design cooperative spectrum management schemes. Based on the architecture, the extended spectrum is capable of managing the occupancy-status of channels, and the performance evaluation demonstrates that WSDs with the extended spectrum map achieve a faster execution in spectrum sensing and less interference to neighbors.

- the proposed extended DHCP, which aims to achieve a faster retrieval of the spectrum map, contributes to increase in the number of activated WSDs by decreasing the estimated time for the connection establishment to white space networks. The performance evaluation confirms that the capacity of white space networks increases when WSDs retrieve the spectrum map in the middle of the DHCP operations.
- the proposed FCB, which aims to not only improve the probability of detection in spectrum sensing but also support channel bonding or aggregation, contributes to increase in the utilization of white space by accommodating more WSDs as the performance evaluation demonstrates.
- the proposed ITPA-based spectrum sharing framework, which aims to assist WSDs initially failed to search unoccupied channels to find shareable channels with neighboring WSDs, contributes to success in the search of shareable channels on some of the WSDs failed in the first channel assignment. The performance evaluation demonstrates that about 30% of the WSDs can have a chance, over 60%, in the success of the channel assignment with the ITPA.

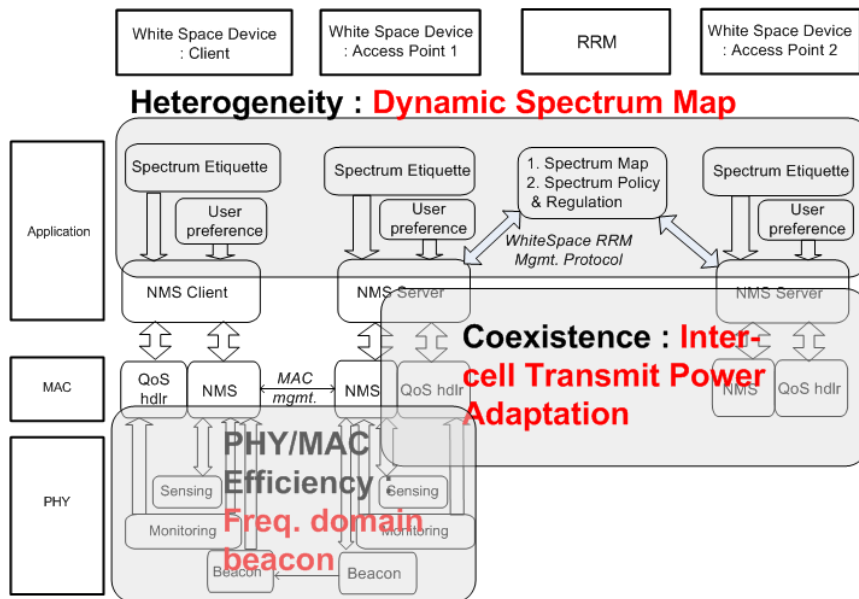


Figure 43: The cross-layer architecture layers with all proposed schemes

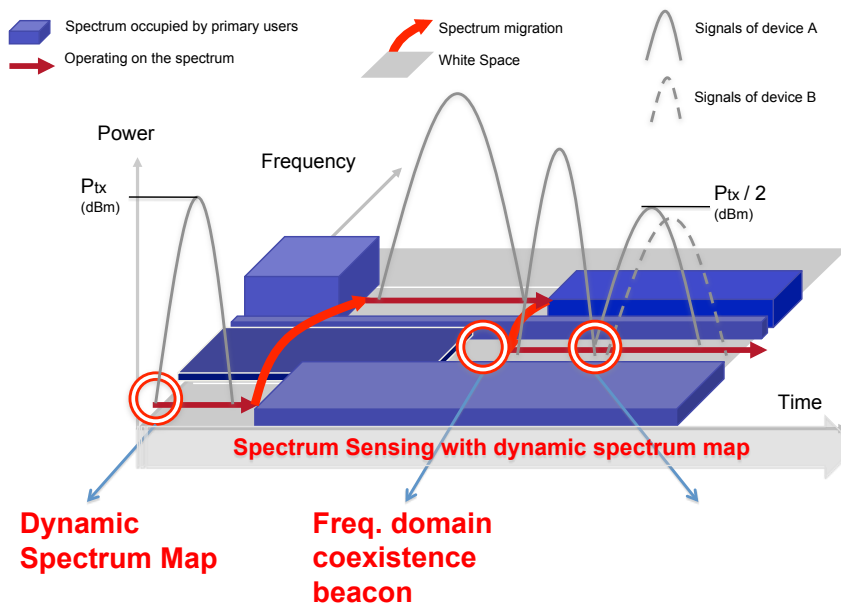


Figure 44: The example of the cross-layer spectrum map management



## REFERENCES

- [1] “Patent: Method and system for discovering vacant dtv channels using dhcp server location (pub.no.: Us 2009/0217333 a1).”
- [2] AKELLA, A., JUDD, G., SESHAN, S., and STEENKISTE, P., “Self-management in chaotic wireless deployment,” in *Mobicom 2005*, 2005.
- [3] ALIMIAN, A. and ABOBA, B., “Analysis of roaming techniques,” tech. rep., 2004.
- [4] AURA, T., ROE, M., and MURDOCH, S. J., “Securing network location awareness with authenticated dhcp,”
- [5] BERLEMANN, L. and MANGOLD, S., *Cognitive radio and dynamic spectrum access*. Wiley.
- [6] BOUDEC, J.-Y. L., “Understanding the simulation of mobility models with palm calculus,” *Performance Evaluation*, vol. 64, 2007.
- [7] BOWICK, C., BLYLER, J., and AJLUNI, C., *RF circuit design, Second Edition*. Newnes.
- [8] BRIK, V., ROZNER, E., BANERJEE, S., and BAHL, P., “Dsap: a protocol for coordinated spectrum access,” in *New Frontiers in Dynamic Spectrum Access Networks, 2005. DySPAN 2005. 2005 First IEEE International Symposium on*, pp. 611–614, 2005.
- [9] BUDDHIKOT, M., HARI, A., SINGH, K., and MILLER, S., “Mobilenat: A new technique for mobility across heterogeneous address spaces,”
- [10] BUDDHIKOT, M. M., KOLODZY, P., MILLER, S., RYAN, K., and EVANS, J., “Dimsumnet: new directions in wireless networking using coordinated dynamic spectrum,” in *World of Wireless Mobile and Multimedia Networks, 2005. WoW-MoM 2005. Sixth IEEE International Symposium on a*, pp. 78–85, 2005.
- [11] CORDEIRO, C. and CHALLAPALI, K., “C-mac: A cognitive mac protocol for multi-channel wireless networks,” in *New Frontiers in Dynamic Spectrum Access Networks, 2007. DySPAN 2007. 2nd IEEE International Symposium on*, pp. 147–157, 2007.
- [12] CORREIA, L. M., *MOBILE BROADBAND MULTIMEDIA NETWORKS*. ACADEMIC PRESS, 2006.

- [13] DIGHAM, F. F., ALOUINI, M. S., and SIMON, M. K., “On the energy detection of unknown signals over fading channels,” *Communications, IEEE Transactions on*, vol. 55, no. 1, pp. 21–24, 2007.
- [14] DUTTA, A., DAS, S., FAMOLARI, D., OHBA, Y., TANIUCHI, K., FAJARDO, V., LOPEZ, M., KODAMA, T., and SCHULZRINNE, H., “Seamless proactive handover across heterogeneous access networks,”
- [15] ECMA, “First cognitive radio networking standard for personal/portable devices in tv white spaces,” 2009.
- [16] EMD, S., “Wireless data transmission based on adaptive modulation and arq control,” *Journal of Engineering and Applied Sciences 3(4), Medwell Journals*, pp. 337–343, 2008.
- [17] FCC, “FCC adopts rules for unlicensed use of television white spaces,” November 2008.
- [18] FCC, “FCC frees up vacant tv airwaves for super wi-fi technologies,” September 2010.
- [19] GARDNER, W. A., “Signal interception: a unifying theoretical framework for feature detection,” *IEEE Transactions on Communications*, vol. 36, pp. 897–906, 1988.
- [20] GILL, P., ARLITT, M., LI, Z., and MAHANTI, A., “Youtube traffic characterization: a view from the edge,” 2007.
- [21] GOLDSMITH, A., *Wireless Communications*. Cambridge University Press, 2005.
- [22] HAUGEN, R. B. and SKOGAN, E., “Queueing systems with stochastic time out,” no. 12, 1980.
- [23] HERATH, S. P., RAJATHEVA, N., and TELLAMBURA, C., “On the energy detection of unknown deterministic signal over nakagami channels with selection combining,” in *Electrical and Computer Engineering, 2009. CCECE '09. Canadian Conference on*, pp. 745–749, 2009.
- [24] IAN F. AKYILDIZ, WON-YEOL LEE, M. C. V. and MOHANTY, S., “Next generation/dynamic spectrum access/cognitive radio wireless networks: A survey,” *COMPUTER NETWORKS JOURNAL (ELSEVIER)*, 2006.
- [25] IEEE 802.22 WORKING GROUP ON WIRELESS REGIONAL AREA.
- [26] KIM, H. and SHIN, K. G., “In-band spectrum sensing in cognitive radio networks: Energy detection or feature detection?,” in *Mobicom 2008*, 2008.
- [27] KOBAYASHI, M., NAKAYAMA, H., ANSARI, N., and KATO, N., “Robust and efficient stream delivery for application layer multicasting in heterogeneous networks,” *IEEE Transaction on Multimedia*, vol. 11, no. 1, 2009.

- [28] KWAN-WOO, K., JONGMIN, P., JINYOUN, C., KYUTAE, L., RAZZELL, C. J., KIHONG, K., CHANG-HO, L., HAKSUN, K., and LASKAR, J., “Interference analysis and sensing threshold of detect and avoid (daa) for uwb coexistence with wimax,” in *Vehicular Technology Conference, 2007. VTC-2007 Fall. 2007 IEEE 66th*, pp. 1731–1735, 2007.
- [29] LEMSTRA, I. W., “Cognitive radio defying spectrum management a collection of four (short) contributions,” 2008.
- [30] LUNDEN, J., “Spectrum sensing for cognitive radio and radar systems,” Ph.D. dissertation, November 2009.
- [31] MLINARSKY, F., “Equipment meeting the complex 600-mbps multipleinput, multiple-output wlan standard will require sophisticated channel-emulation test strategies,” 2007.
- [32] MULLEN, J. and HUANG, H., “Impact of multipath fading in wireless ad hoc networks,” in *Proceedings of the 2nd ACM international workshop on Performance evaluation of wireless ad hoc, sensor, and ubiquitous networks*, pp. 181–188, 2005.
- [33] NEW AMERICAN FOUNDATION, “Measuring the tv white space available for unlicensed wireless broadband,” tech. rep., 2006.
- [34] POLLIN, S., “Coexistence and dynamic sharing in cognitive radio networks,” in *Cognitive Wireless Communication Networks* (HOSSAIN, EKRAM; BHARGAVA, V. K., ed.), Springer, 2007.
- [35] RAPPAPORT, T., *Wireless Communications: Principles and Practice. 2nd ed.* Prentice Hall, 2002.
- [36] RYZHIK, I. S. G. and M., I., *Table of integrals, series and products. Seventh Edition.* Academic Press, 2007.
- [37] SHELLHAMMER, S., JUNIGA, J. C., GOLDHAMMER, M., and HU, W., “Coexistence tutorial material,”
- [38] SHELLHAMMER, S. and TANDRA, R., “An evaluation of dtv pilot power detection,” tech. rep., September 2009.
- [39] SHRIVASTAVA, S., AGRAWAL, D., MISHRA, A., BANERJEE, S., and NADEEM, T., “Understanding the limitations of transmit power control for indoor wlans,” in *IMC 2007*, 2007.
- [40] SNIDER, J. H., “The art of spectrum lobbying americas \$480 billion spectrum giveaway, how it happened, and how to prevent it from recurring,” tech. rep., 2007.
- [41] SPREAD SPECTRUM SCENE, “An introduction to indoor radio propagation,”

- [42] STANOJEV, I., SIMEONE, O., BAR-NESS, Y., and YU, T., “Spectrum leasing via distributed cooperation in cognitive radio,” in *Communications, 2008. ICC '08. IEEE International Conference on*, pp. 3427–3431, 2008.
- [43] SURI, N. R. and NARAHARI, Y., “An auction algorithm for procuring wireless channel in a heterogenous wireless network,” in *Wireless and Optical Communications Networks, 2006 IFIP International Conference on*, pp. 5 pp.–5, 2006.
- [44] TALEB, T., JAMALIPOUR, A., NEMOTO, Y., and KATO, N., “Demaps: A load-transition-based mobility management scheme for an efficient selection of map in mobile ipv6 networks,” *IEEE Transaction on Vehicular Technology*, vol. 58, no. 2, 2009.
- [45] THOMPSON, H. R., “Distribution of distance to nth neighbour in a population of randomly distributed individuals,” *Ecology*, vol. 37, pp. 391–394, 1956.
- [46] TOKGOZ, Y., MESHKATI, F., ZHOU, Y., YAVUZ, M., and NANDA, S., “Uplink interference management for hspa+ and lte femtocells,”
- [47] URKOWITZ, H., “Energy detection of unknown deterministic signals,” in *Proceedings of the IEEE*, vol. 55, pp. 523–531, 1967.
- [48] WANG, W. A., HUANG, C., LI, J., and ROSS, K. W., “Queen: Estimating packet loss rate between arbitrary internet hosts,” in *The tenth Passive and Active Measurement conference*, 2009.
- [49] WEIGLE, M. C., “Improving confidence in network simulations,” pp. 2188–2194, Winter Simulation Conference, 2006.
- [50] YOON, S. and LIM, K., “Frequency-domain coexistence beacon for the coexistence of white space applications,” in *IEEE VTC 2010-Fall*, 2010.
- [51] ZHAO, Q. and SADLER, B. M., “A survey of dynamic spectrum access: Signal processing, networking, and regulatory policy,” *IEEE Signal Processing Mag.*, vol. 24, no. 3, pp. 79–89, 2007.
- [52] ZHAO, Q., TONG, L., and SWAMI, A., “Decentralized cognitive mac for dynamic spectrum access,” in *New Frontiers in Dynamic Spectrum Access Networks, 2005. DySPAN 2005. 2005 First IEEE International Symposium on*, pp. 224–232, 2005.
- [53] ZHENG, H. and LILI, C., “Device-centric spectrum management,” in *New Frontiers in Dynamic Spectrum Access Networks, 2005. DySPAN 2005. 2005 First IEEE International Symposium on*, pp. 56–65, 2005.

## PUBLICATIONS

- [1] Seungil Yoon, Kyutae Lim and Jongman Kim, “Cross-Layer Dynamic Spectrum Map Management Framework for White Space Applications,” in *EURASIP Journal on Wireless Communications and Networking*, vol. 2010, Article ID 870976.
- [2] Seungil Yoon, Kyutae Lim and Jongman Kim, “Practical Analysis of the Inter-cell Transmit Power Adaptation-based Spectrum Sharing,” *IEEE Transaction on Mobile Computing*, submitted.
- [3] Seungil Yoon, Kyutae Lim and Jongman Kim, “Extending Frequency-domain Coexistence Beacon for Supporting Channel Bonding or Aggregation of White Space Applications,” *IEEE Communication Letters*, submitted.
- [4] Seungil Yoon, Kyutae Lim and Jongman Kim, “Enhanced DHCP for the Fast Retrieval of the Spectrum Map for White Space Applications,” in *IEEE Wireless Communications and Networking Conference (WCNC) 2011* April 2011.
- [5] Seungil Yoon, Jongmin Park, Kyutae Lim and Jongman Kim, “Inter-cell Transmit Power Adaptation Algorithm for Coexistence of White Space Applications,” in *IEEE Consumer Communications and Networking Conference (CCNC) 2011* Jan. 2010.
- [6] Seungil Yoon and Kyutae Lim, “Frequency-Domain Coexistence Beacon for the Coexistence of White Space Applications,” in *the 2010 IEEE 72nd Vehicular Technology Conference*, Sept. 2010.

## VITA

Seungil Yoon, a research assistant at the Georgia Electrical Design Center (GEDC) and an Electrical and Computer Engineering (ECE) Ph.D. student at the Georgia Institute of Technology, is responsible for designing network architecture and protocols of cognitive radio systems that will operate on white space, unused TV spectrum.

Seungil Yoon, a leading technical researcher in the standardization of cognitive radio systems, has filed a number of patents and implemented test-bed. He uses his work experience and ability to design practical cognitive radio systems. Prior to joining the GEDC, he worked more than seven years on the Telecommunication and Information division of Samsung Electronics in call processing software design and implementation of CDMA2000 1X/EV-DO systems.

Yoon's greatest strengths are his leadership in software development and his deduction to collaboration with other companies. While working on Samsung Electronics, he led multiple commercial software development projects with a dozen of engineers, and I also led multiple interoperability tests and system demonstration with Qualcomm and Korean cellular service providers.

Yoon received a bachelors degree and a masters degree in Computer Science (CS) from Kwangwoon University in Seoul.